UNIVERSITÀ DI PISA

DIPARTIMENTO DI MATEMATICA
CORSO DI LAUREA TRIENNALE IN MATEMATICA

Efficient Succinct Data Structures on Directed Acyclic Graphs

CANDIDATO

Luca Lombardo

RELATORE

Roberto Grossi

ANNO ACCADEMICO 2024/2025

ABSTRACT

This work introduces a redefinition of the classic rank query, traditionally applied to bit-vectors and strings, for Directed Acyclic Graphs (DAGs). We present a novel succinct data structure that leverages the topology of the input DAG to efficiently support these generalized queries while maintaining space usage below the entropy of the original graph (as there is no need to keep the whole graph to answer the queries). Our approach targets node-weighted DAGs and incorporates a critical algorithmic component: solving a generalized prefix-sum problem along DAG paths. These prefix sums, computed recursively from the root, encapsulate essential meta-information that underpins the succinct representation. The outcome of a query is expressed as a collection of ranges $[l, r]$, each representing a contiguous span of values reachable from the queried node. These ranges capture all possible accumulations (sums) of information derived from paths that originate at the source of the DAG and end at the queried node.

CONTENTS

INTRODUCTION

1.1 WHY SUCCINCT DATA STRUCTURES?

The digital age is characterized by an exponential and seemingly boundless increase in data generation and collection. This phenomenon, while not new, has dramatically shifted in scale and nature over time. We have progressed from early structured databases and text digitization to the vast heterogeneity of the World Wide Web. Subsequently, major scientific endeavors began producing unprecedented data volumes: consider genomics projects sequencing DNA, large-scale climate simulations, or astronomical observatories surveying the cosmos. The rise of social networks then turned billions of users into continuous producers of content (text, images, video) and relational data. More recently, the Internet of Things (IoT) has deployed sensors capturing real-time environmental and operational data, while the ascent of Large Language Models (LLMs) and generative AI relies on training over astronomical datasets and necessitates efficient representations for the models themselves.

This relentless data production often outpaces our ability to process it effectively. While storage technology (hard drives, SSDs, cloud storage) continually improves, allowing us to archive petabytes and exabytes, a persistent bottleneck remains the main memory (RAM) capacity of computers. Accessing data in RAM is crucial for performance, being orders of magnitude faster (typically a factor of $\sim 10^5$) than accessing secondary storage [41]. Consequently, fitting the necessary data - and critically, the auxiliary structures built upon it - into RAM is vital for countless data-intensive applications.

Indeed, the challenge frequently lies not just with the size of the raw data, but with the footprint of the data structures required for efficient querying and manipulation. Classical indices, trees, graphs, and other structures, while enabling fast operations, can demand significantly more space than the data they represent - sometimes one or two orders of magnitude larger. The human genome is a compelling example: the sequence of roughly 3.3 billion bases can be stored in under 800 megabytes using a simple 2-bit encoding. However, powerful structures like suffix trees, essential for many pattern matching and sequence analysis tasks, can easily consume tens of gigabytes, exceeding the RAM capacity of typical machines [41].

Several paradigms exist to cope with massive datasets: secondary-memory algorithms optimizing disk access, streaming algorithms processing data "on the fly" with limited memory, and distributed algorithms partitioning data and computation across clusters. Each has strengths and limitations, often involving trade-offs in performance, accuracy, or applicability. Furthermore, the proliferation of devices with constrained computational and memory resources (from smartphones to embedded sensors) creates scenarios where space is a primary constraint.

Data compression offers a well-established method for reducing storage space. However, most compression algorithms require full or partial decompression before the data can be randomly accessed or queried, making them unsuitable for tasks requiring direct interaction with the compressed form. This is precisely where Succinct Data Structures emerge as a powerful alternative. Situated at the intersection of Data Structures and Information Theory, they aim to represent data using space close to its theoretical minimum (often related to information-theoretic measures like entropy) while simultaneously supporting efficient queries directly on the compressed representation [41].

Succinct data structures strive to achieve the best of both worlds: the space efficiency of compression and the operational efficiency of traditional data structures. By compressing both the data itself and the indexing overhead needed to query it, they enable larger datasets and more complex structures to fit within faster levels of the memory hierarchy (e.g., cache instead of RAM, RAM instead of disk). This not only facilitates solving larger problems on a single machine but can also yield performance improvements due to better memory locality and reduced data transfer costs.

1.2 RESULTS AND CONTRIBUTIONS

This thesis introduces a novel representation for node-weighted Directed Acyclic Graphs (DAGs), specifically designed to efficiently support path-based aggregation queries.

Building upon foundational concepts in data compression (Chapter 2) and established succinct techniques for sequences, particularly Rank and Select operations (Chapter 3), this work addresses the challenge of managing potentially complex path information in weighted DAGs. A key motivation stems from the observation that problems like querying occurrences within degenerate strings (Section 3.3) can be effectively modeled using weighted DAGs (Chapter 4), but the application extends to other domains involving path analysis in acyclic graph structures.

The core technical contribution, presented in Chapter 4, is a space-efficient DAG representation that supports a generalized rank query (4.9). This query aims to characterize the set of possible cumulative weights achievable on paths from a source vertex to a target vertex N, considering the contribution of N's weight itself.

Our approach hinges on a strategic partitioning of the DAG's vertices into explicit nodes (V_E, whose path weight information is stored directly) and implicit nodes (V_I). For implicit nodes, the path weight information ($\mathcal{O}$-sets, 4.5) is reconstructed on demand by following a path defined by a carefully chosen successor function σ (4.11). This traversal relies on compact offset sequences ($\mathcal{I}_v$) stored for each implicit node v, which map indices in $\mathcal{O}_v$ to indices in the $\mathcal{O}$-set of its successor $\sigma(v)$. We provide algorithms (GETVALUE at 10, GETOSET at 11) for reconstructing $\mathcal{O}$-set information (Section 4.3.1) and computing the final rank query (Section 4.3.2) based on this representation.

A crucial aspect is the analysis of compression strategies for the structure's components (Section 4.4), including vertex weights, successor information, and the associated data sequences ($\mathcal{O}_v$ and $\mathcal{I}_v$). We leverage techniques like variable-length integer coding (potentially using implementations like those discussed in Appendix A), Elias-Fano coding for monotonic sequences (Section 2.6.4), and Run-Length Encoding (RLE) to minimize space (Section 4.4.2).

Significantly, we demonstrate (Section 4.5) that the space usage of our proposed structure can be substantially lower than the theoretical 0th-order entropy bound required for a lossless representation of the entire input graph $G = (V, E, w)$. This efficiency is achieved because our structure is specifically tailored to the rank query and does not need to store the full graph topology (all edges E), thereby offering a highly space-efficient solution for its designated task compared to both general-purpose graph encodings and naive precomputation approaches.

1.3   STRUCTURE OF THE THESIS

This thesis is organized as follows. Chapter 1, the current chapter, provides the motivation for studying succinct data structures, outlines the main contributions of this thesis concerning succinct representations for weighted DAGs, and describes the overall structure of the document. Chapter 2 then lays the theoretical groundwork by reviewing fundamental concepts from information theory and essential compression techniques relevant for building compact representations, such as entropy, source coding, integer coding, and statistical coding. Following this, Chapter 3 introduces core building blocks used in many succinct data structures, focusing on Rank and Select

operations, their implementation on bitvectors and wavelet trees, and their application to degenerate strings. The primary research contribution is presented in Chapter 4, which details the proposed succinct representation for weighted DAGs, including the mathematical framework, the structure itself, query algorithms, compression strategies, and space efficiency analysis. Chapter 5 summarizes the findings and contributions, discusses limitations, and proposes future research directions aimed at enhancing query time predictability. Finally, Appendix A provides practical implementation details for a compressed integer vector structure supporting efficient random access, complementing the theoretical discussion of compression techniques.

COMPRESSION PRINCIPLES AND METHODS

Entropy fundamentally represents the minimal average number of bits required to encode information from a source. In the context of uniquely identifying objects within a set U, a related concept is the information content required, which serves as a fundamental measure of the space needed in compressed data representations. The primary goal of compressed data structures is to occupy space close to this theoretical lower bound, while simultaneously enabling efficient query operations. This balance between storage efficiency and query responsiveness is central to optimizing data compression techniques.

Numerous compression techniques exist, yet they often share certain fundamental steps. Figure 1 illustrates typical processes employed for data compression. These procedures depend on the nature of the data, and the specific arrangement or combination of the blocks shown may differ. Numerical manipulation, such as predictive coding and linear transformations, is commonly employed for waveform signals like images and audio. Logical manipulation involves transforming the data into a format more amenable to compression, including techniques such as run-length encoding, zero-trees, set-partitioning information representations, and dictionary methods. Subsequently, source modeling is used to estimate the data's statistical properties, which is crucial for effective entropy coding.

Figure 1: Typical processes in data compression

These initial numerical and logical processing stages typically aim to transform the data, exploiting specific properties like signal correlation or symbol repetition, to reduce specific forms of redundancy and produce a representation more amenable to statistical compression (e.g., yielding symbols with a more skewed frequency distribution or more predictable patterns). A common feature among most compression systems is the incorporation of *entropy coding* as the final process, wherein the processed information is represented in a highly

compact form. This stage can significantly impact the overall compression ratio, as it performs the final reduction in data size based on the modeled statistics. In this chapter, we examine the principles of entropy coding, exploring the fundamental concepts and methods that underpin this crucial stage of data compression.

2.1 WORST-CASE ENTROPY

When considering the task of assigning a unique identifier (*code*, see Section 2.3) to every element of a finite set U, a baseline measure of the required information content is the logarithm of the set size. If we constrain the codes to all have the same length l, then l must be at least $\lceil \log_2 |U| \rceil$ bits to distinguish all elements. The theoretical minimum information content per element, expressed in bits, without the constraint of integer code lengths or specific coding schemes, is defined as the *worst-case entropy* of U [10]

$$H_{wc}(U) = \log_2 |U| \tag{1}$$

where $|U|$ denotes the number of elements in the set U. The term "worst-case" here refers to the scenario where no probability distribution over the elements is assumed (or equivalently, a uniform distribution is assumed), and we seek the theoretical limit for encoding based solely on the set size.

Remark 2.1. If fixed-length binary codes are used, their length l must be an integer. To assign a unique code to each of the $|U|$ elements, we require $2^l \geqslant |U|$. Taking the logarithm base 2 gives $l \geqslant \log_2 |U|$. Since l must be an integer, the minimum required length is $l_{min} = \lceil \log_2 |U| \rceil \geqslant H_{wc}(U)$.

Example 2.2. Let $\mathcal{T}_n$ denote the set of all general ordinal trees [4] with n nodes. In this scenario, each node can have an arbitrary number of children, and their order is distinguished. With n nodes, the number of possible ordinal trees is the $(n-1)$-th Catalan number, given by:

$$|\mathcal{T}_n| = C_{n-1} = \frac{1}{n}\binom{2n-2}{n-1}$$

Using the known asymptotic approximation for Catalan numbers derived from Stirling's formula, for large n:

$$|\mathcal{T}_n| = C_{n-1} \approx \frac{4^{n-1}}{\sqrt{\pi}(n-1)^{3/2}} = \frac{4^n}{4\sqrt{\pi}(n-1)^{3/2}} = \frac{4^n}{n^{3/2}}\Theta(1)$$

$$H_{wc}(\mathcal{T}_n) = \log_2 |\mathcal{T}_n|$$
$$= \log_2 \left(\frac{4^n}{n^{3/2}} \Theta(1) \right)$$
$$= 2n - \Theta(\log_2 n)$$

Thus, we have determined the minimum number of bits required to uniquely identify (encode) a general ordinal tree with n nodes based solely on their count.

2.2 ENTROPY

We now introduce the concept of entropy as a measure of uncertainty of a random variable. While the worst-case entropy H_{wc}, discussed previously, provides a lower bound based solely on the set's cardinality (effectively assuming fixed-length codes or a uniform probability distribution over the elements), Shannon entropy offers a more refined measure. It accounts for the actual probability distribution of the elements, quantifying the *average* uncertainty or information content associated with the random variable. A deeper explanation can be found in standard texts such as [24, 41, 10].

Definition 2.3 (Entropy of a Random Variable). *Let X be a random variable taking values in a finite alphabet $\mathcal{X}$ with the probabilistic distribution $P_X(x) = Pr\{X = x\}$ ($x \in \mathcal{X}$). Then, the entropy of X is defined as*

$$H(X) = H(P_X) \stackrel{\text{def}}{=} E_{P_x}\{-\log P_X(x)\} = -\sum_{x \in \mathcal{X}} P_X(x) \log P_X(x)$$

This is also known as Shannon entropy, named after Claude Shannon, who introduced it in his seminal work [54]

Here, $E_{P_X}[\cdot]$ denotes the expectation with respect to the probability distribution P_X. The logarithm is taken to base 2, and entropy is expressed in bits. From the definition, it follows that the entropy of a discrete random variable is always non-negative[1]. .

Example 2.4. [Toss of a fair coin] Let X be a random variable representing the outcome of a fair coin toss, with $\mathcal{X} = \{\text{Heads}, \text{Tails}\}$. The probability distribution is $P_X(\text{Heads}) = P_X(\text{Tails}) = \frac{1}{2}$. The entropy of X is:

$$H(X) = -\frac{1}{2} \log_2 \frac{1}{2} - \frac{1}{2} \log_2 \frac{1}{2} = -\frac{1}{2}(-1) - \frac{1}{2}(-1) = 1 \text{ bit}$$

This result aligns with the intuition that one bit is required to convey the outcome of a fair coin toss.

---

[1] The entropy is zero if and only if X is deterministic, i.e., $P_X(x) = 1$ for some single value $x = c$.

Remark 2.5. By convention, $H(X)$ denotes the entropy of the random variable X. It is important to note that entropy is not a function of the random variable itself, but rather a functional of its probability distribution P_X. It depends only on the probabilities of the values, not the values themselves.

The entropy $H(X)$ quantifies the average uncertainty associated with the random variable X. It can be interpreted as the average amount of information (in bits) gained upon observing an outcome of X, or equivalently, the minimum average number of bits required to encode the outcomes of X using an optimal compression scheme.

2.2.1 *Properties*

Having introduced the entropy for a single random variable X, we now consider the case of two random variables X and Y. To quantify the total uncertainty associated with the pair (X, Y) considered together, we define the joint entropy:

Definition 2.6 (Joint Entropy). *Let (X, Y) be a pair of discrete random variables (X, Y) with a joint distribution $P_{XY}(x, y) = Pr\{X = x, Y = y\}$. The joint entropy of (X, Y) is defined as*

$$H(X, Y) = H(P_{XY}) = -\sum_{x \in \mathcal{X}} \sum_{y \in \mathcal{Y}} P_{XY}(x, y) \log P_{XY}(x, y)$$

This definition extends naturally to the joint entropy of n random variables $(X_1, X_2, \ldots, X_n)$ as $H(X_1, \ldots, X_n)$.

We also define the conditional entropy $H(Y|X)$, which measures the remaining uncertainty about Y when X is known. It is the expected value of the entropies of the conditional distributions $P_{Y|X}(y|x)$, averaged over X.

Often, it's helpful to conceptualize the relationship between Y and X in terms of information transmission. Given $X = x$, the conditional probability $P_{Y|X}(y|x) = Pr\{Y = y|X = x\}$ describes the likelihood of observing $Y = y$. The collection of these conditional probabilities for all $x \in \mathcal{X}$ and $y \in \mathcal{Y}$ defines a statistical relationship often referred to as a *channel* with *input alphabet* $\mathcal{X}$ and *output alphabet* $\mathcal{Y}$.

Definition 2.7 (Conditional Entropy). *Let (X, Y) be a pair of discrete random variables with a joint distribution $P_{XY}(x, y) = Pr\{X = x, Y = y\}$. The conditional entropy of Y given X is defined as*

$$H(Y|X) = H(W|P_X) \overset{\text{def}}{=} \sum_x P_X(x) H(Y|x)$$

$$= \sum_{x \in \mathcal{X}} P_X(x) \left\{ -\sum_{y \in \mathcal{Y}} W(y|x) \log W(y|x) \right\}$$

$$= -\sum_{x \in \mathcal{X}} \sum_{y \in \mathcal{Y}} P_{XY}(x, y) \log W(y|x)$$

$$= E_{P_{XY}} \{ -\log W(Y|X) \}$$

Since entropy is non-negative, and $H(Y|X)$ is an average of non-negative entropies $H(Y|X = x)$, conditional entropy is also non-negative: $H(Y|X) \geqslant 0$. Furthermore, $H(Y|X) = 0$ if and only if Y is completely determined by X (i.e., $Y = f(X)$ for some deterministic function f with probability one).

The relationship between joint and conditional entropy is established by the chain rule.

Theorem 2.8 (Chain Rule). *Let (X, Y) be a pair of discrete random variables with a joint distribution $P_{XY}(x, y)$. Then, the joint entropy of (X, Y) can be expressed as*

This is also known as additivity of entropy.

$$H(X, Y) = H(X) + H(Y|X)$$

Proof. From the definition of conditional entropy (2.7), we have

$$H(X, Y) = -\sum_{x,y} P_{XY}(x, y) \log W(y|x)$$

$$= -\sum_{x,y} P_{XY}(x, y) \log \frac{P_{XY}(x, y)}{P_X(x)}$$

$$= -\sum_{x,y} P_{XY}(x, y) \log P_{XY}(x, y) + \sum_{x,y} P_X(x) \log P_X(x)$$

$$= H(X, Y) + H(X)$$

Where we used the relation

$$W(y|x) = \frac{P_{XY}(x, y)}{P_X(x)}$$

When $P_X(x) \neq 0$. $\qquad\square$

Corollary 2.9.

$$H(X, Y|Z) = H(X|Z) + H(Y|X, Z)$$

Proof. The proof is analogous to the proof of the chain rule.   □

Corollary 2.10.

$$H(X_1, X_2, \ldots, X_n) = H(X_1) + H(X_2|X_1) + H(X_3|X_1, X_2)$$
$$+ \ldots + H(X_n|X_1, X_2, \ldots, X_{n-1})$$

Proof. We can apply the two-variable chain rule in repetition obtain the result.   □

2.2.2 *Mutual Information*

Having defined measures for the uncertainty of individual variables ($H(X)$), pairs ($H(X, Y)$), and conditional uncertainty ($H(Y|X)$), we can quantify the amount of information that one variable provides about another. This is the mutual information, $I(X; Y)$. It represents the reduction in uncertainty about X obtained by learning the value of Y, or vice versa. Figure 2 provides a visual representation.

Definition 2.11 (Mutual Information)**.** *Let (X, Y) be a pair of discrete random variables with a joint distribution $P_{XY}(x, y)$. The mutual information between X and Y is defined as*

$$I(X; Y) = H(X) - H(X|Y) \tag{1}$$

Using the chain rule (2.8), we can rewrite it as

$$I(X; Y) = H(X) - H(X|Y)$$
$$= H(X) + H(Y) - H(X, Y) \tag{2}$$
$$= -\sum_x P_X(x) \log P_X(x) - \sum_y P_Y(y) \log P_Y(y)$$
$$+ \sum_{x,y} P_{XY}(x, y) \log P_{XY}(x, y) \tag{3}$$
$$= \sum_{x,y} P_{XY}(x, y) \log \frac{P_{XY}(x, y)}{P_X(x)P_Y(y)} \tag{4}$$
$$= E_{P_{XY}} \left\{ \log \frac{P_{XY}(x, y)}{P_X(x)P_Y(y)} \right\} \tag{5}$$

It follows immediately that the mutual information is symmetric, $I(X; Y) = I(Y; X)$.
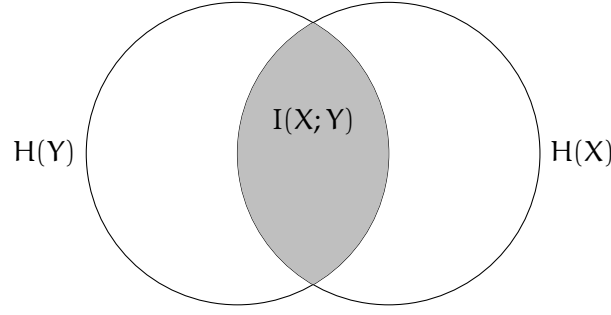
Figure 2: Mutual information between two random variables X and Y.

2.2.3 *Fano's inequality*

Information theory provides fundamental limits on data processing tasks, including compression and inference. It allows us to establish lower bounds on the probability of error when estimating one random variable based on observations of another. Fano's inequality relates the conditional entropy $H(X|Y)$ to the probability of error when estimating X from Y. Recall that $H(X|Y) = 0$ if and only if X is a function of Y, meaning X can be determined from Y with zero error. Fano's inequality bounds the error probability when $H(X|Y) > 0$.

Theorem 2.12 (Fano's Inequality). *Let X and Y be two discrete random variables with X taking values in some discrete alphabet $\mathcal{X}$, we have*

$$H(X|Y) \leqslant Pr\{X \neq Y\}\log(|\mathcal{X}| - 1) + h(Pr\{X \neq Y\})$$

where $h(p) = -p\log p - (1-p)\log(1-p)$ is the binary entropy function.

Proof. Let Z be a random variable defined as follows:

$$Z = \begin{cases} 1 & \text{if } X \neq Y \\ 0 & \text{if } X = Y \end{cases}$$

We can then write

$$\begin{aligned} H(X|Y) = H(X|Y) + H(Z|XY) &= H(XZ|Y) \\ &= H(X|YZ) + H(Z|Y) \\ &\leqslant H(X|YZ) + H(Z) \end{aligned} \tag{6}$$

The last inequality follows from the fact that conditioning reduces entropy. We can then write

$$H(Z) = h(Pr\{X \neq Y\}) \tag{7}$$

Since $\forall y \in \mathcal{Y}$, we can write

$$H(X|Y = y, Z = 0) = 0$$

and

$$H(X|Y = y, Z = 1) \leqslant \log(|\mathcal{X}| - 1)$$

Combining these results, we have

$$H(X|YZ) \leqslant \Pr\{X \neq Y\} \log(|\mathcal{X}| - 1) \tag{8}$$

From equations 6, 7 and 8, we have Fano's inequality. □

Fano's inequality thus provides a tangible link between the conditional entropy $H(X|Y)$, which quantifies the remaining uncertainty about X when Y is known, and the minimum probability of error achievable in any attempt to estimate X from Y. This inequality, along with the foundational concepts of entropy, joint entropy, conditional entropy, and mutual information introduced throughout this section, establishes a robust theoretical framework. These tools are not merely abstract measures; they allow us to quantify information, understand dependencies between data sources, and ultimately, to delineate the fundamental limits governing how efficiently data can be represented and compressed. Understanding these limits is essential as we go deeper into specific encoding techniques.

2.3 SOURCE AND CODE

In the previous section, information-theoretic limits based on the probabilistic nature of data sources were established. Attention now turns to the practical mechanisms for achieving data compression: the interplay between a *source* of information and the *code* used to represent it. A source, in this context, is any process generating a sequence of symbols drawn from a specific alphabet (e.g., letters of text, pixel values in an image, sensor readings). Source coding, or data compression, involves converting this sequence into a different, typically shorter, sequence of symbols from a target coding alphabet (often binary).

The core principle behind efficient coding is the exploitation of the source's statistical properties. Symbols or patterns occurring frequently should ideally be assigned shorter representations (codewords), while less frequent ones can be assigned longer codewords. A classic, intuitive example is Morse code: the most common letter in English text, *E*, is represented by the shortest possible signal, a single dot, whereas infrequent letters like *Q* receive much longer sequences.

2.3.1 *Codes*

A source characterized by a random process generates symbols from a specific alphabet at each time step. The objective is to transform this output sequence into a more concise representation. This data reduction technique, known as *source coding* or *data compression*, utilizes a code to represent the original symbols more efficiently. The device performing this transformation is termed an *encoder*, and the process itself is referred to as *encoding* [24].

Definition 2.13 (Source Code). *A source code for a random variable X is a mapping from the set of possible outcomes of X, denoted $\mathcal{X}$, to $\mathcal{D}^*$, the set of all finite-length strings of symbols from a $\mathcal{D}$-ary alphabet. Let $C(x)$ denote the codeword assigned to x, and let $l(x)$ denote the length of $C(x)$.*

Definition 2.14 (Expected length). *The expected length $L(C)$ of a source code C for a random variable X with probability mass function $P_X(x)$ is defined as*

$$L(C) = \sum_{x \in \mathcal{X}} P_X(x)l(x)$$

where $l(x)$ is the length of the codeword assigned to x.

For simplicity, we assume the $\mathcal{D}$-ary alphabet is $\mathcal{D} = \{0, 1, \dots, K-1\}$, where $K = |\mathcal{D}|$.

Example 2.15. Consider a source code for a random variable X with $\mathcal{X} = \{a, b, c, d\}$ and $P_X(a) = 0.5$, $P_X(b) = 0.25$, $P_X(c) = 0.125$, and $P_X(d) = 0.125$. The code is defined as

$$C(a) = 0$$
$$C(b) = 10$$
$$C(c) = 110$$
$$C(d) = 111$$

The entropy of X is

$$H(X) = -0.5 \log_2 0.5 - 0.25 \log_2 0.25 - 0.125 \log_2 0.125 - 0.125 \log_2 0.125 = 1.75 \text{ bits}$$

The expected length of this code is also 1.75:

$$L(C) = 0.5 \cdot 1 + 0.25 \cdot 2 + 0.125 \cdot 3 + 0.125 \cdot 3 = 1.75 \text{ bits}$$

This example presents a code that achieves the lower bound given by the entropy, as $L(C) = H(X)$.

Definition 2.16 (Nonsingular Code)**.** *A code is nonsingular if every element of the range of* X *maps to a different element of* $\mathcal{D}^*$*. Thus:*

$$x \neq y \implies C(x) \neq C(y)$$

Although a nonsingular code ensures distinct representations for individual source symbols, the primary objective is often the transmission of sequences of these symbols. This potential inefficiency motivates the use of codes where the structure inherently delineates codeword boundaries, eliminating the need for explicit separators. Such codes are often referred to as prefix codes or instantaneous codes. These codes possess a property where the structure itself indicates the end of each codeword. The following definitions formalize this concept [10].

Definition 2.17 (Extension of a Code)**.** *The extension* C^* *of a code* C *is the mapping from finite-length sequences of symbols from* $\mathcal{X}$ *to finite-length strings of symbols from the* $\mathcal{D}$*-ary alphabet defined by*

$$C^*(x_1 x_2 \dots x_n) = C(x_1)C(x_2)\dots C(x_n)$$

where $C(x_1)C(x_2)\dots C(x_n)$ *denotes the concatenation of the codewords assigned to* $x_1, x_2, \dots, x_n$*.*

Example 2.18. If $C(x_1) = 0$ and $C(x_2) = 110$, then $C^*(x_1 x_2) = 0110$.

Definition 2.19 (Unique Decodability)**.** *A code* C *is uniquely decodable if its extension* C^* *is nonsingular.*

Thus, any encoded string in a uniquely decodable code has only one possible source string that could have generated it.

Definition 2.20 (Prefix Code)**.** *A code is a prefix code if no codeword is a prefix of any other codeword.*

Also called instantaneous code

Upon receiving a coded sequence, an *instantaneous code* permits decoding each symbol as soon as its corresponding codeword is completely received. Since the code structure indicates where each codeword ends, the code effectively provides implicit punctuation separating the symbols. This allows the entire message to be decoded by simply reading the string and identifying codeword boundaries without needing subsequent symbols. For instance, using the code from Example 2.15, the binary string `01011111010` is decoded as `0,10,111,110,10` because the code structure naturally separates the symbols [10]. Figure 3 illustrates the relationship between different classes of codes.

Figure 3: Relationship between different types of codes

Example 2.21. [Morse Code] Morse code serves as a classic example. Historically used for telegraphy, it represents text characters using sequences from a ternary alphabet: a short signal (dot, .), a longer signal (dash, -), and a space (pause used as a delimiter). Frequent letters like *E* receive short codes (.), while less common ones like *Q* get longer codes (–.-). The following table summarizes the Morse code for some letters and the SOS distress signal:

Character/Sequence	Code
E	.
T	-
A	. -
N	- .
S	. . .
O	- -
SOS	. . . - - . . .

Nonsingularity: The code is nonsingular because each letter corresponds to a unique sequence of dots and dashes.

Prefix Property: The code does not satisfy the prefix condition. Several codewords are prefixes of others. For example, $C(E) = $. is a prefix of $C(A) = $. - and $C(S) = $ . . .

Unique Decodability: Unique decodability is achieved through the critical use of pauses (spaces) inserted between letters and words accord-

ing to specific timing rules. These pauses function as explicit delimiters. Without these explicit delimiters, the ambiguities arising from the lack of the prefix property would prevent reliable decoding. This contrasts with prefix codes (e.g., Example 2.15), which are inherently uniquely decodable based solely on their structure, without needing external delimiters.

2.3.2 *Kraft's Inequality*

The goal is to construct efficient codes, ideally prefix codes (instantaneous codes), whose expected length approaches the source entropy. A fundamental constraint arises because short lengths cannot be arbitrarily assigned to all symbols while maintaining the prefix property or even unique decodability. Kraft's inequality precisely quantifies this limitation. It establishes a *necessary* condition that the chosen codeword lengths $l(x)$ must satisfy for *any uniquely decodable* code to exist. Crucially, the same inequality also serves as a *sufficient* condition guaranteeing that a *prefix* code with these exact lengths can indeed be constructed. The necessity part for uniquely decodable codes will be stated and proved first.

Denote the size of the source and code alphabets with $J = |\mathcal{X}|$ and $K = |\mathcal{D}|$, respectively. Different proofs of the following theorem can be found in [10, 24]; the proof presented here follows [24], although the one proposed in [10], based on the concept of a source tree, is also very interesting.

Theorem 2.22 (Kraft's Inequality)**.** *The codeword lengths $l(x)$, $x \in \mathcal{X}$, of any uniquely decodable code C over a K-ary alphabet must satisfy the inequality*

$$\sum_{x \in \mathcal{X}} K^{-l(x)} \leqslant 1 \tag{1}$$

Proof. Consider the n-th power of the sum in the inequality (1):

$$\left(\sum_{x \in \mathcal{X}} K^{-l(x)} \right)^n = \sum_{x_1 \in \mathcal{X}} \sum_{x_2 \in \mathcal{X}} \cdots \sum_{x_n \in \mathcal{X}} K^{-l(x_1)} K^{-l(x_2)} \ldots K^{-l(x_n)}$$

$$= \sum_{x^n \in \mathcal{X}^\setminus} K^{-l(C^*(x^n))}$$

where $l(C^*(x^n)) = l(C(x_1)) + l(C(x_2)) + \ldots + l(C(x_n))$ is the length of the concatenation of the codewords assigned to $x_1, x_2, \ldots, x_n$. Grouping terms by the length m of the resulting codeword extension $C^*(x^n)$, we obtain:

$$\sum_{x^n \in \mathcal{X}^\setminus} K^{-l(C^*(x^n))} = \sum_{m=1}^{nl_{max}} A(m) K^{-m}$$

where $A(m)$ denotes the number of source sequences $x^n \in \mathcal{X}^n$ whose extended codeword $C^*(x^n)$ has length m, and $l_{max} = \max_{x \in \mathcal{X}} l(x)$ is the maximum length of a codeword in the code C. Since the code C is uniquely decodable, its extension C^* is nonsingular. Consequently, any two distinct source sequences x^n and y^n must map to distinct coded sequences $C^*(x^n)$ and $C^*(y^n)$. For a fixed length m, the number of distinct coded sequences $C^*(x^n)$ having length m cannot exceed the total number of possible K-ary sequences of length m, which is K^m. Thus, $A(m) \leqslant K^m$. This implies that each term $A(m)K^{-m}$ in the sum is less than or equal to 1. Therefore, the sum is bounded by the number of possible values for m:

$$\left(\sum_{x \in \mathcal{X}} K^{-l(x)} \right)^n = \sum_{m=1}^{nl_{max}} A(m)K^{-m} \leqslant \sum_{m=1}^{nl_{max}} 1 = nl_{max}$$

Thus,

$$\sum_{x \in \mathcal{X}} K^{-l(x)} \leqslant (nl_{max})^{1/n}$$

Taking the limit as $n \to \infty$, and noting that $\lim_{n \to \infty} (nl_{max})^{1/n} = \lim_{n \to \infty} \exp\left(\frac{\ln(nl_{max})}{n} \right) = e^0 = 1$, yields

$$\sum_{x \in \mathcal{X}} K^{-l(x)} \leqslant 1$$

This completes the proof. $\square$

2.4 EMPIRICAL ENTROPY

The concept of empirical entropy builds upon the foundational notion of Shannon entropy. For a binary source emitting symbols from the alphabet $\mathcal{U} = \{0, 1\}$ with respective probabilities p_0 and $p_1 = 1 - p_0$, the Shannon entropy is defined as:

$$H(p_0) = -p_0 \log_2 p_0 - (1 - p_0) \log_2(1 - p_0)$$

This definition can be extended to sequences generated by such sources. Consider first a memoryless (or zero-order) source, where the probability of emitting a symbol is independent of previously emitted symbols. For such a source generating sequences of length n, the alphabet of possible sequences is Σ^n, where Σ is the alphabet of individual symbols. If the source emits symbols from a general alphabet Σ of size $|\Sigma| = \sigma$, with each symbol $s \in \Sigma$ having a probability p_s (such that $\sum_{s \in \Sigma} p_s = 1$), the Shannon entropy of the source is given by:

$$H(P) = H(p_1, \ldots, p_\sigma) = -\sum_{s \in \Sigma} p_s \log p_s = \sum_{s \in \Sigma} p_s \log \frac{1}{p_s}$$

For a memoryless source, the entropy of a sequence of length n is $nH(P)$.

Remark 2.23. If a single symbol s_i occurs with probability $p_{s_i} = 1$ (implying all other symbols have probability 0), then the entropy $H(P) = 0$. Conversely, if all symbols have the same probability $p_s = \frac{1}{\sigma}$, the entropy reaches its maximum value, $H(P) = \log \sigma$. Consequently, for a sequence of n symbols drawn independently from this uniform distribution, the total entropy is $n \log \sigma$.

2.4.1 *Bit Sequences*

In practice, the true probabilities p_s governing the source are often unknown. Often, observation is limited to a single sequence generated by the source. Empirical entropy provides a method to estimate the information content based directly on the observed frequencies within that sequence. This concept is first examined for binary sequences.

Consider a binary sequence $B[1, n]$, for which compression is sought without access to an explicit model of the source. Instead, only the sequence B itself is available. Without a source model, it can be hypothesised that B may exhibit a statistical bias (e.g., towards more 0s or more 1s). Consequently, compression can be attempted based on this observed characteristic. Specifically, B can be modelled as the output of a zero-order source. If m denotes the count of 1s in B, it is postulated that the source emits 1s with probability $p = m/n$. This motivates the definition of zero-order empirical entropy:

Definition 2.24 (Zero-order empirical entropy)**.** *Given a binary sequence* $B[1, n]$ *containing m occurrences of 1 and $n - m$ occurrences of 0, the zero-order empirical entropy of B is defined as:*

$$\mathcal{H}_0(B) = \mathcal{H}\left(\frac{m}{n}\right) = \frac{m}{n} \log \frac{n}{m} + \frac{n - m}{n} \log \frac{n}{n - m}$$

where logarithms are typically base 2 for information content measured in bits.

The zero-order empirical entropy establishes a lower bound: if compression of B is attempted using a fixed codeword $C(1)$ for 1s and $C(0)$ for 0s, it is impossible to compress B to fewer than $n\mathcal{H}_0(B)$ total bits. Achieving a compressed length $m|C(1)| + (n - m)|C(0)| < n\mathcal{H}_0(B)$ would contradict the source coding theorem derived from Shannon entropy.

CONNECTION WITH WORST CASE ENTROPY   A connection exists between the zero-order empirical entropy $\mathcal{H}_0(B)$ and the worst-case entropy H_{wc} (Section 2.1). Define the set $\mathcal{B}_{n,m}$ as the collection of all binary sequences of length n containing exactly m ones. The sequence B belongs to this set. The number of bits required to assign a unique identifier to each sequence *within this specific set* $\mathcal{B}_{n,m}$, which corresponds to the worst-case entropy if selection within the set is uniform, is $H_{wc}(\mathcal{B}_{n,m}) = \log |\mathcal{B}_{n,m}| = \log \binom{n}{m}$. Using Stirling's approximation for the binomial coefficient, it can be shown that this quantity relates to the total empirical entropy $n\mathcal{H}_0(B)$:

$$\log \binom{n}{m} \approx n\mathcal{H}_0(B) - O(\log n)$$

Thus, the total empirical entropy $n\mathcal{H}_0(B)$ approximates the number of bits required to uniquely identify a sequence within the set $\mathcal{B}_{n,m}$, offering an interpretation of empirical entropy related to the combinatorial complexity of sequences with a fixed composition [41].

2.4.2 *Entropy of a Text*

Analogously, for a text $S[1, n]$ drawn from an alphabet $\Sigma = \{s_1, \ldots, s_\sigma\}$, where each symbol $s \in \Sigma$ occurs n_s times in S (such that $\sum_{s \in \Sigma} n_s = n$), the zero-order empirical entropy is defined based on the observed relative frequencies:

Definition 2.25 (Zero-order empirical entropy of a text). *Given a text $S[1, n]$ over alphabet Σ, where symbol s appears n_s times, the zero-order empirical entropy of S is:*

$$\mathcal{H}_0(S) = \mathcal{H}\left(\frac{n_{s_1}}{n}, \ldots, \frac{n_{s_\sigma}}{n}\right) = \sum_{s \in \Sigma} \frac{n_s}{n} \log \frac{n}{n_s}$$

Example 2.26. Consider $S = $ "abracadabra". The length is $n = 11$. The symbol counts are $n_a = 5$, $n_b = 2$, $n_c = 1$, $n_d = 1$, $n_r = 2$. The alphabet size is $\sigma = 5$. The zero-order empirical entropy of S is:

$$\mathcal{H}_0(S) = \frac{5}{11} \log_2 \frac{11}{5} + \frac{2}{11} \log_2 \frac{11}{2} + \frac{1}{11} \log_2 \frac{11}{1}$$
$$+ \frac{1}{11} \log_2 \frac{11}{1} + \frac{2}{11} \log_2 \frac{11}{2} \approx 2.04 \text{ bits/symbol}$$

This suggests a theoretical lower bound for compression based on symbol frequencies of $n\mathcal{H}_0(S) \approx 11 \times 2.04 \approx 22.44$ bits for the entire sequence. This is lower than the $n \log \sigma = 11 \log_2 5 \approx 25.54$ bits corresponding to the uniform distribution over the alphabet.

This zero-order definition has limitations, particularly for sources like natural language text where symbol occurrences often exhibit dependencies. For instance, in English, the character *q* is almost invariably followed by *u*. Higher-order entropy models (Section 2.5), which account for the conditional probability of a symbol given its preceding context, provide a more refined measure of the information content for such sources. This principle of exploiting context underlies compression techniques such as Huffman coding (Section 2.7); however, Huffman coding itself is typically applied in a zero-order fashion unless specifically adapted for context.

2.5 HIGHER ORDER ENTROPY

The zero-order empirical entropy $\mathcal{H}_0(S)$, discussed in the previous section, provides a useful baseline for compression by considering the frequency of individual symbols. However, it operates under the implicit assumption that symbols are generated independently, a condition seldom met in practice, especially for data like natural language text. For instance, the probability of encountering the letter *u* in English text dramatically increases if the preceding letter is *q*. To capture such dependencies and obtain a more accurate measure of the information content considering local context, the concept of *higher-order empirical entropy* is introduced. This approach conditions the probability of a symbol's occurrence on the sequence of k symbols that immediately precede it.

Definition 2.27 (Redundancy). *For an information source X generating symbols from an alphabet Σ, the redundancy R is the difference between the maximum possible entropy per symbol and the actual entropy $H(X)$ of the source:*

$$R = \log_2 |\Sigma| - H(X)$$

This redundancy value, R, quantifies the degree of predictability or statistical structure inherent in the source. A high redundancy signifies that the source is far from random, exhibiting patterns (like non-uniform symbol probabilities or inter-symbol dependencies) that can potentially be exploited for compression. Conversely, a source with low redundancy behaves more randomly, leaving less room for compression beyond the theoretical minimum dictated by $H(X)$.

However, evaluating redundancy directly using Definition 2.27 often proves impractical, as determining the true source entropy $H(X)$ for the process generating a given string S is typically unfeasible. This limitation necessitates alternative, empirical approaches. To address this issue, the concept of the *k-th order empirical entropy* of a string S,

denoted as $\mathcal{H}_k(S)$, is introduced. In statistical coding (Section 2.7), a scenario with $k = 0$ will be examined, relying on symbol frequencies within the string. With $\mathcal{H}_k(S)$, the objective is to extend the entropy concept by examining the frequencies of k-grams in string S. This requires analyzing subsequences of symbols with a length of k, thereby capturing the *compositional structure* of S [13].

Let S be a string of length $n = |S|$ over an alphabet Σ of size $|\Sigma| = \sigma$. Let ω denote a k-gram (a sequence of k symbols from Σ), and let n_ω be the number of occurrences of ω in S. Let $n_{\omega\sigma_i}$ be the number of times the k-gram ω is followed by the symbol $\sigma_i \in \Sigma$ in S. [2]

Definition 2.28 (k-th Order Empirical Entropy). *The* k-th order empirical entropy *of a string* S *is defined as:*

$$\mathcal{H}_k(S) = \frac{1}{n} \sum_{\omega \in \Sigma^k} \left(\sum_{\sigma_i \in \Sigma} n_{\omega\sigma_i} \log_2 \left(\frac{n_\omega}{n_{\omega\sigma_i}} \right) \right) \tag{1}$$

where terms with $n_{\omega\sigma_i} = 0$ *contribute zero to the sum, following the convention* $0\log(a/0) = 0$.

This definition calculates the average conditional entropy based on the preceding k symbols. An equivalent and often more intuitive way to express this is by averaging the zero-order empirical entropies of the sequences formed by the symbols following each distinct k-gram context:

$$\mathcal{H}_k(S) = \sum_{\omega \in \Sigma^k, n_\omega > 0} \frac{n_\omega}{n} \cdot \mathcal{H}_0(S_\omega) \tag{2}$$

where S_ω is the string formed by concatenating all symbols that immediately follow an occurrence of the k-gram ω in S (its length is $|S_\omega| = n_\omega$). The sum is taken over all k-grams ω that actually appear in S (i.e., $n_\omega > 0$).

Example 2.29. Consider the example from 2.26, where S = "abracadabra" ($n = 11$) and $\Sigma = \{a, b, c, d, r\}$ ($\sigma = 5$). The zero-order empirical entropy is $\mathcal{H}_0(S) \approx 2.04$ bits/symbol. Now, let's calculate the first-order ($k = 1$) empirical entropy using Equation (2). The contexts are the single characters. For context *a* ($n_a = 5$), the following symbols form S_a = "bcdb$" (assuming $ denotes an end-of-string marker), yielding $\mathcal{H}_0(S_a) \approx 1.922$ bits/symbol (assuming $ is a unique symbol contributing to the calculation). For context *b* ($n_b = 2$), the sequence is S_b = "rr", resulting in $\mathcal{H}_0(S_b) = 0$ bits/symbol. Similarly, for contexts *c* ($n_c = 1$), *d* ($n_d = 1$), and *r* ($n_r = 2$), the subsequent sequences are

---

2 The notation $\omega \in \Sigma^k$ signifies that ω is a k-gram.

S_c = "a", S_d = "a", and S_r = "aa", respectively, all leading to zero-order empirical entropies of 0 bits/symbol. Therefore, the first-order empirical entropy of S is:

$$\mathcal{H}_1(S) = \frac{n_a}{n}\mathcal{H}_0(S_a) + \frac{n_b}{n}\mathcal{H}_0(S_b) + \cdots + \frac{n_r}{n}\mathcal{H}_0(S_r)$$
$$= \frac{5}{11} \cdot (1.922) + \frac{2}{11} \cdot 0 + \cdots + \frac{2}{11} \cdot 0 \approx 0.874 \text{ bits/symbol}$$

This value is significantly lower than the zero-order empirical entropy $\mathcal{H}_0(S)$, reflecting the predictability introduced by considering the preceding character.

The quantity $n\mathcal{H}_k(S)$ serves as a lower bound for the minimum number of bits attainable by any encoding of S, under the condition that the encoding of each symbol may rely only on the k symbols preceding it in S. Consistently, any compressor achieving fewer than $n\mathcal{H}_k(S)$ bits would imply the ability to compress symbols originating from the related k-th order Markov source to a level below its Shannon entropy.

Remark 2.30. As k grows large (up to $k = n-1$, and often sooner), the k-th order empirical entropy $\mathcal{H}_k(S)$ tends towards zero, given that most long k-grams appear only once, making their subsequent symbol perfectly predictable within the sequence S. This renders the model ineffective as a lower bound for practical compressors when k is very large relative to n. Even before reaching $\mathcal{H}_k(S) = 0$, achieving compression close to $n\mathcal{H}_k(S)$ bits becomes practically challenging for high k values. This is due to the necessity of storing or implicitly representing the conditional probabilities (or equivalent coding information) for all σ^k possible contexts, which requires significant space overhead ($\approx \sigma^{k+1} \log n$ bits in simple models). In theory, it is commonly assumed that S can be compressed up to $n\mathcal{H}_k(S) + o(n)$ bits for any k such that $k + 1 \leqslant \alpha \log_\sigma n$ for some constant $0 < \alpha < 1$. Under this condition, the overhead for storing the model ($\sigma^{k+1} \log n \leqslant n^\alpha \log n$) becomes asymptotically negligible compared to the compressed data size ($o(n)$ bits) [41].

Definition 2.31 (Coarsely Optimal Compression Algorithm). *A compression algorithm is* coarsely optimal *if, for every fixed value of* $k \geqslant 0$, *there exists a function* $f_k(n)$ *such that* $\lim_{n\to\infty} f_k(n) = 0$, *and for all sequences* S *of length* n, *the compression size achieved by the algorithm is bounded by* $n(\mathcal{H}_k(S) + f_k(n))$ *bits.*

The *Lempel-Ziv* algorithm family, particularly LZ78, serves as a prominent example of coarsely optimal compression techniques, as demonstrated by Plotnik et al. [47]. These algorithms typically rely on dictionary-based compression. However, as highlighted by Kosaraju and Manzini

[32], the notion of coarse optimality does not inherently guarantee practical effectiveness across all scenarios. The additive term $n \cdot f_k(n)$ might still lead to poor performance on some sequences, especially if $f_k(n)$ converges slowly or if the sequence length n is not sufficiently large for the asymptotic behavior to dominate.

2.5.1 *Source Coding Theorem*

Having established the properties of different code types in Section 2.3 and the fundamental constraint imposed by Kraft's inequality (Theorem Theorem 2.22), we now arrive at a cornerstone result in information theory: the Source Coding Theorem. Attributed to Shannon [54], this theorem provides the definitive answer to the question of the ultimate limit of lossless data compression. It establishes that the entropy $\mathcal{H}(X)$ of the source (representing the underlying probability distribution, distinct from the empirical entropy $\mathcal{H}_k(S)$ of a specific string) is not just a theoretical measure of information, but the precise operational limit for the average length of any uniquely decodable code representing that source.

The theorem consists of two crucial parts: a lower bound on the achievable average length, and a statement about the existence of codes that approach this bound. The theorem will be stated for a K-ary code alphabet $\mathcal{D}$, using $\mathcal{H}_K(X) = \mathcal{H}(X)/\log K$ to denote the theoretical source entropy measured in K-ary units (assuming $\mathcal{H}(X)$ is calculated using base 2 logarithms unless otherwise specified).

Theorem 2.32 (Source Coding Theorem). *Let X be a random variable generating symbols from an alphabet Σ with probability mass function $P_X(x)$. Let $\mathcal{D}$ be a code alphabet of size $K \geqslant 2$.*

1. *(Lower Bound) The expected length $L(C)$ of any uniquely decodable code $C : \Sigma \to \mathcal{D}^*$ for X satisfies*

$$L(C) \geqslant \mathcal{H}_K(X) = \frac{\mathcal{H}(X)}{\log K} \tag{3}$$

2. *(Achievability) There exists a prefix code $C : \Sigma \to \mathcal{D}^*$ such that its expected length $L(C)$ satisfies*

$$L(C) < \mathcal{H}_K(X) + 1 \tag{4}$$

Proof. Part (i) - Lower Bound: Let C be any uniquely decodable code with codeword lengths $l(x)$ for $x \in \Sigma$. By Theorem 2.22, these lengths must satisfy Kraft's inequality: $S = \sum_{x \in \Sigma} K^{-l(x)} \leqslant 1$. Let an auxiliary probability distribution $Q(x)$ over Σ be defined as $Q(x) = K^{-l(x)}/S$. Note that $\sum_{x \in \Sigma} Q(x) = 1$, so Q is a valid probability distribution.

Consider the expected length $L(C)$:

$$
\begin{aligned}
L(C) &= \sum_{x \in \Sigma} P_X(x) l(x) \\
&= \sum_{x \in \Sigma} P_X(x) \log_K \left(K^{l(x)} \right) \\
&= \sum_{x \in \Sigma} P_X(x) \log_K \left(\frac{S}{Q(x)} \right) \quad \text{(since } K^{-l(x)} = SQ(x)) \\
&= \sum_{x \in \Sigma} P_X(x) \left(\log_K S - \log_K Q(x) \right) \\
&= (\log_K S) \sum_{x \in \Sigma} P_X(x) - \sum_{x \in \Sigma} P_X(x) \log_K Q(x) \\
&= \log_K S - \sum_{x \in \Sigma} P_X(x) \log_K Q(x)
\end{aligned}
$$

Relating the last term to the relative entropy (Kullback-Leibler divergence) $D(P_X\|Q)$ and the entropy $\mathcal{H}_K(X)$:

$$
\begin{aligned}
D(P_X\|Q) &= \sum_{x \in \Sigma} P_X(x) \log_K \frac{P_X(x)}{Q(x)} \\
&= \sum_{x \in \Sigma} P_X(x) \log_K P_X(x) - \sum_{x \in \Sigma} P_X(x) \log_K Q(x) \\
&= -\mathcal{H}_K(X) - \sum_{x \in \Sigma} P_X(x) \log_K Q(x)
\end{aligned}
$$

Thus, $-\sum P_X(x) \log_K Q(x) = D(P_X\|Q) + \mathcal{H}_K(X)$. Substituting this back into the expression for $L(C)$:

$$
L(C) = \log_K S + D(P_X\|Q) + \mathcal{H}_K(X)
$$

Since $S \leqslant 1$, $\log_K S \leqslant \log_K 1 = 0$. Also, the relative entropy is always non-negative, $D(P_X\|Q) \geqslant 0$. Therefore,

$$
L(C) \geqslant 0 + 0 + \mathcal{H}_K(X) = \mathcal{H}_K(X)
$$

This establishes the lower bound (3). This line of proof closely follows [10].

Part (ii) - Achievability: It must be shown that a prefix code exists whose expected length satisfies (4). Consider choosing codeword lengths $l(x)$ for each $x \in \Sigma$ as:

$$
l(x) = \lceil -\log_K P_X(x) \rceil
$$

where $\lceil \cdot \rceil$ denotes the ceiling function. These lengths are positive integers (assuming $P_X(x) \leqslant 1$ and $P_X(x) > 0$).

First, verify that these lengths satisfy Kraft's inequality. From the definition of the ceiling function:

$$
-\log_K P_X(x) \leqslant l(x) < -\log_K P_X(x) + 1
$$

Exponentiating the left inequality with base K:

$$K^{-\log_K P_X(x)} \geqslant K^{-l(x)} \implies P_X(x) \geqslant K^{-l(x)}$$

Summing over all $x \in \Sigma$:

$$\sum_{x \in \Sigma} K^{-l(x)} \leqslant \sum_{x \in \Sigma} P_X(x) = 1$$

Since the chosen lengths satisfy Kraft's inequality, the sufficiency part of Kraft's theorem guarantees that there exists a *prefix* code C with these exact lengths $l(x) = \lceil -\log_K P_X(x) \rceil$ [10, 24].

Now, calculate the expected length $L(C)$ for this prefix code:

$$
\begin{aligned}
L(C) &= \sum_{x \in \Sigma} P_X(x) l(x) \\
&= \sum_{x \in \Sigma} P_X(x) \lceil -\log_K P_X(x) \rceil \\
&< \sum_{x \in \Sigma} P_X(x) \left(-\log_K P_X(x) + 1 \right) \quad \text{(using } \lceil y \rceil < y + 1 \text{)} \\
&= \sum_{x \in \Sigma} -P_X(x) \log_K P_X(x) + \sum_{x \in \Sigma} P_X(x) \cdot 1 \\
&= \mathcal{H}_K(X) + 1
\end{aligned}
$$

Thus, it has been shown that there exists a prefix code C with $L(C) < \mathcal{H}_K(X) + 1$, proving the achievability part (4). $\qquad \square$

The Source Coding Theorem is a profound result. It states that the source entropy $\mathcal{H}_K(X)$ is the fundamental lower limit on the average number of K-ary symbols required per source symbol for reliable (lossless) representation using any uniquely decodable code. Furthermore, it guarantees that a prefix code (which is instantaneously decodable) can always be found whose average length is within 1 symbol of this theoretical minimum.

The gap of 1 in the achievability part arises from the constraint that codeword lengths must be integers, while $-\log_K P_X(x)$ is generally not. This gap can be made arbitrarily small (per source symbol) by encoding blocks of source symbols together.

If blocks $X^n = (X_1, \ldots, X_n)$ from an independent and identically distributed source are considered, the entropy per symbol is $\mathcal{H}(X^n)/n = \mathcal{H}(X)$. Applying the theorem to the block source Σ^n, a prefix code can be found with expected length L_n such that $\mathcal{H}_K(X^n) \leqslant L_n < \mathcal{H}_K(X^n) + 1$. Dividing by n, the average length per original source symbol, L_n/n, satisfies:

$$\mathcal{H}_K(X) \leqslant \frac{L_n}{n} < \frac{\mathcal{H}_K(X^n)}{n} + \frac{1}{n} = \mathcal{H}_K(X) + \frac{1}{n}$$

As the block length n increases, the average codeword length per source symbol approaches the entropy $\mathcal{H}_K(X)$. This demonstrates that the entropy limit is asymptotically achievable. Practical codes like Huffman coding (Section 2.7.1) provide methods to construct optimal prefix codes for a given distribution, while techniques like arithmetic coding (Section 2.7.2) effectively approximate the block coding concept to approach the entropy bound closely even for moderate sequence lengths.

2.6 INTEGER CODING

This section presents methods for representing a sequence of positive integers, $S = \{x_1, x_2, \ldots, x_n\}$, potentially containing repetitions, as a compact sequence of bits. The primary objective is to minimize the total number of bits used. A fundamental requirement for such representations is that they must be *self-delimiting* [58]. This property ensures that when the binary codes for individual integers are concatenated, a decoder can unambiguously determine the boundaries between consecutive codes, allowing for the correct reconstruction of the original sequence.

The practical importance of efficient integer coding significantly impacts both storage requirements and processing speed in numerous computing applications. A prominent example is found in *search engines*, which maintain vast indexes mapping terms to lists of document identifiers (IDs). These lists, often called *posting lists*, can enumerate billions of integer IDs [53]. Efficient storage is crucial. A widely adopted technique involves sorting the document IDs within each list and then encoding the differences (gaps) between consecutive IDs using variable-length integer codes. This approach assigns shorter binary codes to smaller, more frequent gaps [58]. The engineering considerations for constructing practical data structures based on these principles, particularly concerning random access capabilities, are explored further in Appendix A, which details a library developed as part of this work.

Another significant application arises in the final encoding stage of various *data compression algorithms*. Techniques such as LZ77, Move-to-Front (MTF), Run-Length Encoding (RLE), and the Burrows-Wheeler Transform (BWT) often produce intermediate outputs consisting of sequences of integers, where smaller values typically appear more frequently. An effective integer coding scheme is therefore necessary to convert these intermediate integer sequences into a final, compact bitstream. Similarly, compressing natural language text can involve mapping words or characters to integer token IDs; the resulting sequence of IDs, often reflecting token frequencies, is then compressed

using integer codes that assign shorter representations to smaller values [58].

This section explores various techniques for designing variable-length, prefix-free binary representations for integer sequences, focusing on methods that optimize space efficiency while ensuring correct decodability.

2.6.1   Unary Code

The unary code is one of the simplest integer encoding methods. It represents a positive integer $x \geqslant 1$ as a sequence of $x - 1$ zeros followed by a single one, denoted as $U(x)$. The decoding process is straightforward: the decoder identifies the end of the code upon encountering the first 1, and the value x corresponds to the total number of bits read.

This coding method requires x bits to represent x. While simple, this length is exponentially greater than the $\lceil \log_2 x \rceil$ bits needed by the standard binary representation $B(x)$. Consequently, unary coding is efficient only for very small values of x and becomes rapidly impractical as x increases. According to Shannon's source coding theorem (Theorem 2.32), the ideal code length for a symbol x with probability $P(x)$ is $-\log_2 P(x)$ bits. The unary code's length of x bits corresponds precisely to this ideal length only if the integers follow the specific geometric probability distribution $P(x) = 2^{-x}$ [58, 52].

Theorem 2.33. *The unary code $U(x)$ of a positive integer $x \geqslant 1$ requires x bits, and it is optimal for the geometric distribution $P(x) = 2^{-x}$.*

Despite its theoretical optimality for the $P(x) = 2^{-x}$ distribution, the unary code can face practical performance challenges. Its implementation often involves numerous bit shifts or bit-level operations during decoding, which can be relatively slow for large values of x.

0	0	0	0	1

Figure 4: Unary code $U(5) = \texttt{00001}$. It uses $x = 5$ bits, consisting of $x - 1 = 4$ zeros followed by a one.

2.6.2   Elias Codes

While unary code is simple, its inefficiency for larger integers motivated the development of *universal codes*. These codes, introduced by Elias [11], are designed such that the length of the codeword for

an integer x grows proportionally to the length of its minimal binary representation, typically $O(\log x)$, rather than $O(x)$ as in unary code. Compared to the standard binary code $B(x)$, which requires $\lceil \log_2 x \rceil$ bits but lacks the prefix property, the Elias γ and δ codes are only marginally longer while possessing the crucial property of being prefix-free.

GAMMA (γ) CODE   The γ code represents a positive integer $x \geqslant 1$ by encoding its magnitude (specifically, the length of its binary representation) along with its value. Let $l = \lfloor \log_2 x \rfloor + 1$ be the number of bits in the standard binary representation $B(x)$. The γ code, $\gamma(x)$, is formed by concatenating the unary code of this length, $U(l)$, with the $l - 1$ least significant bits of x (effectively, $B(x)$ without its leading 1 bit). The leading 1 is implicitly encoded by the terminating 1 of $U(l)$.

The decoding process involves reading the initial unary sequence $U(l)$ to determine the length l. Then, the subsequent $l - 1$ bits are read. Prepending a 1 to these $l - 1$ bits reconstructs the integer x. The total length of $\gamma(x)$ is:

$$|U(l)| + (l - 1) = l + (l - 1) = 2l - 1 = 2\big(\lfloor \log_2 x \rfloor + 1\big) - 1$$

bits. This code structure is known to be optimal for sources where integer probabilities decay approximately as $P(x) \propto 1/x^2$ [58].

Theorem 2.34. *The γ code of a positive integer $x \geqslant 1$ takes $2(\lfloor \log_2 x \rfloor + 1) - 1$ bits. It is optimal for distributions where $P(x) \propto 1/x^2$. Its length is within a factor of two (minus one bit) of the length of the standard binary code $B(x)$.*

0	0	1	1	0

Figure 5: Elias γ code for $x = 6$. Binary $B(6) = 110$, length $l = 3$. The code consists of $U(3) = 001$ followed by the $l - 1 = 2$ trailing bits (10). Result: $\gamma(6) = 00110$ (5 bits).

The primary inefficiency in the γ code stems from the unary encoding of the length l, which grows linearly with $\log x$. The δ code addresses this aspect.

DELTA (δ) CODE   The δ code improves upon γ by encoding the length parameter $l = \lfloor \log_2 x \rfloor + 1$ more efficiently, using the γ code itself. The δ code, $\delta(x)$, is constructed by first computing $\gamma(l)$ and then appending the same $l - 1$ least significant bits of x (i.e., $B(x)$ without its leading 1) used in $\gamma(x)$.

Decoding $\delta(x)$ requires first decoding the initial $\gamma(l)$ segment to retrieve the length l. Then, the next $l-1$ bits are read. Prepending a 1 to these bits reconstructs x. The total number of bits is

$$|\gamma(l)| + (l-1) = (2\lfloor \log_2 l \rfloor + 1) + (l-1) = 2\lfloor \log_2 l \rfloor + l.$$

Asymptotically, this length is approximately $\log_2 x + 2\log_2 \log_2 x + O(1)$ bits [58]. This is only marginally longer (by a factor of $1 + o(1)$) than the raw binary representation $B(x)$. The δ code achieves optimality for distributions where $P(x) \propto 1/(x(\log_2 x)^2)$.

Theorem 2.35. *The δ code of a positive integer $x \geqslant 1$ takes $2\lfloor \log_2(\lfloor \log_2 x \rfloor + 1) \rfloor + \lfloor \log_2 x \rfloor + 1$ bits, approximately $\log_2 x + 2\log_2 \log_2 x$. It is optimal for distributions $P(x) \propto 1/(x(\log_2 x)^2)$ and is within a factor $1 + o(1)$ of the length of $B(x)$.*

0	1	1	1	0

Figure 6: Elias δ code for $x = 6$. $B(6) = \text{110}$, length $l = 3$. First, encode $l = 3$ using γ: $\gamma(3) = \text{011}$. Then, append the $l-1 = 2$ trailing bits (\text{10}). Result: $\delta(6) = \text{01110}$ (5 bits).

Similar to the unary code, decoding Elias codes often involves bit-level operations, which might impact performance for very large integers compared to codes that operate on byte or word boundaries.

2.6.3   *Rice Code*

While Elias codes offer universality, they might be suboptimal if the distribution of integers is known or expected to cluster around values other than powers of two. Rice codes [49], which represent a specific instance of the more general Golomb codes [19], provide a parametric alternative better suited to certain distributions. These codes depend on a parameter $k > 0$, typically chosen based on the statistics of the integers being encoded.

Given an integer $x \geqslant 1$ and the parameter k, the Rice code $R_k(x)$ is computed by first determining the quotient q and the remainder r:

$$q = \lfloor (x-1)/2^k \rfloor \qquad r = (x-1) \pmod{2^k}$$

The codeword $R_k(x)$ is then constructed by concatenating the unary code of the quotient plus one, $U(q+1)$, followed by the remainder r represented using exactly k bits. This k-bit binary representation of r, denoted $B_k(r)$, might require padding with leading zeros if $r < 2^{k-1}$ (assuming $k > 0$). This structure is particularly efficient when integers frequently yield small values for the quotient q, which occurs when x

is often slightly larger than a multiple of 2^k. An example illustrating this construction for $x = 13$ and $k = 3$ is shown in Figure 7.

The total number of bits required to represent x using $R_k(x)$ is given by $|U(q+1)| + k = (q+1) + k$. Rice codes are known to be optimal for geometric distributions, where the probability of integer x is given by $P(x) = p(1-p)^{x-1}$ for some parameter p. Optimality is achieved when the parameter k is chosen such that 2^k closely approximates the mean or median of the distribution [58]. More precisely, the optimal k satisfies the condition

$$2^k \approx -\frac{\log 2}{\log(1-p)}$$

The fixed length (k bits) of the remainder part $B_k(r)$ can facilitate faster decoding procedures in certain hardware or software implementations compared to the variable-length components found in Elias codes.

0	1	1	0	0

Figure 7: Rice code for $x = 13$ with parameter $k = 3$. Calculate $q = \lfloor (13 - 1)/2^3 \rfloor = 1$ and $r = (13-1) \pmod 8 = 4$. The code is $U(q+1) = U(2) = $ `01` followed by $r = 4$ in $k = 3$ bits, $B_3(4) = $ `100`. Result: $R_3(13) = $ `01100` (5 bits).

2.6.4 *Elias-Fano Representation*

The Elias-Fano representation, based on the work developed independently by Elias [11] and Fano [12], provides an elegant method for compressing monotonically increasing sequences of integers. Its modern utility stems from its ability to achieve near-optimal space usage, often only slightly exceeding the information-theoretic minimum, while critically enabling efficient query operations directly on the compressed data. The capability for efficient queries relies on advancements in succinct data structures, particularly for rank and select operations [51]. This combination has proven highly effective in applications such as inverted index compression for search engines [57, 44].

REPRESENTATION STRUCTURE   Consider a strictly increasing sequence of n non-negative integers $S = \{s_0, s_1, \ldots, s_{n-1}\}$, where $0 \leqslant s_0 < s_1 < \ldots < s_{n-1} < u$. The integers belong to a universe of size u. It is assumed $u > n$. Each integer s_i requires $b = \lceil \log_2 u \rceil$ bits in its standard binary form.

The core idea of Elias-Fano is to partition these b bits into two segments based on a parameter l. The parameter l is chosen as $l =$

$\lfloor \log_2(u/n) \rfloor$ (setting $l = 0$ if $u \leqslant n$), a choice known to minimize the total space required [11]. This splits each s_i into: the *lower bits*, $L(s_i)$, comprising the l least significant bits; and the *upper bits*, $H(s_i)$, comprising the remaining $h = b - l$ most significant bits.

The representation consists of two primary components. First, a *Lower Bits Array*, denoted L, is created by concatenating the l-bit values $L(s_0)L(s_1)\ldots L(s_{n-1})$. This array occupies exactly $n \cdot l$ bits.

Second, an *Upper Bits Bitvector*, denoted H, encodes the distribution of the upper bit values. For each possible h-bit value j (ranging from 0 to $2^h - 1$), let c_j be the count of elements s_i in S such that $H(s_i) = j$. The bitvector H is formed by concatenating the sequences $1^{c_j}0$ for $j = 0, 1, \ldots, 2^h - 1$. In essence, it uses a unary code (1^{c_j}) to indicate how many elements share the upper bits value j, followed by a zero delimiter. This structure yields a bitvector H of length exactly $n + 2^h$ bits. It contains n ones (one for each element s_i) and 2^h zeros (one delimiter per possible upper bits value). Note that $2^h \approx n$, so the length of H is typically around $2n$.

Theorem 2.36 (Elias-Fano Space Complexity [57, 51]). *The Elias-Fano encoding of a strictly increasing sequence S of n integers in the range $[0, u)$ requires*

$$n\lfloor \log_2(u/n) \rfloor + n + 2^h$$

bits, where

$$h = \lceil \log_2 u \rceil - \lfloor \log_2(u/n) \rfloor$$

This space is upper bounded by $n\log_2(u/n) + 2n$ bits, which is provably less than 2 bits per integer above the information-theoretic lower bound. The representation can be constructed in $O(n)$ time.

An example of this encoding is provided in Figure 8 for the sequence $S = \{1, 4, 7, 18, 24, 26, 30, 31\}$. Here $n = 8$, $u = 32$, leading to $l = 2$ lower bits and $h = 3$ upper bits. The array L concatenates the 2-bit lower parts ($L(1) = \texttt{01}, L(4) = \texttt{00}, \ldots$). The bitvector H encodes the counts of each upper bit value (H = 0 appears once, H = 1 twice, H = 2 zero times, etc.) using unary codes (1^{c_j}) separated by zeros.

QUERY OPERATIONS   The practical power of the Elias-Fano representation arises when the upper bits bitvector H is augmented with auxiliary data structures supporting constant-time *rank* (rank_0, rank_1) and *select* (select_0, select_1) queries, as detailed in Section 3.1. These structures typically add a $o(n)$ bits overhead. With this machinery, key operations can be performed efficiently [51, 57].

i	s_i	$H(s_i)$	$L(s_i)$
0	1	0 (000)	1 (01)
1	4	1 (001)	0 (00)
2	7	1 (001)	3 (11)
3	18	4 (100)	2 (10)
4	24	6 (110)	0 (00)
5	26	6 (110)	2 (10)
6	30	7 (111)	2 (10)
7	31	7 (111)	3 (11)

$$L = \texttt{0100111000101011} \ (n \cdot l = 8 \times 2 = 16 \text{ bits})$$
$$H = \texttt{1011000100110110} \ (n + 2^h = 8 + 2^3 = 16 \text{ bits})$$

Figure 8: Elias-Fano encoding example for the sequence $S = \{1, 4, 7, 18, 24, 26, 30, 31\}$ with parameters $n = 8$, $u = 32$, $l = 2$, $h = 3$. The table shows the decomposition of each s_i into its upper $H(s_i)$ and lower $L(s_i)$ bits. Below the table are the resulting concatenated lower bits array L and the upper bits bitvector H.

Access(i) retrieves the i-th element s_i (with $0 \leqslant i < n$). First, the lower l bits, $L(s_i)$, are read directly from array L starting at bit position $i \cdot l$. Second, the position p corresponding to the $(i + 1)$-th 1 in H is found using $p = \text{select}_1(H, i + 1)$. Third, the value of the upper h bits, $H(s_i)$, is determined by counting the number of zeros preceding position p; this count is given by $H(s_i) = p - (i + 1)$ or equivalently $H(s_i) = \text{rank}_0(H, p)$. Finally, the integer is reconstructed by combining the parts: $s_i = (H(s_i) \ll l) \vee L(s_i)$. Since each step operates in constant time, *Access(i)* has an overall $O(1)$ time complexity.

Successor(x) (or *NextGEQ(x)*) finds the smallest element $s_i \in S$ such that $s_i \geqslant x$, given $x \in [0, u)$. First, the query value x is decomposed into its upper bits $H(x)$ and lower bits $L(x)$. Using select_0 queries on H, the range of indices $[p_1, p_2)$ in S corresponding to elements whose upper bits are exactly $H(x)$ is identified. Specifically, p_1 (the index of the first element with upper bits $H(x)$) is derived from the position of the $H(x)$-th zero, and p_2 (the index of the first element with upper bits $H(x) + 1$) is derived from the position of the $(H(x) + 1)$-th zero. A search is then conducted within the segment $L[p_1 \cdot l \ldots p_2 \cdot l - 1]$ of the lower bits array to find the smallest index $k \in [p_1, p_2)$ for which $L(s_k) \geqslant L(x)$. If such a k is found, the successor is $s_k = (H(x) \ll l) \vee L(s_k)$. If no such k exists in the range, the successor must be the first element with upper bits greater than $H(x)$, which is s_{p_2} (assuming $p_2 < n$), retrievable via *Access(p_2)*. The dominant cost is the search within the lower bits, potentially involving $O(u/n)$ candidates. Using binary search, this takes $O(\log(u/n))$ time. The select operations contribute $O(1)$ time, leading to a total complexity of $O(1 + \log(u/n))$ for *Successor(x)* *Predecessor(x)* finds the largest element $s_i \in S$ such that $s_i \leqslant x$. It uses a symmetric ap-

proach. The same index range $[p_1, p_2)$ based on $H(x)$ is located. A search is performed on the corresponding lower bits in L to find the largest index $k \in [p_1, p_2)$ such that $L(s_k) \leqslant L(x)$. If found, the predecessor is $s_k = (H(x) \ll l) \vee L(s_k)$. If no element within the range $[p_1, p_2)$ satisfies $s_k \leqslant x$, the predecessor must be the last element with upper bits strictly less than $H(x)$, namely s_{p_1-1} (assuming $p_1 > 0$), which is retrieved using *Access(p$_1$ − 1)*. The time complexity is also $O(1 + \log(u/n))$.

2.7 STATISTICAL CODING

This section explores a technique called *statistical coding*: a method for compressing a sequence of symbols (*texts*) drawn from a finite alphabet Σ. The idea is to divide the process in two key stages: modeling and coding. During the modeling phase, statistical characteristics of the input sequence are analyzed to construct a model, typically estimating the probability $P(\sigma)$ for each symbol $\sigma \in \Sigma$. In the coding phase, this model is utilized to generate codewords for the symbols, which are then employed to compress the input sequence. Two popular statistical coding methods will be focused upon: Huffman coding and Arithmetic coding.

2.7.1 *Huffman Coding*

Compared to the methods seen in Section 2.6, Huffman Codes, introduced by David A. Huffman in his landmark 1952 paper [27], offer broader applicability. They construct optimal prefix-free codes for a given set of symbol probabilities, without requiring specific assumptions about the underlying distribution itself (beyond non-zero probabilities). This versatility makes them suitable for diverse data types, including text where symbol frequencies often lack a simple mathematical pattern.

For instance, in English text, the letter *e* is far more frequent than *z*, and simple integer codes based on alphabetical order would be highly inefficient. Huffman coding directly addresses this by assigning shorter codewords to more frequent symbols.

CONSTRUCTION OF HUFFMAN CODES   The construction algorithm is greedy and builds a binary tree bottom-up. Each symbol $\sigma \in \Sigma$ initially forms a leaf node, typically weighted by its probability $P(\sigma)$ or its frequency count n_σ. The algorithm repeatedly selects the two

nodes (initially leaves, later internal nodes representing merged sub-trees) with the smallest current weights, merges them into a new internal node whose weight is the sum of the two merged weights, and places the two selected nodes as its children. This process continues until only one node, the root, remains.

The prefix-free code for each symbol σ is then determined by the path from the root to the leaf corresponding to σ. Conventionally, a 0 is assigned to traversing a left branch and a 1 to a right branch (or vice versa). The concatenation of these bits along the path forms the Huffman code for the symbol. More formal descriptions and variations can be found in [13, 52, 24, 10].
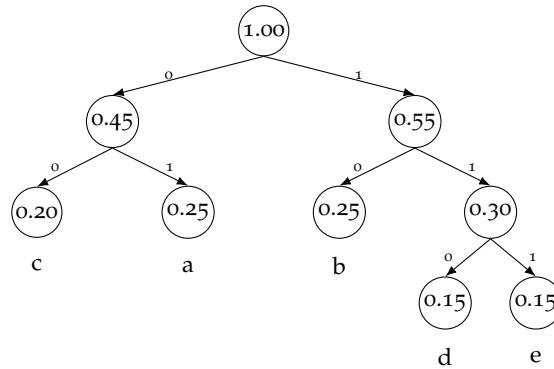
Figure 9: Huffman tree for the example probabilities ($P(a) = 0.25, P(b) = 0.25, P(c) = 0.2, P(d) = 0.15, P(e) = 0.15$). The resulting codes (0 for left, 1 for right) are: $C(a) = 01$, $C(b) = 10$, $C(c) = 00$, $C(d) = 110$, $C(e) = 111$.

Example 2.37. [Huffman Coding Construction] Let $\Sigma = \{a, b, c, d, e\}$ with probabilities $P(a) = 0.25$, $P(b) = 0.25$, $P(c) = 0.2$, $P(d) = 0.15$, $P(e) = 0.15$.

1. Initial nodes: (a: 0.25), (b: 0.25), (c: 0.2), (d: 0.15), (e: 0.15).

2. Merge smallest: d and e. Create node (de: 0.30). Current nodes: (a: 0.25), (b: 0.25), (c: 0.2), (de: 0.30).

3. Merge smallest: c and a. Create node (ca: 0.45). Current nodes: (b: 0.25), (de: 0.30), (ca: 0.45). (Note: Choosing c and a over c and b is arbitrary here; another valid tree exists).

4. Merge smallest: b and de. Create node (bde: 0.55). Current nodes: (ca: 0.45), (bde: 0.55).

5. Merge last two: ca and bde. Create root (root: 1.00).

The resulting tree and codes (assigning 0 to left, 1 to right) are shown in Figure 9.

Let $L_C = \sum_{\sigma \in \Sigma} P(\sigma) \cdot l(\sigma)$ be the average codeword length for a prefix-free code C, where $l(\sigma)$ is the length of the codeword assigned

to symbol σ. The Huffman coding algorithm produces a code C_H that is optimal among all possible prefix-free codes for the given probability distribution.

Theorem 2.38 (Optimality of Huffman Codes)**.** *Let C_H be a Huffman code generated for a given probability distribution P over alphabet Σ. For any other prefix-free code C' for the same distribution, the average codeword length satisfies $L_{C_H} \leqslant L_{C'}$.*

This optimality signifies that no other uniquely decodable code assigning fixed codewords to symbols can achieve a shorter average length. The proof typically relies on induction or an exchange argument, demonstrating that any deviation from the greedy merging strategy cannot improve the average length [13, 52, 24, 10].

The length of individual Huffman codewords can vary. In the worst case, the longest codeword might approach $|\Sigma| - 1$ bits (in a highly skewed distribution). However, a tighter bound related to the minimum probability p_{min} exists: the maximum length is $O(\log(1/p_{min}))$ [41]. If probabilities derive from empirical frequencies in a text of length n, then $p_{min} \geqslant 1/n$, bounding the maximum codeword length by $O(\log n)$. The encoding process itself, once the tree (or equivalent structure) is built, is typically linear in the length of the input sequence S, i.e., $O(|S|)$.

Decoding uses the Huffman Tree (or an equivalent lookup structure). Bits are read sequentially from the compressed stream, traversing the tree from the root according to the bit values (e.g., 0 for left, 1 for right) until a leaf node is reached. The symbol associated with that leaf is output, and the process restarts from the root for the next symbol. The total decoding time is proportional to the total number of bits in the compressed sequence. Since individual codes have length $O(\log n)$ in the empirical case, decoding a single symbol takes at most $O(\log n)$ bit reads and tree traversals.

While optimal among prefix codes, Huffman coding still assigns an integer number of bits to each symbol. This leads to a slight inefficiency compared to the theoretical entropy limit, as quantified by the following theorem.

Theorem 2.39. *Let $\mathcal{H} = \sum_{\sigma \in \Sigma} P(\sigma) \log_2(1/P(\sigma))$ be the entropy of a source emitting symbols from Σ according to distribution P. The average length L_H of the corresponding Huffman code is bounded by*

$$\mathcal{H} \leqslant L_H < \mathcal{H} + 1.$$

Proof. The lower bound $\mathcal{H} \leqslant L_H$ follows from Shannon's source coding theorem (Theorem 2.32), which states that $\mathcal{H}$ is the minimum possible average length for any uniquely decodable code.

For the upper bound, assign to each symbol σ the ideal codeword length $l'_\sigma = -\log_2 P(\sigma)$. Since codeword lengths must be integers, set $l_\sigma = \lceil -\log_2 P(\sigma) \rceil$. Then

$$l_\sigma < -\log_2 P(\sigma) + 1.$$

These l_σ satisfy Kraft's inequality:

$$\sum_{\sigma \in \Sigma} 2^{-l_\sigma} \leqslant \sum_{\sigma \in \Sigma} 2^{-(-\log_2 P(\sigma))} = \sum_{\sigma \in \Sigma} P(\sigma) = 1,$$

so a prefix code C' with these lengths exists. Its average length is

$$L_{C'} = \sum_{\sigma \in \Sigma} P(\sigma) l_\sigma < \sum_{\sigma \in \Sigma} P(\sigma)(-\log_2 P(\sigma) + 1) = \mathcal{H} + 1.$$

Since Huffman coding is optimal (Theorem 2.38), $L_H \leqslant L_{C'} < \mathcal{H} + 1$. Thus,

$$\mathcal{H} \leqslant L_H < \mathcal{H} + 1.$$

$\square$

This theorem highlights that the average Huffman code length is always within one bit of the source entropy. The gap $(L_H - \mathcal{H})$ represents the inefficiency due to the constraint of using integer bit lengths for each symbol's codeword. This gap is significant only when some symbol probabilities are very high (close to 1).

2.7.2 *Arithmetic Coding*

Introduced conceptually by Peter Elias in the 1960s and later developed into practical algorithms by Rissanen [50] and Pasco [45] in the 1970s, Arithmetic Coding offers a more powerful approach to statistical compression than Huffman coding. Its key advantage lies in its ability to approach the theoretical entropy limit more closely, often achieving better compression ratios, especially when dealing with skewed probability distributions or when encoding sequences rather than individual symbols.

Unlike Huffman coding, which assigns a distinct, fixed-length (integer number of bits) prefix-free code to each symbol, Arithmetic coding represents an entire sequence of symbols as a single fraction within the unit interval $[0, 1)$. The length of the binary representation of this fraction effectively corresponds to the information content (entropy) of the entire sequence, allowing for an average representation that can use a fractional number of bits per symbol. This overcomes the inherent inefficiency of Huffman coding, which is bounded by $\mathcal{H} \leqslant L_H < \mathcal{H} + 1$. Arithmetic coding aims to achieve a compressed size very close to $n\mathcal{H}$ bits for a sequence of length n.

2.7.2.1   *Encoding and Decoding*

Let $S = S[1]S[2]\ldots S[n]$ be the input sequence of symbols drawn from alphabet Σ, and let $P(\sigma)$ be the probability of symbol σ according to the chosen statistical model.

The core idea of the encoding process (Algorithm 1) is to progressively narrow down a sub-interval of $[0,1)$. Initially, the interval is $[l_0, h_0) = [0,1)$. For each symbol $S[i]$ in the sequence, the current interval $[l_{i-1}, h_{i-1})$ of size $s_{i-1} = h_{i-1} - l_{i-1}$ is partitioned into smaller sub-intervals, one for each symbol $\sigma \in \Sigma$. The size of the sub-interval for σ is proportional to its probability, $s_{i-1} \cdot P(\sigma)$. The algorithm then selects the sub-interval corresponding to the actual symbol $S[i]$ and makes it the new current interval $[l_i, h_i)$ for the next step. The cumulative probability function $C(\sigma) = \sum_{\sigma' < \sigma} P(\sigma')$ (summing probabilities of symbols lexicographically smaller than σ) is used to efficiently calculate the start (l_i) of the correct sub-interval. After processing all n symbols, the final interval is $[l_n, h_n) = [l_n, l_n + s_n)$, where $s_n = \prod_{i=1}^{n} P(S[i])$.

Algorithm 1 Arithmetic Coding

Require: Sequence $S = S[1..n]$, Probabilities $P(\sigma)$ for $\sigma \in \Sigma$
Ensure: A sub-interval $[l_n, l_n + s_n)$ uniquely identifying S.
  1: Compute cumulative probabilities $C(\sigma) = \sum_{\sigma' < \sigma} P(\sigma')$
  2: $l \leftarrow 0$
  3: $s \leftarrow 1$ $\triangleright$ Initial interval $[0, 1)$, size 1
  4: **for** $i = 1$ to n **do**
  5:     $l_{new} \leftarrow l + s \cdot C(S[i])$ $\triangleright$ Calculate start of sub-interval
  6:     $s_{new} \leftarrow s \cdot P(S[i])$ $\triangleright$ Calculate size of sub-interval
  7:     $l \leftarrow l_{new}$
  8:     $s \leftarrow s_{new}$
  9: **end for**
10: **return** $[l, l + s)$ $\triangleright$ Final interval represents the sequence

---

The final output of the encoder is not the interval itself, but rather a binary fraction x that falls within this final interval $[l_n, l_n + s_n)$ and can be represented with the fewest possible bits. Practical implementations use techniques to incrementally output bits as soon as they are determined (i.e., when the interval lies entirely within $[0, 0.5)$ or $[0.5, 1)$) and rescale the interval to maintain precision using fixed-point arithmetic [40, 13].

The decoding process (Algorithm 2) essentially reverses the encoding. The decoder needs the compressed bitstream (representing the fraction x), the same probability model $P(\sigma)$, and the original sequence length n. It starts with the interval $[0, 1)$. In each step i, it determines which symbol σ's sub-interval $[l + s \cdot C(\sigma), l + s \cdot C(\sigma) + s \cdot P(\sigma))$ contains the encoded fraction x. That symbol σ must be $S[i]$. The decoder outputs σ and updates its current interval to be this sub-interval, just

as the encoder did. This is repeated n times to reconstruct the original sequence S.

Algorithm 2 Arithmetic Decoding

Require: Encoded fraction x, Probabilities $P(\sigma)$, Sequence length n.
Ensure: Original sequence $S[1..n]$.
1: Compute cumulative probabilities $C(\sigma) = \sum_{\sigma' < \sigma} P(\sigma')$
2: $l \leftarrow 0$
3: $s \leftarrow 1$
4: $S \leftarrow$ empty sequence
5: **for** $i = 1$ to n **do**
6:      Find symbol σ s.t $l + s \cdot C(\sigma) \leqslant x < l + s \cdot (C(\sigma) + P(\sigma))$
7:      Append σ to S
8:      $l_{new} \leftarrow l + s \cdot C(\sigma)$
9:      $s_{new} \leftarrow s \cdot P(\sigma)$
10:      $l \leftarrow l_{new}$
11:      $s \leftarrow s_{new}$
12: **end for**
13: **return** S

2.7.2.2 *Efficiency of Arithmetic Coding*

The final interval size $s_n = \prod_{i=1}^{n} P(S[i])$ is crucial. If empirical probabilities $P(\sigma) = n_\sigma/n$ are used, where n_σ is the frequency of σ in S, then $s_n = \prod_{\sigma \in \Sigma} (n_\sigma/n)^{n_\sigma}$. As noted before, the number of bits required to uniquely specify a number within an interval of size s_n is approximately $-\log_2 s_n$.

Calculating $-\log_2 s_n$ with empirical probabilities gives:

$$-\log_2 \left(\prod_{\sigma \in \Sigma} \left(\frac{n_\sigma}{n} \right)^{n_\sigma} \right) = - \sum_{\sigma \in \Sigma} n_\sigma \log_2 \left(\frac{n_\sigma}{n} \right)$$

$$= n \sum_{\sigma \in \Sigma} \frac{n_\sigma}{n} \log_2 \left(\frac{n}{n_\sigma} \right)$$

$$= n \mathcal{H}$$

where $\mathcal{H}$ is the empirical (0-th order) entropy of the sequence S. This demonstrates that the *ideal* number of bits needed by arithmetic coding matches the entropy of the sequence exactly.

The connection between the final interval size s_n and the actual number of output bits deserves clarification. The encoder needs to transmit a binary representation of *some* number x that lies within the final interval $[l_n, l_n + s_n)$. To ensure the decoder can uniquely identify this interval (and thus the sequence), the chosen number x must be distinguishable from any number lying in adjacent potential intervals. This requires a certain precision. The minimum number of bits k needed to represent such an x as a dyadic fraction (i.e., a number of the form

$N/2^k$) must satisfy $2^{-k} \leqslant s_n$. This condition ensures that the precision 2^{-k} is fine enough to pinpoint a unique value within the target interval of size s_n. Taking logarithms, this implies $k \geqslant -\log_2 s_n$. To guarantee that such a fraction actually *exists* within the interval, and to handle the process of incrementally outputting bits, practical arithmetic coding requires slightly more bits than the theoretical minimum $-\log_2 s_n$. A careful analysis shows that at most 2 extra bits are needed beyond the ideal $n\mathcal{H}$.

Theorem 2.40. *The number of bits emitted by arithmetic coding for a sequence S of n symbols, using probabilities $P(\sigma)$ derived from the empirical frequencies within S, is at most $2 + n\mathcal{H}$, where $\mathcal{H}$ is the empirical entropy of the sequence S.*

Proof. Formal proofs can be found in standard texts on information theory and data compression [13, 52, 24, 10]. The core idea, as outlined above, relates the required number of bits k to the final interval size $s_n = 2^{-n\mathcal{H}}$ via $k \approx -\log_2 s_n = n\mathcal{H}$. The additive constant accounts for representing a specific point within the interval. $\square$

Remark 2.41. Practical arithmetic coders do not use floating-point numbers due to precision issues. They employ integer arithmetic, maintaining the interval bounds $[L, H]$ as large integers within a fixed range (e.g., 16 or 32 bits). As the conceptual interval shrinks, common leading bits of L and H are output, and the integer interval is rescaled (e.g., doubled) to occupy the full range again, effectively shifting the conceptual interval. Special handling ("underflow") is needed when the interval becomes very small but straddles the midpoint (e.g., 0.5), preventing immediate output of the next bit. These implementation details ensure correctness and efficiency with fixed-precision arithmetic [40].

RANK AND SELECT

Building upon the concepts of data compression and information theory from the preceding chapters, we now address the construction of *succinct data structures*. As motivated in Section 1.1, the objective is to represent discrete structures using space close to their information-theoretic minimum, while supporting efficient query operations directly on their compressed representation.

This chapter focuses on the fundamental rank and select operations. Given a sequence, rank counts occurrences of specified elements up to a given position, whereas select finds the position of the i-th occurrence of a specified element. The efficient implementation of these queries is critical for the functionality of many succinct data structures. We will investigate methods to support rank and select efficiently, typically achieving constant query time, through the use of auxiliary structures whose space requirement is sublinear relative to the input size.

Our examination proceeds in three stages. First, we consider the foundational case of *bitvectors* (binary sequences). We will analyze techniques, including hierarchical decomposition methods, for constructing auxiliary structures that use $o(n)$ bits of space, where n is the bitvector length, enabling constant-time rank and select queries on the original bitvector. Second, we generalize these concepts to sequences defined over larger, finite alphabets. We will study *Wavelet Trees*, a structure that reduces rank and select operations on general strings to corresponding operations performed on underlying bitvectors. Finally, the chapter addresses the more recent case of *degenerate strings*, which are sequences where each position may represent a subset of characters from the alphabet. We will review approaches that extend rank and select capabilities to this setting, by adapting the principles established for standard strings and bitvectors.

3.1 BITVECTORS

We begin our study with the most fundamental sequence type, the *bitvector* $B[1..n]$, a sequence of n bits from $\{0, 1\}$. Our primary objective is to support two essential query operations on B efficiently: $rank_b(B, i)$, which counts the occurrences of bit b in the prefix $B[1..i]$, and $select_b(B, i)$, which finds the index of the i-th occurrence of bit

b in B. While these operations can be answered by scanning B in $O(n)$ time, we seek constant-time solutions, $O(1)$, by augmenting B with *succinct* auxiliary data structures. These structures should occupy $o(n)$ bits, leading to a total space usage of $n + o(n)$ bits when storing B explicitly. We now formally define these operations.

Definition 3.1 (Rank). *Given a bitvector* $B[1..n]$*, the rank of an index* i *($1 \leqslant i \leqslant n$) relative to a bit* $c \in \{0, 1\}$ *is the number of occurrences of* c *in the prefix* $B[1..i]$*. We denote it as* $\mathrm{rank}_c(i)$*. Specifically, for* $c = 1$:

$$\mathrm{rank}_1(i) = \sum_{j=1}^{i} B[j]$$

The rank for $c = 0$ *can be derived as* $\mathrm{rank}_0(i) = i - \mathrm{rank}_1(i)$.

Definition 3.2 (Select). *Given a bitvector* $B[1..n]$*, the select of the* i*-th occurrence of a bit* $c \in \{0, 1\}$ *is the index* j *such that* $B[j] = c$ *and* $\mathrm{rank}_c(j) = i$*. We denote it as* $\mathrm{select}_c(i)$*. If the* i*-th occurrence of* c *does not exist,* $\mathrm{select}_c(i)$ *is undefined (or returns a special value). Unlike rank,* $\mathrm{select}_0(i)$ *cannot generally be computed directly from* $\mathrm{select}_1(i)$ *in constant time.*
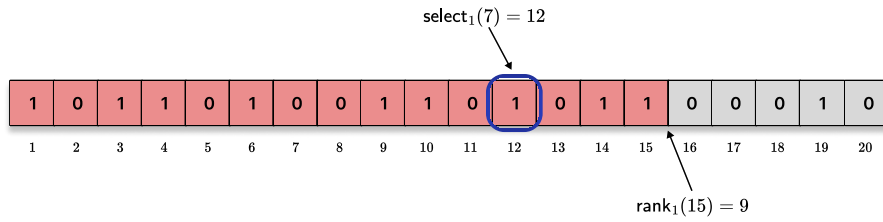
Figure 10: Example of a bitvector $B[1..20]$. The prefix $B[1..15]$ (shaded red) contains 9 ones, so $\mathrm{rank}_1(15) = 9$. The 7th 1 (circled blue) occurs at index 12, so $\mathrm{select}_1(7) = 12$.

Example 3.3. Let B be the bitvector of length $n = 20$ shown in Figure 10:

$$B = 10110100110101110010$$

- $\mathrm{rank}_1(15)$: We count the number of 1s in the prefix $B[1..15]$.

$$B[1..15] = \underbrace{101101001101011}_{15 \text{ bits}}$$

By scanning, there are 9 ones. Therefore, $\mathrm{rank}_1(15) = 9$.

- $\mathrm{select}_1(7)$: We find the index of the 7th occurrence of 1 in B. Scanning B: the 1st 1 is at index 1, 2nd at 3, 3rd at 4, 4th at 6, 5th at 9, 6th at 10, and the 7th 1 is at index 12. Therefore, $\mathrm{select}_1(7) = 12$.

Bitvectors supporting efficient rank and select operations are indeed foundational components for many compressed and succinct data structures. Attaining high performance for these operations is therefore a central concern. The following sections will describe methods to construct the $o(n)$-bit auxiliary structures that achieve constant query times. Furthermore, it is often the case that bitvectors encountered in applications exhibit skewed distributions of 0s and 1s (i.e., they are sparse). While the $n + o(n)$ structures operate on the explicit bitvector, separate lines of research have explored compressing the bitvector B itself by leveraging these statistical properties, thereby reducing the initial n-bit storage requirement.

Remark 3.4. Applying standard symbol-wise coding techniques from Chapter 2 (such as Huffman or Arithmetic coding) directly to a bitvector B typically yields a compressed size related to its zero-order entropy, approximately $n\mathcal{H}_0(B)$ bits. While potentially reducing space, especially for biased bitvectors, this form of compression generally obstructs efficient random access and the direct computation of rank and select queries without significant decompression overhead. The specialized structures detailed in this chapter are expressly designed to provide both space efficiency and fast query capabilities.

3.1.1 *Rank*

A fundamental approach to support rank queries in constant time using sublinear additional space was introduced by Jacobson [29]. The technique relies on a hierarchical decomposition of the bitvector $B[1..n]$ and precomputation of ranks at different granularities. The auxiliary structures occupy $o(n)$ bits in total.

The structure typically employs two levels of blocking on top of the original bitvector B. First, B is conceptually divided into *superblocks* of size Z. Second, each superblock is further divided into *blocks* of size z. Common parameter choices yielding $o(n)$ overhead are $Z = \Theta(\log^2 n)$ and $z = \Theta(\log n)$, for example $Z = \lfloor \log^2 n \rfloor$ and $z = \lfloor (1/2) \log n \rfloor$. We assume for simplicity that z divides Z and Z divides n.

Two auxiliary arrays store precomputed rank information. The first array, R_S, stores the absolute rank at the beginning of each superblock:

$$R_S[k] = \text{rank}_1(B, k \cdot Z) \qquad k = 0, \ldots, n/Z - 1$$

The second array, R_B, stores the rank within a superblock at the beginning of each block, relative to the start of the superblock. Specifically, for the l-th block overall, which belongs to superblock $k = \lfloor l \cdot z/Z \rfloor$

$$R_B[l] = \text{rank}_1(B, l \cdot z) - \text{rank}_1(B, k \cdot Z)$$

Finally, a *lookup table*, often denoted T, is used to determine the rank within a small block of size z. For every possible z-bit pattern p, and every position $j \in [1, z]$, $T[p][j]$ stores the value $rank_1(p, j)$, i.e., the number of set bits in the first j positions of the pattern p.

Figure 11 shows a visual representation of the hierarchical data structure.
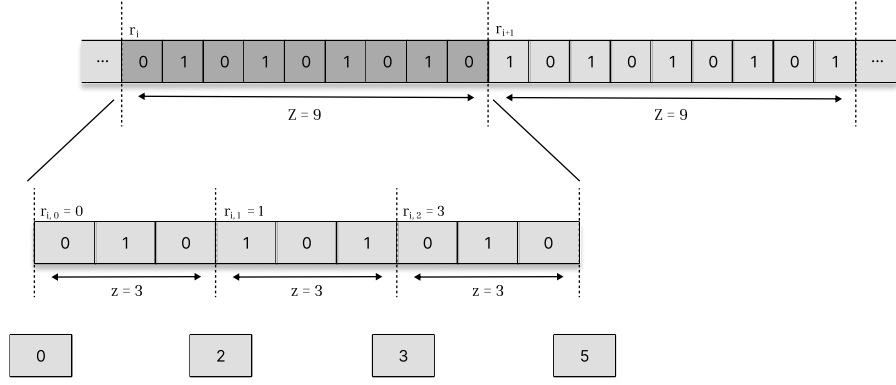
Figure 11: The hierarchical rank data structure. The first level is composed of superblocks of size Z (storing absolute ranks r_i), the second level of blocks of size z (storing relative ranks $r_{i,j}$), and the third level uses a lookup table (represented by the bottom row).

The lookup table T allows determining the number of set bits within any prefix of a z-bit block in constant time. Table 1 shows an example for $z = 3$. For a block p, the entry in column j (corresponding to $rank_1(p, j)$) gives the precomputed result.

block	$r_{i,0}$	$r_{i,1}$	$r_{i,2}$
000	0	0	0
001	0	0	1
010	0	1	1
011	0	1	2
100	1	1	1
101	1	1	2
110	1	2	2
111	1	2	3

Table 1: Example of a lookup table T for intra-block rank computation with $z = 3$. Each row corresponds to a possible z-bit pattern p. The cell for pattern p and index j stores $rank_1(p, j)$.

We can state the following theorem regarding the space and time complexity [28].

Theorem 3.5. *Given a bitvector* $B[1..n]$, *there exists an auxiliary data structure using* $o(n)$ *bits that allows computing* $rank_b(B, i)$ *for any* $i \in [1, n]$

and $b \in \{0, 1\}$ *in* $O(1)$ *time. The original bitvector* B *is accessed only in read mode. The total space required is* $n + o(n)$ *bits.*

Proof. We construct the auxiliary data structure using a standard two-level hierarchical decomposition of the bitvector B. We define a *superblock* size $Z = \lfloor \log^2 n \rfloor$ and a *block* size $z = \lfloor (1/2) \log n \rfloor$. For analytical simplicity, assume n is a multiple of Z, and Z is a multiple of z.

The structure comprises three main components designed to store precomputed rank information at different scales.

First, the *Superblock Rank Directory (*R_S*)* is an array storing the absolute rank at the start of each superblock. Specifically, for $k \in [0, n/Z - 1]$, $R_S[k] = \text{rank}_1(B, k \cdot Z)$. Since each rank value is at most n, storing these requires $\lceil \log n \rceil$ bits per entry. The total space for R_S is:

$$\text{Space}(R_S) = \frac{n}{Z} \lceil \log n \rceil = \frac{n}{\lfloor \log^2 n \rfloor} \lceil \log n \rceil$$

$$= O\left(\frac{n \log n}{\log^2 n} \right) = O(n/\log n) \text{ bits.}$$

Second, the *Block Rank Directory (*R_B*)* stores ranks relative to the start of the containing superblock. For each block index $l \in [0, n/z - 1]$, let $k = \lfloor l \cdot z/Z \rfloor$ be its superblock index. $R_B[l]$ stores the relative rank $\text{rank}_1(B, l \cdot z) - \text{rank}_1(B, k \cdot Z)$. This value is at most Z, requiring $\lceil \log Z \rceil$ bits per entry. The total space for R_B is:

$$\text{Space}(R_B) = \frac{n}{z} \lceil \log Z = \frac{n}{\lfloor (1/2) \log n \rfloor} \lceil \log(\lfloor \log^2 n \rfloor) \rceil$$

$$= O\left(\frac{n}{\log n} \log(\log^2 n) \right)$$

$$= O\left(\frac{n \log \log n}{\log n} \right) \text{ bits.}$$

We verify that the space complexity for both directories R_S and R_B is sublinear, i.e., $o(n)$. For R_S, we have $O(n/\log n)$. As $n \to \infty$, $(n/\log n)/n = 1/\log n \to 0$. For R_B, we have $O(n \log \log n/\log n)$. As $n \to \infty$, $(n \log \log n/\log n)/n = \log \log n/\log n \to 0$. Thus, both $\text{Space}(R_S)$ and $\text{Space}(R_B)$ are $o(n)$.

Third, the *Intra-Block Rank Mechanism (*T*)* is responsible for determining the rank within any z-bit block in constant time. A direct precomputation approach involves storing, for each of the 2^z possible z-bit patterns p and each position $j \in [1, z]$, the value $\text{rank}_1(p, j)$. The space requirement for such a naive table would be:

$$\text{Space}(\text{Naive } T) = O(2^z \cdot z \cdot \log z).$$

Substituting $z = \lfloor (1/2) \log n \rfloor$, this becomes

$$O(2^{(1/2)\log n} \log n \log \log n) = O(\sqrt{n} \log n \log \log n)$$

which is not sublinear ($o(n)$). The crucial insight, originally provided by Jacobson [28], is that this intra-block rank functionality can indeed be implemented using auxiliary structures occupying only $o(n)$ bits while still supporting $O(1)$ query time. This often involves techniques like further table compression or specialized indexing strategies not detailed here, but whose existence and performance guarantees we rely upon.

The total auxiliary space is the sum of the space complexities for R_S, R_B, and the efficient implementation of T. This sum is $O(n/\log n) + O(n \log \log n / \log n) + o(n)$, which simplifies to $o(n)$. Therefore, the total space including the original bitvector is $n + o(n)$ bits. $\square$

It is worth noting a crucial optimization for practical implementations, especially when the block size z is chosen such that it fits within a machine word (e.g., $z \leqslant 64$ on standard 64-bit architectures). In this scenario, the theoretical $o(n)$-bit lookup mechanism T for intra-block rank can often be replaced by direct computation using highly optimized hardware instructions.

Specifically, to compute the rank within the z-bit block $p = B[l \cdot z + 1..(l+1) \cdot z]$ up to position j, i.e., $\text{rank}_1(p,j)$, one can perform bitwise operations. First, isolate the j-bit prefix of p^1. Then, the number of set bits in this prefix can be computed efficiently using the processor's population count (popcount) instruction. Modern programming languages often expose this functionality directly; for instance, the Rust standard library provides the `count_ones()` method on primitive integer types. This operation is typically executed in constant time (often a single machine instruction) and can be significantly faster in practice than accessing a more complex precomputed table structure, especially for small values of z. We will discuss this in more detail in Section 3.1.5.

To answer a query $\text{rank}_1(B,i)$, we perform the following constant-time steps: Calculate the relevant indices: superblock $k = \lfloor (i-1)/Z \rfloor$, block $l = \lfloor (i-1)/z \rfloor$, and intra-block position $j = (i-1) \pmod z + 1$. Retrieve the precomputed ranks: $\text{rank}_S = R_S[k]$ from the superblock directory and $\text{rank}_B = R_B[l]$ from the block directory. Access the z-bit block $p = B[l \cdot z + 1..(l+1) \cdot z]$ from the original bitvector B. This access takes $O(1)$ time on a Word RAM where the word size $w \geqslant \log n \geqslant z$. Compute the intra-block rank $\text{rank}_T = T(p,j)$ using

---

1 For example, using a bitmask like $p \;\&\; ((1 \ll j) - 1)$

the $o(n)$-space constant-time mechanism T. The final rank is obtained by summing these components:

$$\text{rank}_1(B, i) = \text{rank}_S + \text{rank}_B + \text{rank}_T.$$

All steps involve only constant-time operations (arithmetic, array lookups, memory access of z bits, and the T lookup), hence the total query time is $O(1)$.

The query $\text{rank}_0(B, i)$ is then computed simply as $i - \text{rank}_1(B, i)$, also in constant time.

3.1.2 *Select*

The select operation serves as the inverse to rank. Formally, for a bitvector B and an integer i, $\text{select}_b(B, i)$ returns the index j such that $B[j] = b$ and $\text{rank}_b(B, j) = i$. This relationship can be expressed as:

$$\text{rank}_b(B, \text{select}_b(B, i)) = i$$

provided the i-th occurrence of b exists.

Supporting select queries efficiently requires a different auxiliary structure compared to the fixed-size blocking used for rank. An approach providing constant-time select within this space framework was developed by Clark [8]. It relies on a multi-level hierarchy guided by the number of set bits (specifically, 1s, as select_0 can be handled symmetrically or via select_1 on the complemented bitvector with additional rank structures). The core idea is to partition the bitvector B based on the cumulative count of 1s and use multiple levels of indexing structures to locate the i-th 1 quickly.

We begin by designing the first level of the select data structure. The bitvector B is conceptually divided into variable-length *chunks*, such that each chunk (except possibly the last) contains exactly K set bits. A typical choice is $K = \Theta(\log n \log \log n)$. We store an array P_1 containing the starting position (index in B) of each chunk. The number of chunks is $\lceil m/K \rceil$, where $m = \text{rank}_1(B, n)$ is the total number of 1s. The space for P_1 is

$$O(m/K \cdot \log n) = O(n/(\log n \log \log n) \cdot \log n) = O(n/\log \log n)$$

which is $o(n)$. Given a query $\text{select}_1(i)$, the relevant chunk index can be determined as $k = \lceil i/K \rceil$, and its starting position retrieved from P_1.

The second step addresses how to find the target 1 within its chunk. Let the length of a chunk be Z. We categorize chunks into two types based on their density. A chunk is considered *sparse* if its length Z is

large compared to K, specifically $Z > K^2$. Conversely, a chunk is *dense* if $Z \leqslant K^2$. For sparse chunks, we can afford to store the relative positions (offsets from the chunk's start) of the K set bits explicitly. The total space required across all sparse chunks for these offsets can be shown to be $o(n)$ [8]. If the target 1 falls within a sparse chunk, its position is found by calculating its relative rank $i' = (i-1) \pmod{K} + 1$ and retrieving the i'-th stored offset. For dense chunks ($Z \leqslant K^2$), explicitly storing offsets is too costly. Instead, we introduce a second level of structure within these dense chunks.

This second level structure subdivides each dense chunk into smaller variable-length *sub-chunks*, each containing exactly k set bits, where $k = \Theta((\log \log n)^2)$. We store an array P_2 for each dense chunk, holding the starting positions of these sub-chunks relative to the start of the dense chunk. The total space for all P_2 structures across all dense chunks is $O(m/k \cdot \log Z_{max}) = O(n/k \cdot \log K^2) = O(n/(\log \log n)^2 \cdot \log(\log n \log \log n)) = o(n)$.

Finally, we need to handle the sub-chunks. Let a sub-chunk have length z. Similar to the chunk level, we distinguish between *sparse sub-chunks* ($z > k^2$) and *dense sub-chunks* ($z \leqslant k^2$). For sparse sub-chunks, we again store the relative positions of the k set bits explicitly; the total space across all sparse sub-chunks remains $o(n)$ [8]. For dense sub-chunks ($z \leqslant k^2$), we require a mechanism to find the i''-th 1 (where i'' is the rank relative to the sub-chunk start) within the z bits in constant time. It is known [8] that constant-time select within a block of size $z = O(\text{polylog } n)$ can be achieved using an auxiliary structure of size $o(z)$ bits associated with the block (e.g., using precomputed tables or other techniques). Summing over all dense sub-chunks, the total space for these Level 3 mechanisms is $o(n)$.

The overall query process involves navigating this hierarchy. The algorithm can be summarized by the following pseudocode.

As for the rank data structure, we can state the following theorem:

Theorem 3.6. *Given a bitvector $B[1..n]$, there exists an auxiliary data structure using $o(n)$ bits that allows computing* select$_b(B, i)$ *for any valid i and $b \in \{0, 1\}$ in $O(1)$ time. The original bitvector B is accessed only in read mode. The total space required is $n + o(n)$ bits.*

Proof. The constant query time follows from the algorithm described, where each step (calculating indices, accessing pointer structures P_1, P_2, retrieving stored offsets for sparse cases, or using the constant-time Level 3 dense mechanism) takes $O(1)$ time. The total auxiliary space is the sum of the space required for P_1, the relative offsets for sparse chunks, the P_2 arrays, the relative offsets for sparse sub-chunks, the Level 3 dense sub-chunk mechanisms, and the structures needed

---

Algorithm 3 Select$_1$ Algorithm

1: **function** Select$_1$(B, i)
2:     $k \leftarrow \lceil i/K \rceil$
3:     $pos_1 \leftarrow$ GetChunkStartPos(k)
4:     ChunkInfo $\leftarrow$ GetChunkInfo(k)
5:     **if** ChunkInfo indicates *sparse* ($Z > K^2$) **then**
6:         $i' \leftarrow (i-1) \pmod{K} + 1$
7:         offset $\leftarrow$ GetSparseChunkOffset(k, i')
8:         **return** $pos_1 +$ offset
9:     **else**
10:         $i' \leftarrow (i-1) \pmod{K} + 1$
11:         $l \leftarrow \lceil i'/k \rceil$
12:         $pos_2 \leftarrow$ GetSubChunkStartPos(k, l)
13:         SubChunkInfo $\leftarrow$ GetSubChunkInfo(k, l)
14:         **if** SubChunkInfo indicates *sparse* ($z > k^2$) **then**
15:             $i'' \leftarrow (i'-1) \pmod{k} + 1$
16:             offset $\leftarrow$ GetSparseSubChunkOffset(k, l, i'')
17:             **return** $pos_1 + pos_2 +$ offset
18:         **else**
19:             $i'' \leftarrow (i'-1) \pmod{k} + 1$
20:             offset $\leftarrow$ DenseSubChunkSelect(k, l, i'')
21:             **return** $pos_1 + pos_2 +$ offset
22:         **end if**
23:     **end if**
24: **end function**

---

to distinguish between sparse and dense cases. As analyzed during the description, each component requires $o(n)$ bits with parameters $K = \Theta(\log n \log \log n)$ and $k = \Theta((\log \log n)^2)$, relying on established results [8]. Therefore, the total auxiliary space is $o(n)$ bits, yielding an overall space of $n + o(n)$ bits.   □

Remark 3.7. The threshold

$$k^2 = \Theta((\log \log n)^4)$$

for handling the smallest dense blocks can be extremely small for practical values of n. In implementations, if k is small enough (e.g., fits within a machine word or cache line), scanning the dense sub-chunk directly to find the i''-th occurrence of 1 might be faster than using the more complex theoretical $o(n)$ mechanism or precomputed tables. This again relates to broadword programming techniques, similar to the optimization mentioned for rank.

3.1.3 *Entropy-Compressed Rank/Select Structures*

While the preceding structures achieve optimal query time with sublinear additive space overhead, they still require the explicit storage

of the n-bit vector B. An alternative line of research focuses on compressing the bitvector itself, aiming for space usage closer to the information-theoretic minimum while preserving efficient query capabilities. The structure developed by Raman, Raman, and Rao [48] provides such a solution, offering constant-time rank and select operations within space related to the zero-order entropy of the bitvector.

The core strategy involves partitioning the bitvector $B[1..n]$ into blocks of a fixed size b, commonly chosen as $b = \lfloor \frac{1}{2} \log_2 n \rfloor$ to facilitate the construction of lookup tables within $o(n)$ space. Each block B_j (representing $B[(j-1)b+1..jb]$) is not stored directly but is replaced by a pair (c_j, o_j) that implicitly encodes its content. The first component, c_j, denotes the *class* of the block, defined as the population count (number of set bits) within B_j. The number of possible classes is $b+1$, requiring $\lceil \log_2(b+1) \rceil$ bits per class value. The second component, o_j, is the *offset*, which uniquely identifies the specific pattern of B_j among all possible b-bit blocks belonging to class c_j. There are precisely $\binom{b}{c_j}$ such blocks. The offset o_j is an integer in the range $[0, \binom{b}{c_j} - 1]$, assigned based on a fixed enumeration (e.g., lexicographical order) of the blocks within each class. Storing o_j requires $\lceil \log_2 \binom{b}{c_j} \rceil$ bits.

The compressed representation of B primarily consists of two sequences: a sequence $C = c_1 c_2 \dots c_{n/b}$ containing the classes of all blocks, and a sequence $O = o_1 o_2 \dots o_{n/b}$ containing the corresponding offsets. Note that the space required for each offset o_j varies depending on its class c_j. This variable-length nature contributes significantly to the overall compression, as blocks with very few or very many set bits (low c_j or high c_j) result in small values of $\binom{b}{c_j}$, thus requiring fewer bits for their offsets.

To support constant-time queries, we need to store some auxiliary information. The structure utilizes a hierarchical approach, grouping the small blocks into superblocks, typically of size $Z = \Theta(\log^2 n)$ bits (containing $s = Z/b = \Theta(\log^2 n / \log n)$ small blocks). Thus, we employ two main auxiliary structures:

1. A superblock directory stores, for each superblock boundary $k \cdot Z$, the absolute rank $\text{rank}_1(B, k \cdot Z)$. This resembles the R_S array from Section 3.1.1 and occupies $O(n/\log n)$ bits.

2. An index structure provides pointers to the beginning of the offset data o_j for the first block j of each superblock within the sequence O. Since the offsets have variable lengths, this typically involves storing prefix sums of the offset lengths, which can be done within $o(n)$ bits overhead while supporting constant-time access. Similar structures might be needed for the class sequence if it is further processed.

Furthermore, precomputed lookup tables are essential for constant-time intra-block operations. Let T_{rank} be a table such that $T_{rank}[c][o][k]$ returns the rank within the k-th position of the block uniquely identified by class c and offset o. Similarly, let T_{select} be a table such that $T_{select}[c][k']$ returns the offset o and the position p of the k'-th set bit within any block of class c. With $b = \lfloor \frac{1}{2} \log_2 n \rfloor$, the total size of these tables can be bounded by $o(n)$ bits.

To compute $rank_1(B, i)$, the algorithm first determines the superblock k and the block j containing index i. The absolute rank up to the start of superblock k is retrieved from the superblock directory. The ranks contributed by the full blocks between the start of superblock k and block j are calculated by summing their respective class values c_l (retrieved from sequence C). Finally, the class c_j and offset o_j for block j are retrieved, and the intra-block rank up to the relative position within B_j is found using the T_{rank} lookup table. All these steps take constant time.

The $select_1(B, i)$ query uses the superblock directory to identify the superblock k containing the i-th set bit via binary search or related techniques on the precomputed ranks (achievable in $O(1)$ time with appropriate auxiliary structures). Then, it determines the specific block j within that superblock by examining the class sequence C and potentially using the offset pointers. Finally, the T_{select} table is used with the class c_j and the relative rank within the block to find the intra-block position.

Combining these techniques, Raman, Raman, and Rao established the following result for their indexable dictionary structure, which is equivalent to a compressed bitvector supporting rank and select:

Theorem 3.8 ([48]). *Given a bitvector* $B[1..n]$ *containing* m *set bits, there exists a data structure using*

$$B(n, m) + o(n) + O(\log \log n)$$

bits, where $B(n, m) = \lceil \log_2 \binom{n}{m} \rceil$, *that supports* rank$_b(B, i)$ *and* select$_b(B, i)$ *queries for any valid* i *and* $b \in \{0, 1\}$ *in* $O(1)$ *time on the Word RAM model.*

The term $B(n, m)$ represents the information-theoretic minimum space required to store an arbitrary subset of size m from a universe of size n. For $m = p \cdot n$, Stirling's approximation shows that

$$B(n, m) \approx n(-p \log_2 p - (1-p) \log_2(1-p)) = n\mathcal{H}_0(B)$$

bits, where $\mathcal{H}_0(B)$ is the zero-order empirical entropy of the bitvector. Thus, this structure achieves space close to the entropy bound, providing significant compression for biased bitvectors while maintaining optimal query performance. The small additive $O(\log \log n)$ term originates from auxiliary structures related to universe reduction techniques employed in the full construction [48].

3.1.4 *Compressing Sparse Bitvectors*

The preceding sections presented methods for supporting rank and select queries, ranging from structures operating on the plain n-bit vector with $o(n)$ additive overhead (3.1.1, 3.1.2) to entropy-compressed representations aiming for space close to the information-theoretic minimum $B(n, m)$ (3.1.3). While structures like the one presented by Raman, Raman and Rao [48] provide general compression adapting to the bitvector's density, scenarios involving high sparsity, where the number of set bits $m = \text{rank}_1(B, n)$ is substantially smaller than the total length n ($m \ll n$), admit specialized compression techniques. These methods focus directly on the properties inherent to sparse sets, potentially offering different space-time trade-offs compared to general entropy-based approaches.

In such sparse settings, we can leverage compression techniques that exploit the low density of set bits. The Elias-Fano representation, previously introduced in Section 2.6.4, provides a highly effective method for this task. Recall that Elias-Fano encodes a monotonically increasing sequence of m integers up to a maximum value n. We can represent the bitvector B by encoding the sequence of indices $\{i \mid B[i] = 1\}$.

As detailed in [57] in the context of quasi-succinct indices for information retrieval, the Elias-Fano representation achieves a space complexity of approximately $m \log_2(n/m) + O(m)$ bits. This is remarkably close to the information-theoretic lower bound for representing a subset of size m from a universe of size n, often expressed as $n\mathcal{H}_0(B) + O(m)$ bits. The crucial advantage is that the space depends primarily on m, the number of set bits, rather than the full length n, leading to significant compression when m is small.

This compressed representation directly supports efficient operations. The $\text{select}_1(i)$ operation, can typically be implemented in constant time on average, often leveraging auxiliary pointers within the Elias-Fano structure as engineered for example in [57]. However, this space efficiency comes at the cost of potentially slower rank_1 and accessing $B[i]$ operations compared to the structures seen previously. These operations usually involve decoding parts of the Elias-Fano structure and may take $O(\log(n/m))$ time or depend on the specific implementation details [41].

3.1.5 *Practical Considerations*

While the asymptotic analysis guarantees $O(1)$ query time and $o(n)$ extra space for the rank and select structures presented before, achiev-

ing high performance in practice requires careful consideration of architectural factors and constant overheads hidden in the $o(n)$ term. Memory latency, cache efficiency, and instruction-level parallelism often dominate the actual running time on modern processors.

A particularly effective approach for optimizing rank and select implementations leverages *broadword programming* (also known as SWAR - SIMD within a Register). This technique treats machine registers as small parallel processors, performing operations on multiple data fields packed within a single word using standard arithmetic and logical instructions. Vigna [55] applied these techniques to rank and select queries, leading to highly efficient practical implementations.

The rank9 structure proposed by Vigna [55] exemplifies this approach. It employs a two-level hierarchy, similar in concept to the structure in Section 3.1.1, but critically relies on broadword algorithms for the final rank computation within a machine word (specifically, sideways addition or population count). Instead of large precomputed lookup tables for small blocks, rank9 uses carefully designed constants and bitwise operations (detailed in Algorithm 1 of [55]) to compute the rank within a 64-bit word quickly. This typically involves storing relative counts for sub-blocks (e.g., seven 9-bit counts within a 64-bit word) in the second level. The advantages of this approach include speed, resulting from the exploitation of fast register operations and the avoidance of large table lookups, often outperforming other methods in practice. It also offers space efficiency, requiring relatively low overhead (typically around 25% on top of the original bitvector B) mainly for the cumulative counts. Furthermore, broadword algorithms are generally branch-free, benefiting performance on modern pipelined processors by avoiding potential misprediction penalties.

Similarly, Vigna [55] developed broadword algorithms for selection within a word (Algorithm 2 in the paper). The companion select9 structure integrates these intra-word selection capabilities with a multi-level inventory scheme. The objective of select9 is to support high-performance selection queries, often achieving near constant-time execution, through hierarchical indexing combined with efficient broadword search for the final location. This capability involves an additional space cost, typically measured at approximately 37.5% relative to the rank9 structure.

Furthermore, a major bottleneck in rank/select operations is often memory access latency. To mitigate this, *interleaving* the auxiliary data structures is highly recommended. For instance, storing a first-level (superblock) rank count immediately followed by its corresponding second-level (sub-block) counts increases the probability that all necessary auxiliary information for a query resides within the same cache line. This simple layout optimization can dramatically reduce

cache misses compared to storing different levels of the hierarchy in separate arrays.

3.2 WAVELET TREES

Building upon the concepts established for bitvectors in Section 3.1, we now extend our focus to sequences over general alphabets using *Wavelet Trees*. Introduced by Grossi, Gupta, and Vitter [21], the wavelet tree is a highly versatile data structure. It functions as a self-index, capable of representing a sequence $S[1..n]$ drawn from an alphabet $\Sigma = \{1, \ldots, \sigma\}$ within space close to its compressed size, while supporting fundamental query operations directly on this representation and allowing reconstruction of the original sequence data. This characteristic makes wavelet trees a cornerstone in applications like compressed full-text indexing, for example within the FM-index [15], where they provide efficient support for the essential rank queries during the backward search phase [42].

While the core idea of hierarchical alphabet partitioning shares conceptual similarities with earlier structures, such as Chazelle's structure for geometric point grids [7] and Kärkkäinen's work on repetition-based indexing [30], the specific formulation and operational capabilities defined by Grossi et al. [21] established the wavelet tree as a broadly applicable tool for sequence processing [42]. Its flexibility derives from its capacity to represent data variously as sequences, permutations, or point grids [42, 23, 14].

We consider a sequence $S[1..n] = s_1 s_2 \ldots s_n$, with $s_i \in \Sigma = \{1, \ldots, \sigma\}$. The primary operations of interest are generalizations of those defined for bitvectors:

- Access(S, i): $S \times [1..n] \to \Sigma$. Returns the symbol $S[i]$.

- $\mathrm{rank}_c(S, i)$: $S \times \Sigma \times [0..n] \to [0..n]$. Returns the number of occurrences of symbol c in the prefix $S[1..i]$, i.e., $|\{j \mid 1 \leqslant j \leqslant i, S[j] = c\}|$. We define $\mathrm{rank}_c(S, 0) = 0$.

- $\mathrm{select}_c(S, j)$: $S \times \Sigma \times [1..n] \to [1..n] \cup \{\bot\}$. Returns the position (index) k such that $S[k] = c$ and $\mathrm{rank}_c(S, k) = j$. If the j-th occurrence does not exist, it returns a special symbol $\bot$.

A naive approach using σ distinct bitvectors B_c (where $B_c[i] = 1$ if and only if $S[i] = c$) reduces these operations to bitvector rank/select ($\mathrm{rank}_c(S, i) = \mathrm{rank}_1(B_c, i)$ and $\mathrm{select}_c(S, j) = \mathrm{select}_1(B_c, j)$). However, augmenting these bitvectors for $O(1)$ time queries using the methods of Section 3.1 requires $n\sigma + o(n\sigma)$ total bits, which is inefficient compared to the $n\lceil \log \sigma \rceil$ bits of the plain representation, especially for

large σ [41]. Wavelet trees offer a significantly more space-conscious solution.

3.2.1   *Structure and construction*

The standard wavelet tree for a sequence $S[1..n]$ over $\Sigma = \{1, \ldots, \sigma\}$ is a balanced binary tree structure. Each node v corresponds to an alphabet sub-range $[a_v, b_v] \subseteq \Sigma$ and implicitly represents the subsequence S_v containing all characters s_i from the original sequence S such that $s_i \in [a_v, b_v]$, maintaining their relative order.

The construction proceeds recursively:

- The root node v_{root} corresponds to the full alphabet range $[1, \sigma]$ and the entire sequence $S_{v_{root}} = S$.

- For an internal node v representing the range $[a_v, b_v]$ with $a_v < b_v$:

  1. Define a midpoint $m_v = \lfloor (a_v + b_v)/2 \rfloor$.

  2. Store a bitmap $B_v[1..|S_v|]$ where $B_v[k] = 0$ if the k-th character of S_v is in $[a_v, m_v]$, and $B_v[k] = 1$ if it is in $[m_v + 1, b_v]$.

  3. Recursively construct the left child v_l for the alphabet range $[a_v, m_v]$ and the subsequence S_{v_l} formed by characters $s \in S_v$ with $s \leqslant m_v$.

  4. Recursively construct the right child v_r for the alphabet range $[m_v + 1, b_v]$ and the subsequence S_{v_r} formed by characters $s \in S_v$ with $s > m_v$.

- A leaf node v represents a single symbol alphabet range $[a_v, a_v]$ (i.e., $a_v = b_v$) and stores no bitmap.

The height of this tree is $h = \lceil \log \sigma \rceil$. The construction process, detailed in Algorithm 4, takes $O(n \log \sigma)$ time, as each symbol from S is processed at each level of the tree.

The space usage of this pointer-based wavelet tree consists of the bitmaps and the pointers. The bitmaps across all nodes at any given level collectively store exactly n bits. With $h = \lceil \log \sigma \rceil$ levels, the total space for bitmaps is $n\lceil \log \sigma \rceil$. The tree has σ leaves and $\sigma - 1$ internal nodes. Storing child and parent pointers (e.g., $3(\sigma - 1)$ pointers, each $\approx \log \sigma$ bits) adds an overhead of $O(\sigma \log \sigma)$ bits (or $O(\sigma \log n)$ if indices into an array are used), which can dominate for large σ. Each bitmap B_v must also be augmented with $o(|S_v|)$ bits to support constant-time rank/select (Section 3.1), contributing an additional $o(n \log \sigma)$ bits overall.

Algorithm 4 Building a wavelet tree

---

function BUILD_WT(S, n)
   $T \leftarrow \text{build}(S, n, 1, \sigma)$
   return T
end function
function BUILD(S, n, a, b)   ▷ Takes a string $S[1, n]$ over $[a, b]$
   if $a = b$ **then**
      Free S
      return null
   end if
   $v \leftarrow$ new node
   $m \leftarrow \lfloor (a + b)/2 \rfloor$
   $z \leftarrow 0$ ▷ number of elements in S that are $\leqslant m$
   for $i \leftarrow 1$ to n **do**
      if $S[i] \leqslant m$ **then**
         $z \leftarrow z + 1$
      end if
   end for
   Allocate strings $S_{\text{left}}[1, z]$ and $S_{\text{right}}[1, n - z]$
   Allocate bitmap $v.B[1, n]$
   $z \leftarrow 0$
   for $i \leftarrow 1$ to n **do**
      if $S[i] \leqslant m$ **then**
         bitclear($v.B, i$)   ▷ set i-th bit of $v.B$ to 0
         $z \leftarrow z + 1$
         $S_{\text{left}}[z] \leftarrow S[i]$
      else
         bitset($v.B, i$)   ▷ set i-th bit of $v.B$ to 1
         $S_{\text{right}}[i - z] \leftarrow S[i]$
      end if
   end for
   Free S
   $v.\text{left} \leftarrow \text{build}(S_{\text{left}}, z, a, m)$
   $v.\text{right} \leftarrow \text{build}(S_{\text{right}}, n - z, m + 1, b)$
   Pre-process $v.B$ for rank and select queries
   return v
end function

Tracking symbols

The wavelet tree supports the primary sequence operations by translating them into traversals involving bitvector rank/select queries.

3.2.1.1   *Access*

Computing access(S, i) involves a top-down traversal from the root v_{root}. At each internal node v (representing range $[a_v, b_v]$ with midpoint m_v), we examine the bit $B_v[i_v]$, where i_v is the current index within the node's implicit sequence S_v. If $B_v[i_v] = 0$, we pro-

```
                    wookies_wield_wicked_weapons_with_wisdom$
                    1111001010010010010001001111010101001010111

              0                                      1

      ie_ied_iced_ea_ih_id$                   wookswlwkwponswtwsom
      110111010110100110110                   11101101011101111110

         0        1                              0          1

    __c_a__$        ieiediedeihid        klknm          wooswwwposwtwso
    00101000        1010010001110        00011          100111100111110

      0    1          0      1           0    1          0          1

  _____$   ca    eededed  iiiihi     klk    nm      oopoo      swwwswtws
  000001    10    1101010  111101     010    10      00100      1011101110

  0  1  0  1      0   1    0   1      0  1  0  1    0   1      0      1

  $   _  a  c     d   e    h   i      k  l  m  n    o   p      s    wwwwtw
                                                                   111101

                                                                   0    1

                                                                   t    w
```
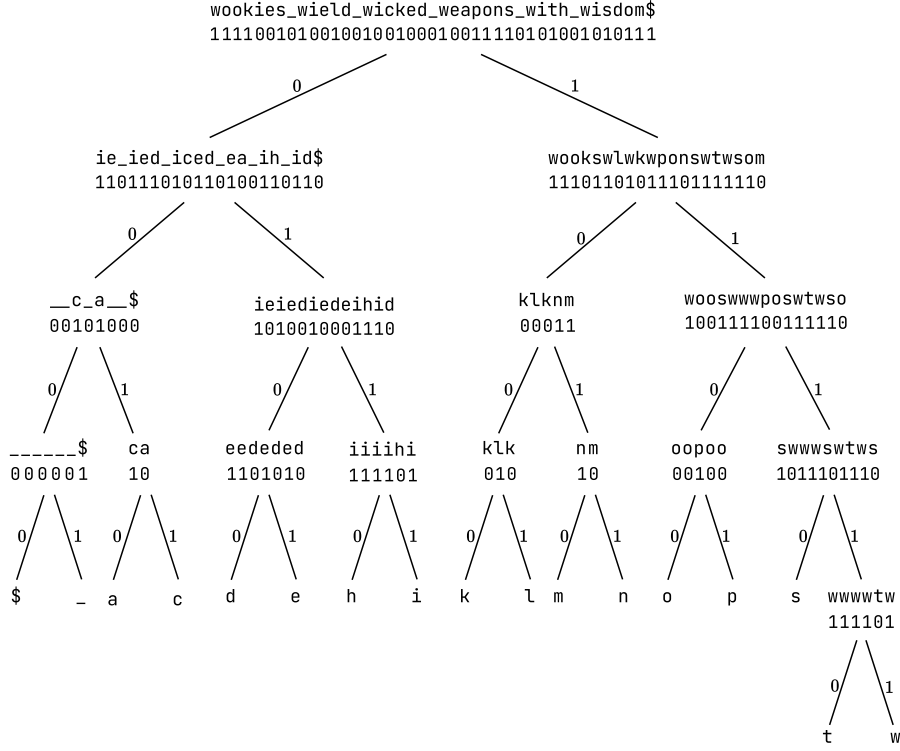
Figure 12: Wavelet tree for the sequence `wookies_wield_`...

ceed to the left child v_l (range $[a_v, m_v]$) and update the index to $i_{v_l} = \text{rank}_0(B_v, i_v)$. If $B_v[i_v] = 1$, we proceed to the right child v_r (range $[m_v + 1, b_v]$) and update the index to $i_{v_r} = \text{rank}_1(B_v, i_v)$. This repeats until a leaf node representing a single symbol $[a, a]$ is reached; this a is $S[i]$. The process performs $\lceil \log \sigma \rceil$ bitvector rank operations in $O(\log \sigma)$ time. Algorithm 5 details this.

Algorithm 5 Access queries on a wavelet tree

> **function** ACCESS(T, i)   ▷ T is the sequence S seen as a wavelet tree
> $v \leftarrow T_{root}$ ▷ start at the root node
> $[a, b] \leftarrow [1, \sigma]$
>   **while** $a \neq b$ **do**
>   **if** $access(v.B, i) = 0$ **then**   ▷ i-th bit of the bitmap of v
> $i \leftarrow \text{rank}_0(v.B, i)$
> $v \leftarrow v.\text{left}$ ▷ move to the left child of node v
> $b \leftarrow \lfloor (a + b)/2 \rfloor$
>   **else**
> $i \leftarrow \text{rank}_1(v.B, i)$
> $v \leftarrow v.\text{right}$ ▷ move to the right child of node v
> $a \leftarrow \lfloor (a + b)/2 \rfloor + 1$
>   **end if**
>   **end while**
>   **return** a
> **end function**

3.2.1.2 *Select*

Computing $select_c(S, j)$ involves an upward traversal from the leaf node u corresponding to symbol c. Let the index within the leaf level be $j_u = j$. To move to the parent v, we determine if u is the left (v_l) or right (v_r) child. If $u = v_l$, the corresponding index in the parent's bitmap B_v is $j_v = select_0(B_v, j_u)$. If $u = v_r$, the index is $j_v = select_1(B_v, j_u)$. We repeat this process, updating j at each level, until the root node is reached. The final index j_{root} is the position of the j-th c in S. This requires $\lceil \log \sigma \rceil$ bitvector select operations in $O(\log \sigma)$ time. Algorithm 6 shows the recursive structure.

Algorithm 6 `Select` queries on a wavelet tree

---

    function $\textsc{select}_c(S, j)$
        return $select(T._{root}, 1, \sigma, c, j)$
    end function
    function $\textsc{select}(v, a, b, c, j)$
        if $a = b$ **then**
            return j
        end if
        if $c \leqslant \lfloor (a + b)/2 \rfloor$ **then**
            $j \leftarrow select(v.left, a, \lfloor (a + b)/2 \rfloor, c, j)$ **return** $select_0(v.B, j)$
        else
            $j \leftarrow select(v.right, \lfloor (a + b)/2 \rfloor + 1, b, c, j)$
            return $select_1(v.B, j)$
        end if
    end function

3.2.1.3 *Rank*

Computing $rank_c(S, i)$ uses a top-down traversal similar to access. We start at the root v_{root} with index $i_{root} = i$. At each node v (range $[a_v, b_v]$, midpoint m_v), we check if the target symbol c belongs to the left sub-range ($c \leqslant m_v$) or the right sub-range ($c > m_v$). If $c \leqslant m_v$, we descend to the left child v_l and update the index to $i_{v_l} = rank_0(B_v, i_v)$. If $c > m_v$, we descend to the right child v_r and update the index to $i_{v_r} = rank_1(B_v, i_v)$. The traversal continues until the leaf node u corresponding to symbol c is reached. The final index i_u at this leaf is the value $rank_c(S, i)$. This requires $\lceil \log \sigma \rceil$ bitvector rank operations in $O(\log \sigma)$ time. Algorithm 7 formalizes this.

Example 3.9. Consider the computation of $rank_e(S, 13)$ shown in Figure 13. We start at the root with index $i = 13$. Here, *e* corresponds to bit 0, so we compute $rank_0(13) = 6$ and descend left with the new index $i = 6$. At this node, *e* corresponds to bit 1; evaluating $rank_1(6) = 5$, we proceed right with index $i = 5$. In the next node, *e* maps to bit 0; calculating $rank_0(5) = 3$, we descend left with $i = 3$. We reach the

node for *e*, where it corresponds locally to bit 1. The final computation is $\text{rank}_1(3) = 2$. Thus, $\text{rank}_e(S, 13) = 2$.
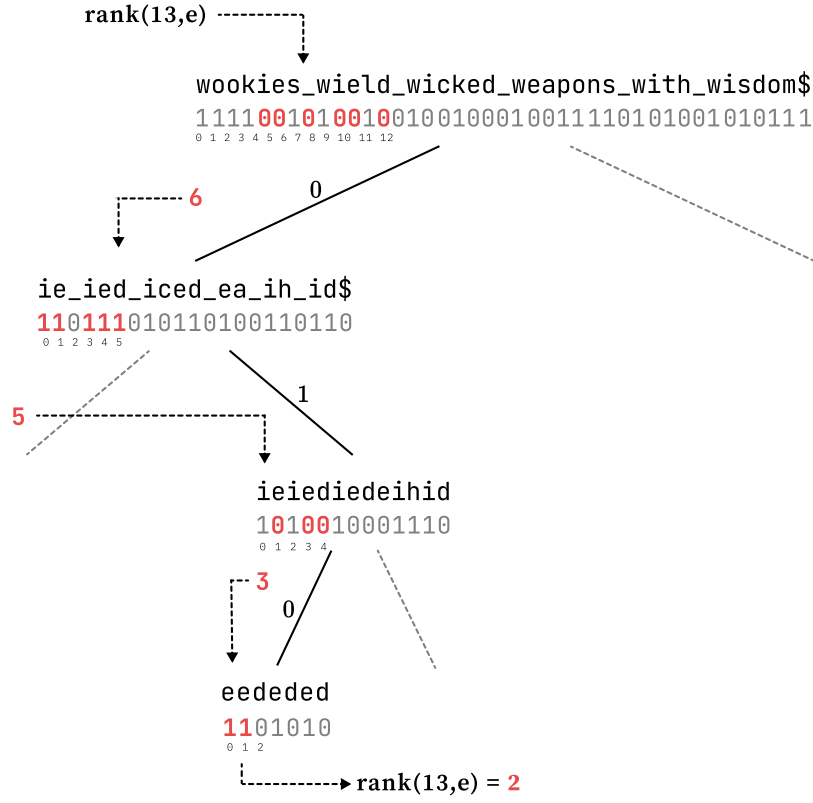

rank(13,e)

wookies_wield_wicked_weapons_with_wisdom$
1111**00**10**1**0**0**10010010001001111101010010101011
0 1 2 3 4 5 6 7 8 9 10 11 12

6   0

ie_ied_iced_ea_ih_id$
110111010110100110110
0 1 2 3 4 5

5   1

ieiediedeihid
1**0100**10001110
0 1 2 3 4

3
0

eededed
1101010
0 1 2

rank(13,e) = 2

Figure 13: $\text{rank}_e(S, 13)$ on the wavelet tree of Figure 12.

Algorithm 7 Rank queries on a wavelet tree
_____

function $\text{RANK}_c(S, i)$
   $v \leftarrow T_{\text{root}}$ ▷ start at the root node
   $[a, b] \leftarrow [1, \sigma]$
   while $a \neq b$ **do**
      if $c \leqslant \lfloor (a + b)/2 \rfloor$ **then**
         $i \leftarrow \text{rank}_0(v.B, i)$
         $v \leftarrow v.\text{left}$ ▷ move to the left child of node v
         $b \leftarrow \lfloor (a + b)/2 \rfloor$
      else
         $i \leftarrow \text{rank}_1(v.B, i)$
         $v \leftarrow v.\text{right}$ ▷ move to the right child of node v
         $a \leftarrow \lfloor (a + b)/2 \rfloor + 1$
      end if
   end while
   return i
end function
_____

Pointerless Representation: To remove the $O(\sigma \log \sigma)$ pointer overhead, the pointerless wavelet tree concatenates bitmaps level-wise [37, 36]. Let B_l be the concatenated bitmap for level l. If a node v at level l

corresponds to the range $[s_v, e_v]$ in B_l, its left child's range in B_{l+1} is

$$[(l+1)n + \text{rank}_0(B_l, s_v - 1) + 1, (l+1)n + \text{rank}_0(B_l, e_v)]$$

Its right child's range is

$$[(l+1)n + z_l + \text{rank}_1(B_l, s_v - 1) + 1, (l+1)n + z_l + \text{rank}_1(B_l, e_v)]$$

where $z_l = \text{rank}_0(B_l, n)$ is the total 0-count at level l. This achieves $n\lceil \log \sigma \rceil + o(n \log \sigma)$ total space. Navigation requires extra rank operations per level compared to the pointer-based version ([9]), which can impact practical performance, although the asymptotic query time remains $O(\log \sigma)$.

3.2.2 *Compressed Wavelet Trees*

The standard wavelet tree representations (pointer-based and pointerless) achieve space proportional to $n \log \sigma$. However, when the sequence S itself is compressible (i.e., its empirical entropy is lower than $\log \sigma$), it is desirable for the index structure to reflect this compressibility. Wavelet trees can be adapted to achieve space bounds related to the empirical entropy of S, primarily through two main strategies: directly compressing the bitmaps stored within the nodes, or reshaping the tree based on symbol frequencies.

3.2.2.1 *Compressing the Bitvectors*

This approach maintains the balanced binary structure of the wavelet tree but replaces the plain bitmaps B_v at each internal node v with compressed representations that still support efficient rank and select queries. As explored in Section 3.1.4, various techniques exist for compressing sparse or biased bitvectors. If we employ a representation for each B_v (of length $N_v = |S_v|$) that uses $N_v \mathcal{H}_0(B_v) + o(N_v)$ bits while maintaining $O(1)$ query times for rank and select (e.g., using structures based on Raman et al. [48] or improved variants [46]), the total space complexity aggregates advantageously.

Theorem 3.10 (Entropy-Compressed WT Space (Bitmaps) [21, 41, 16])**.** *A wavelet tree for $S[1..n]$ over $\Sigma = \{1, \ldots, \sigma\}$, using node bitmaps compressed to their zero-order entropy with $O(1)$-time rank/select support, can be stored in*

$$n\mathcal{H}_0(S) + o(n \log \sigma) \text{ bits.}$$

The query times for access*,* rank*, and* select *remain* $O(\log \sigma)$.

Proof sketch. The core idea relies on the property that the sum of zero-order entropies of the bitmaps at any level l is upper bounded by the sum at level $l - 1$. Summing across all internal nodes, the total space for the compressed bitmaps relates directly to the zero-order entropy of the original sequence S:

$$\sum_{v \text{ internal}} |S_v| \mathcal{H}_0(B_v) = n \mathcal{H}_0(S)$$

The $o(n \log \sigma)$ term arises from aggregating the sublinear $o(N_v)$ overheads from each node's rank/select structure across all levels. Since rank/select on each compressed bitmap is $O(1)$, the total query time remains determined by the tree height, $O(\log \sigma)$. □

While theoretically achieving optimal space relative to $H_0(S)$, practical implementations using compressed bitmaps (like those based on RRR found in libraries such as SDSL [18]) can exhibit higher query latency compared to using plain, uncompressed bitmaps due to the computational overhead of performing rank/select on the compressed format [9].

3.2.2.2 *Huffman-Shaped Wavelet Trees*

Instead of compressing the content (bitmaps), this strategy compresses the structure itself by adapting the tree shape to the symbol frequencies $f_c = \text{rank}_c(S, n)$ in S. The wavelet tree is given the shape of a Huffman tree [26] constructed for the symbols based on their frequencies [22, 35]. In this structure, a symbol c occurring f_c times resides at a leaf at depth $|h(c)|$, where $h(c)$ is its Huffman code. The bitmaps B_v are stored uncompressed at the internal nodes.

The total number of bits stored in the plain bitmaps across the entire tree is precisely the length of the Huffman-encoded sequence:

$$\sum_{c \in \Sigma} f_c |h(c)| \quad \leqslant \quad n(\mathcal{H}_0(S) + 1) \text{ bits.}$$

Adding the overhead for rank/select support on these plain bitmaps ($o(n(\mathcal{H}_0(S) + 1))$ total) and the space to store the Huffman model itself (e.g., $O(\sigma \log \sigma)$ bits, reducible for canonical codes [9]), gives the total space.

Theorem 3.11 (Huffman-Shaped WT Performance [35, 41]). *A Huffman-shaped wavelet tree using plain bitmaps (with* $O(1)$ *rank/select support) occupies space bounded by*

$$n(\mathcal{H}_0(S) + 1) + o(n(\mathcal{H}_0(S) + 1)) + O(\sigma \log \sigma) \text{ bits.}$$

It supports access, rank, and select. The worst-case query time is $O(d_{max})$, *where* d_{max} *is the maximum depth (potentially* $O(n)$, *but typically bounded to* $O(\log \sigma)$ *[43]). The average query time, assuming queries are distributed according to symbol frequencies* (f_c/n), *is* $O(1 + \mathcal{H}_0(S))$.

This approach achieves compression related to $\mathcal{H}_0(S)$ through structural adaptation rather than bitmap compression, often leading to faster average query times $(O(1 + \mathcal{H}_0(S))$ vs $O(\log \sigma))$ for statistically skewed query distributions, while using potentially simpler and faster plain bitmap rank/select structures. Pointerless versions based on canonical Huffman codes are also possible [9].

3.2.2.3 *Higher-Order Entropy Compression*

To capture statistical dependencies beyond symbol frequencies, wavelet trees are often used on the Burrows-Wheeler Transformed [6] sequence S^{BWT}. The BWT groups symbols preceded by the same context of length k, making S^{BWT} highly compressible by methods sensitive to local statistics. The k-th order empirical entropy, $H_k(S)$, quantifies this context-dependent compressibility (see Section 2.5). It is known that $\sum_{A \in \Sigma^k} |S_A| \mathcal{H}_0(S_A) = n\mathcal{H}_k(S)$, where S_A is the sequence of symbols following context A [38].

Building a single wavelet tree over the entire S^{BWT} and using zero-order entropy compression on its internal bitmaps (as in Section 3.2.2.1) allows the structure to achieve space related to $H_k(S)$ for the original sequence S.

Theorem 3.12 (H_k-Compressed WT [43, 14]). *Let* S^{BWT} *be the Burrows-Wheeler Transform of* S. *A wavelet tree built over* S^{BWT} *using node bitmaps compressed to their zero-order entropy (requiring* $N_v \mathcal{H}_0(B_v) + o(N_v)$ *bits per node* v) *occupies a total space of*

$$n\mathcal{H}_k(S) + o(n \log \sigma) \text{ bits}$$

for any $k \leqslant \alpha \log_\sigma n$ $(0 < \alpha < 1)$.

Proof sketch. The space bound follows because the zero-order entropy of the wavelet tree bitmaps over S^{BWT} sums to $n\mathcal{H}_0(S^{BWT})$, and $\mathcal{H}_0(S^{BWT})$ effectively captures $\mathcal{H}_k(S)$ due to the context-grouping property of the BWT [38, 43]. The $o(n \log \sigma)$ term accumulates the overheads of the compressed rank/select structures. $\square$

This structure supports the rank operations on S^{BWT} needed for FM-index pattern matching in $O(\log \sigma)$ time per operation.

This connection is crucial for compressed full-text indexing. Practical variants exist, such as partitioning S^{BWT} and using Huffman-shaped wavelet trees on the blocks [31], which may offer different practical performance trade-offs. The choice between RLE and GE for bitmap encoding in this context was analyzed in [14], favoring RLE-like approaches for achieving H_k.

3.2.3 Wavelet Matrices and Quad Vectors

Further refinements address practical performance bottlenecks, primarily memory latency during tree traversal and the overhead associated with large alphabets in pointerless or Huffman representations.

3.2.3.1 The Wavelet Matrix

The wavelet matrix [9] provides an alternative layout for the pointerless wavelet tree that simplifies navigation and improves speed. It maintains the level-wise concatenated bitmaps $B_0, B_1, \ldots, B_{h-1}$ (where $h = \lceil \log \sigma \rceil$) and stores the counts $z_l = \mathrm{rank}_0(B_l, n)$ for each level l. The key difference lies in the mapping between levels: a position i in B_l corresponding to a 0-bit maps to position $\mathrm{rank}_0(B_l, i)$ in B_{l+1}, while a position corresponding to a 1-bit maps to position $z_l + \mathrm{rank}_1(B_l, i)$ in B_{l+1}.

Theorem 3.13 (Wavelet Matrix Performance [9]). *The wavelet matrix represents* $S[1..n]$ *using*

$$n \lceil \log \sigma \rceil + o(n \log \sigma) \text{ bits}$$

(where $o(n \log \sigma)$ *is for rank/select support on the* h *bitmaps, and the* z_l *values require negligible* $O(\log \sigma \log n)$ *bits). It supports* access, rank, *and* select *queries in* $O(\log \sigma)$ *time, executing exactly one bitvector rank or select operation per level traversed.*

This simplified navigation avoids the extra rank operations needed in the strict pointerless WT and eliminates pointer overhead, making it practically faster than pointerless trees and competitive with pointer-based trees, especially for large σ [9]. It can also be combined with bitmap compression or specialized Huffman shaping [9].

3.2.3.2   *4-ary (Quad) Wavelet Trees*

To combat the $O(\log \sigma)$ cache misses inherent in traversing a binary tree, 4-ary wavelet trees reduce the tree height to $h' = \lceil (\log \sigma)/2 \rceil$ [39]. Each internal node partitions its alphabet range $[a_v, b_v]$ into four sub-ranges based on the next two bits in the symbols' binary representation. Instead of a bitmap, each node stores a *quad vector* Q_v (a sequence over $\{0, 1, 2, 3\}$ or $\{00, 01, 10, 11\}$) indicating to which of the four children each symbol belongs.

Supporting queries requires specialized rank/select operations on these quad vectors. Structures achieving $O(1)$ time for quad vector rank/select with $o(N_v \log 4) = o(N_v)$ bits of overhead per node (where N_v is the quad vector length) have been developed [39].

Theorem 3.14 (4-ary WT Performance [39])**.** *A 4-ary wavelet tree using* $O(1)$-*time rank/select structures on quad vectors represents* $S[1..n]$ *in*

$$n \lceil \log \sigma \rceil + o(n \log \sigma) \text{ bits}$$

and supports access, rank, *and* select *in* $O(\log \sigma)$ *time, specifically requiring* $O(\lceil (\log \sigma)/2 \rceil)$ *quad vector rank or select operations.*

Proof sketch. Each level effectively stores 2 bits per original symbol. With $\approx (\log \sigma)/2$ levels, the total space for the quad vectors is $n \times 2 \times (\log \sigma)/2 = n \log \sigma$ bits. The $o(n \log \sigma)$ term accounts for the aggregated overhead of the quad vector rank/select structures. The query time is determined by the reduced tree height. $\square$

The principal advantage lies in the potential halving of cache misses during queries, leading to significant practical speedups in latency-bound scenarios, as demonstrated experimentally in [39], particularly when implemented as a 4-ary wavelet matrix.

3.3   DEGENERATE STRINGS

The concepts of rank and select queries, fundamental tools in string processing and succinct data structures as explored earlier in this chapter (Section 3.1, Section 3.2), can be extended to the domain of *degenerate strings*. This representation is often used to model uncertainty or variability in sequences, particularly in biological contexts.

Recall that a standard *string* S of length n over a finite non-empty alphabet Σ is a sequence $S = s_1 s_2 \ldots s_n$ where each $s_i \in \Sigma$. A degenerate string generalizes this:

Definition 3.15 (Degenerate String [17]). *A degenerate string is a sequence $X = X_1 X_2 \ldots X_n$, where each X_i is a subset of the alphabet Σ (i.e., $X_i \subseteq \Sigma$). The value n is termed the* length *of X. The* size *of X, denoted by N, is defined as $N = \sum_{i=1}^{n} |X_i|$. We denote the number of empty sets ($\emptyset$) among $X_1, \ldots, X_n$ by n_0.*

Degenerate strings were introduced by Fischer and Paterson [17] and are frequently employed in bioinformatics, for example, to represent DNA sequences with ambiguities (using IUPAC codes) or to model sequence variations within a population [2, 3].

Alanko et al. [2] introduced the counterparts of rank and select for degenerate strings:

Definition 3.16 (Subset Rank and Select [2]). *Given a degenerate string $X = X_1 \ldots X_n$ over alphabet Σ, a character $c \in \Sigma$, an index $i \in \{1, \ldots, n\}$, and a rank $j \in \mathbb{N}^+$, we define:*

- *subset-rank$_X(i, c)$: Returns the number of sets among the first i sets $X_1, \ldots, X_i$ that contain the symbol c. Formally, $|\{k \mid 1 \leqslant k \leqslant i \text{ and } c \in X_k\}|$.*

- *subset-select$_X(j, c)$: Returns the index k such that X_k is the j-th set in the sequence X (from left to right) that contains the symbol c. If fewer than j such sets exist, the result is undefined or signals an error.*

Example 3.17. Let $X = \{T\}\{G\}\{A, C, G, T\}\{\}\{\}\{C, G\}\{\}\{A\}\{\}\{A\}\{A, C\}\{\}\{\}\{A\}\{A\}$ be a degenerate string of length $n = 15$ over $\Sigma = \{A, C, G, T\}$. Then:

- subset-rank$_X(8, A) = 2$, as the sets containing 'A' up to index 8 are X_3 and X_8.

- subset-select$_X(2, G) = 3$, as the sets containing 'G' are X_2 (index 2, 1st), X_3 (index 3, 2nd), and X_6 (index 6, 3rd). The index of the 2nd such set is 3.

The motivation for studying these queries in [2] arose from pangenomics applications, particularly for fast membership queries on de Bruijn graphs represented via the Spectral Burrows-Wheeler Transform (SBWT) [1]. In the SBWT framework, a k-mer query translates to $2k$ subset-rank queries on a specific degenerate string.

A naive solution involves storing a bitvector B_c of length n for each $c \in \Sigma$, marking the presence of c in X_k at $B_c[k]$. Standard $O(1)$-time rank and select on these bitvectors suffice (subset-rank$_X(i, c) = \text{rank}_1(B_c, i)$ and subset-select$_X(j, c) = \text{select}_1(B_c, j)$), but the total space is $O(\sigma n)$ bits, which is impractical for large σ or n.

3.3.1   *Subset Wavelet Trees*

To address the space issue, Alanko et al. [2] introduced the *Subset Wavelet Tree (SWT)*, generalizing the standard Wavelet Tree (Section 3.2) to degenerate strings.

STRUCTURE   The SWT is a balanced binary tree over Σ. Each node v represents an alphabet partition A_v (root is Σ), with children representing halves of A_v. A sequence Q_v at node v contains subsets X_k from the original string that intersect with A_v (plus empty sets at the root). Each node v stores two bitvectors, L_v and R_v, of length $|Q_v|$, preprocessed for rank/select:

- $L_v[k] = 1 \iff$ the k-th set in Q_v intersects the *first* half of A_v.

- $R_v[k] = 1 \iff$ the k-th set in Q_v intersects the *second* half of A_v.

Often, L_v and R_v are combined into a base-4/base-3 sequence requiring specialized rank support.

QUERIES   subset-rank$_X(i, c)$ is answered by traversing from the root to the leaf for c. At node v, if c is in the left partition, update $i \leftarrow \text{rank}_1(L_v, i)$ and go left; otherwise, update $i \leftarrow \text{rank}_1(R_v, i)$ and go right. The final i is the result (Algorithm 8).

subset-select$_X(j, c)$ is answered by traversing from the leaf for c up to the root. Moving from child v to parent u, if v is the left child, update $j \leftarrow \text{select}_1(L_u, j)$; otherwise, update $j \leftarrow \text{select}_1(R_u, j)$. The final j is the result (Algorithm 9).

COMPLEXITY   With constant-time rank/select on node bitvectors, SWT queries take $O(\log \sigma)$ time. The space complexity depends on the structure of the sets. A key case highlighted in [2] is that of *balanced* degenerate strings, where the total size N equals the length n (implicitly, each non-empty set has size 1, relevant for SBWT applications).

Theorem 3.18 (SWT Space Complexity for Balanced Strings [2])**.** *The subset wavelet tree of a balanced degenerate string takes $2n \log \sigma + o(n \log \sigma)$ bits of space and supports* **subset-rank** *and* **subset-select** *queries in $O(\log \sigma)$ time.*

The $o(n \log \sigma)$ term covers the overhead for rank/select structures on the node bitvectors. Practical performance hinges on efficient rank (especially rank-pair queries [2]) on the internal base-3/4 sequences.

Algorithm 8 Subset-Rank Query using SWT [2]

Require: Character c from $[1, \sigma]$, index i
Ensure: The number of subsets X_k such that $k \leqslant i$ and $c \in X_k$
  1: **function** SUBSETRANK(c, i)
  2:    $v \leftarrow$ root
  3:    $[l, r] \leftarrow [1, \sigma]$
  4:    **while** $l \neq r$ **do**
  5:       $mid \leftarrow \lfloor (l + r - 1)/2 \rfloor$
  6:       **if** $c \leqslant mid$ **then**
  7:          $r \leftarrow mid$
  8:          $i \leftarrow \text{rank}_1(L_v, i)$
  9:          $v \leftarrow$ left child of v
 10:       **else**
 11:          $l \leftarrow mid + 1$
 12:          $i \leftarrow \text{rank}_1(R_v, i)$
 13:          $v \leftarrow$ right child of v
 14:       **end if**
 15:    **end while**
 16:    **return** i
 17: **end function**

3.3.2 *Improved Reductions and Bounds*

While the SWT offered a valuable first step, Bille et al. [5] revisited the subset rank-select problem, achieving significant theoretical and practical advances by focusing on reductions to standard rank-select operations on regular strings.

They made three significant contributions in this context. First, they introduced the parameter N and revisited the problem through reductions to the regular rank-select problem, deriving flexible complexity bounds based on existing rank-select structures, as detailed in Theorem 3.19. Second, they established a worst-case lower bound of $N \log \sigma - o(N \log \sigma)$ bits for structures supporting subset-rank or subset-select, and demonstrated that, by leveraging standard rank-select structures, their bounds often approach this lower limit while maintaining optimal query times (Theorem 3.20). Lastly, they implemented and compared their reductions to prior implementations, achieving twice the query speed of the most compact structure from [2] while maintaining comparable space usage. Additionally, they designed a vectorized structure that offers a 4-7x speedup over compact alternatives, rivaling the fastest known solutions.

Theorem 3.19 (General Upper Bound [5]). *Let X be a degenerate string of length n, size N, and containing n_0 empty sets over an alphabet $[1, \sigma]$. Let $\mathcal{D}$ denote a $\mathcal{D}_b(\ell, \sigma)$-bit data structure for a length-ℓ string over $[1, \sigma]$, supporting:*

Algorithm 9 Subset-Select Query using SWT [2]

Require: Character c from $[1, \sigma]$, rank j
Ensure: The index k such that X_k is the j-th set containing c
 1: **function** SUBSETSELECT(c, j)
 2:     $v \leftarrow$ leaf node corresponding to c
 3:     **while** $v \neq$ root **do**
 4:         $u \leftarrow$ parent of v
 5:         **if** $v =$ left child of u **then**
 6:             $j \leftarrow \text{select}_1(L_u, j)$
 7:         **else**
 8:             $j \leftarrow \text{select}_1(R_u, j)$
 9:         **end if**
10:         $v \leftarrow u$
11:     **end while**
12:     **return** j
13: **end function**

- *rank queries in $\mathcal{D}_r(\ell, \sigma)$ time, and*

- *select queries in $\mathcal{D}_s(\ell, \sigma)$ time.*

The subset rank-select problem on X can be solved under the following conditions:

(i) *(Case $n_0 = 0$): The structure requires:*

$$\mathcal{D}_b(N, \sigma) + N + o(N) \text{ bits,}$$

and supports:

    subset-rank in $\mathcal{D}_r(N, \sigma) + O(1)$ time,

    subset-select in $\mathcal{D}_s(N, \sigma) + O(1)$ time.

(ii) *(Case $n_0 > 0$): The bounds from case (i) apply with the following substitutions:*

$$N' = N + n_0 \quad and \quad \sigma' = \sigma + 1.$$

(iii) *(Alternative Bound): The structure uses additional $\mathcal{B}_b(n, n_0)$ bits of space and supports:*

    subset-rank in $\mathcal{D}_r(N, \sigma) + \mathcal{B}_r(n, n_0)$ time,

    subset-select in $\mathcal{D}_s(N, \sigma) + \mathcal{B}_s(n, n_0)$ time.

Here, $\mathcal{B}$ refers to a data structure on the length-n bitstring E (indicating empty sets) that contains n_0 1s, which:

- *uses $\mathcal{B}_b(n, n_0)$ bits,*

- *supports $\text{rank}_1(\cdot)$ in $\mathcal{B}_r(n, n_0)$ time, and*

- *supports select$_0(\cdot)$ in $\mathcal{B}_s(n, n_0)$ time.*

By applying succinct rank-select structures (like Golynski et al. [20]) to these bounds, [5] achieved improvements in query times without significantly increasing space usage compared to the SWT approach. For instance, substituting the Golynski et al. structure into Theorem 3.19 (i) results in a data structure occupying $N \log \sigma + N + o(N \log \sigma + N)$ bits, supporting subset-rank in $O(\log \log \sigma)$ time and subset-select in constant time. This improves the space constant from 2 to $1 + 1/\log \sigma$ compared to Alanko et al. [2] for balanced strings, while exponentially reducing query times.

For $n_0 > 0$, Theorem 3.19 (ii) modifies the bounds to $(N + n_0) \log(\sigma + 1) + (N + n_0) + o(n_0 \log \sigma + N \log \sigma + N + n_0)$ bits, maintaining the same improved query times. When $n_0 = o(N)$ and $\sigma = \omega(1)$, the space matches the $n_0 = 0$ case. Alternatively, Theorem 3.19(iii) allows for tailored bitvector structures sensitive to n_0.

Theorem 3.20 (Space Lower Bound [5]). *Let X be a degenerate string of size N over an alphabet $[1, \sigma]$. Any data structure supporting subset-rank or subset-select on X must use at least $N \log \sigma - o(N \log \sigma)$ bits in the worst case.*

In Theorem 3.20 we aim to establish a lower bound on the space required to represent X while supporting subset-rank or subset-select. Since these operations allow us to reconstruct X fully, any valid data structure must encode X completely. Our approach is to determine the number L of distinct degenerate strings possible for given parameters N and σ, and to show that distinguishing between these instances necessitates at least $\log_2 L$ bits.

Proof. Let N be sufficiently large, and let $\sigma = \omega(\log N)$. Without loss of generality, assume $\log N$ and $N/\log N$ are integers. Consider the class of degenerate strings $X_1, \ldots, X_n$ where $|X_i| = \log N$ for each i and $n = N/\log N$. The number of such strings is given by

$$\binom{\sigma}{\log N}^{N/\log N} \tag{1}$$

This is because each X_i can be formed by choosing $\log N$ characters from σ symbols, and there are n such subsets. The number of bits required to represent any degenerate string X must be at least:

$$\log \binom{\sigma}{\log N}^{N/\log N} = \frac{N}{\log N} \log \binom{\sigma}{\log N}$$

$$\geqslant \frac{N}{\log N} \log \left(\frac{\sigma - \log N}{\log N} \right)^{\log N}$$

$$= N \log \left(\frac{\sigma - \log N}{\log N} \right)$$

$$= N \log \sigma - o(N \log \sigma).$$

Thus, any representation of X that supports subset-rank or subset-select must use at least $N \log \sigma - o(N \log \sigma)$ bits in the worst case, concluding the proof. $\qquad\square$

3.3.2.1 *Reductions*

Let $X, \mathcal{D}, \mathcal{B}$ be as in Theorem 3.19 and consider $\mathcal{V}$ a data structure (for example the one described by Jacobson in [28]), which uses $n + o(n)$ bits for a bitstring of length n and supports rank and select in $O(1)$ time.

The reductions in Theorem 3.19 rely on the construction of two auxiliary strings S and R derived from the sets X_i. When $n_0 = 0$, each S_i is the concatenation of elements in X_i (in arbitrary order), and R_i is a single 1 followed by $|X_i| - 1$ 0s. The global strings S and R are formed by concatenating these sequences $S_1 \ldots S_n$ and $R_1 \ldots R_n$, appending a final 1 after R_n. The data structure consists of $\mathcal{D}$ built over S and Jacobson's structure $\mathcal{V}$ over R, using $\mathcal{D}_b(N, \sigma) + N + o(N)$ bits. Figure 14 from [5] illustrates this reduction for $n_0 = 0$.

Figure 14: *Left:* A degenerate string X over the alphabet $\{A, C, G, T\}$ where $n = 4$ and $N = 8$. *Right:* The reduction from Theorem 3.19 (i) on X. White space is for illustration purposes only. [5]

Queries are supported as follows: To compute subset-rank$_X(i, c)$, first find the start position $k = \text{select}_1(R, i+1)$ of the representation of X_{i+1} in R. The end position of the representation of X_i in S is $k-1$. Then return rank$_c(S, k-1)$. Conversely, to compute subset-select$_X(j, c)$, find the index $k = \text{select}_c(S, j)$ of the j-th occurrence of c in S. Then,

identify the corresponding set index by computing $\mathrm{rank}_1(R, k)$. Let's consider the practical example in Figure 14: to compute subset-$\mathrm{rank}_X(2, A)$, we first compute $\mathrm{select}_1(R, 3) = 6$. Now we know that S_2 ends at position $k - 1 = 5$, so we return $\mathrm{rank}_A(S, 5) = 2$. To compute subset-$\mathrm{select}_X(2, G)$ we compute $\mathrm{select}_G(S, 2) = 8$, and compute $\mathrm{rank}_1(R, 8) = 4$ to determine that position 8 corresponds to X_4.

Since rank and select on R are constant time using $\mathcal{V}$, these operations achieve $\mathcal{D}_r(N, \sigma) + O(1)$ and $\mathcal{D}_s(N, \sigma) + O(1)$ time, as required by Theorem 3.19 (i).

For $n_0 \neq 0$, empty sets are replaced by singletons containing a new character $\sigma + 1$, effectively reducing the problem to the $n_0 = 0$ case with $N' = N + n_0$ and $\sigma' = \sigma + 1$. This achieves the bounds of Theorem 3.19 (ii).

ALTERNATIVE BOUND   Let E be a bitvector of length n, where $E[i] = 1$ if $X_i = \emptyset$ and $E[i] = 0$ otherwise. Define X' as the degenerate string derived from X by removing all empty sets. The data structure consists of reduction (i) applied to X', along with a bitvector structure $\mathcal{B}$ built on E. This requires $\mathcal{D}_b(N, \sigma) + N + o(N) + \mathcal{B}_b(n, n_0)$ bits of space.

To support subset-$\mathrm{rank}_X(i, c)$, calculate $k = i - \mathrm{rank}_1(E, i)$, which maps X_i to its corresponding set X'_k in the string without empty sets. Then, return subset-$\mathrm{rank}_{X'}(k, c)$ (computed using the reduction (i) on X'). This operation runs in $\mathcal{B}_r(n, n_0) + \mathcal{D}_r(N, \sigma) + O(1)$ time.

To support subset-$\mathrm{select}_X(j, c)$, first determine $k = $ subset-$\mathrm{select}_{X'}(j, c)$ (using reduction (i) on X'), and then return $\mathrm{select}_0(E, k)$, which identifies the position of the k-th zero in E (i.e., the index of the k-th nonempty set in the original string X). This operation runs in $\mathcal{B}_s(n, n_0) + \mathcal{D}_s(N, \sigma) + O(1)$, achieving the stated performance bounds.

Empirical Results

Experimental evaluations by Bille et al. [5] compared subset rank structures on *E. coli* and human metagenome datasets, testing both within a k-mer index and via isolated subset-rank queries. The authors benchmarked Subset Wavelet Tree variants [2] against their designs based on the reductions presented in Section 3.3.2.1.

Their work introduced the dense-sparse decomposition (DSD) method, optimizing the reduction strategy for skewed set distributions common in genomic data by handling empty, singleton, and larger sets differently. Implementations incorporated techniques like SIMD instructions. Results showed that DSD structures offered competitive space-time tradeoffs compared to SWT variants. For instance, the

SIMD-enhanced DSD was 4-7 times faster than the Concat(ef) reduction baseline [1] at similar space, while DSD(rrr) doubled the query speed of Concat(ef) using comparable space. Structures like DSD(scan) demonstrated a balance between space usage and query time relative to other tested methods.

SUCCINCT WEIGHTED DAGS FOR PATH QUERIES

The preceding chapters have established a foundation in data compression (Chapter 2) and succinct data structures, particularly focusing on rank and select operations (Chapter 3). These sequence-based tools provide efficient ways to handle queries on linear data.

Building upon this foundation, we now shift our focus to graph structures, specifically directed acyclic graphs (DAGs) where nodes carry weights. A key motivation for this shift comes from revisiting the *degenerate string problem* introduced in Section 3.3. This problem can be viewed through a different lens, that of graph representation. As we detail below, a degenerate string and a target character can be naturally modeled as a specific type of weighted DAG.

Degenerate Strings as DAGs

Given a degenerate string $X = X_1 X_2 \ldots X_n$ over an alphabet Σ (as defined in Section 3.3), we construct a weighted DAG $G_c = (V_c, E_c, w_c)$ for a specified character $c \in \Sigma$. This construction provides a mapping from the sequence structure to a graph structure.

First, we define the set of vertices V_c. Let s be a unique source vertex. For each index k ($1 \leqslant k \leqslant n$) and each character $a \in X_k$, we introduce a unique vertex, denoted as $v_{k,a}$. The vertex set V_c is the union of the source and all such vertices:

$$V_c = \{s\} \cup \{v_{k,a} \mid 1 \leqslant k \leqslant n, a \in X_k\}.$$

These vertices $v_{k,a}$ represent the choice of character a at position k of the degenerate string.

The weight function $w_c : V_c \to \mathbb{N}_0$ is defined as follows: the weight of the source vertex s is $w_c(s) = 0$. For any other vertex $v_{k,a} \in V_c \setminus \{s\}$, its weight depends on whether the character a matches the target character c:

$$w_c(v_{k,a}) = \begin{cases} 1 & \text{if } a = c \\ 0 & \text{if } a \neq c \end{cases}.$$

This function assigns a positive weight only to vertices corresponding to the specific character c we are focusing on.

The edge set E_c connects the source to the vertices representing the first set X_1, and subsequently connects vertices between adjacent positions k and $k + 1$:

$$E_c = \{(s, v_{1,a}) \mid a \in X_1\} \cup \{(v_{k,a}, v_{k+1,b}) \mid 1 \leqslant k < n, a \in X_k, b \in X_{k+1}\}.$$

Since edges only connect vertices associated with index k to vertices associated with index $k + 1$, the graph (V_c, E_c) contains no directed cycles and is therefore a DAG.

Figure 15 shows an example degenerate string. The weighted DAG G_A derived from this degenerate string for character $c = A$, following the construction detailed above, is illustrated in Figure 16. In the figure, the notation (k, a) inside a node identifies the vertex $v_{k,a}$.

$$X = \left\{ \begin{matrix} A \\ C \\ G \end{matrix} \right\} \quad \left\{ \begin{matrix} A \\ T \end{matrix} \right\} \quad \left\{ \begin{matrix} T \\ C \\ A \end{matrix} \right\} \quad \left\{ \begin{matrix} A \\ G \end{matrix} \right\}$$

$$\quad\quad X_1 \quad\quad X_2 \quad\quad X_3 \quad\quad X_4$$

Figure 15: An example degenerate string $X = X_1 X_2 X_3 X_4$ over $\Sigma = \{A, C, G, T\}$.
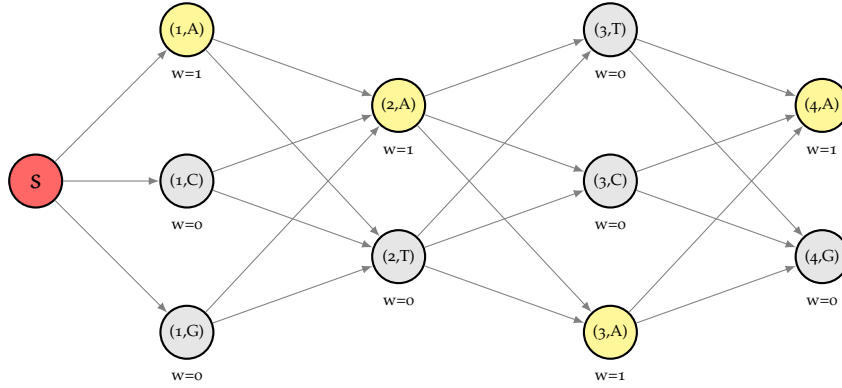

Figure 16: The weighted DAG G_A derived from the degenerate string in Figure 15 for character $c = A$. Nodes visually labeled (k, a) represent the vertices $v_{k,a}$. Nodes with $w_A(v_{k,a}) = 1$ are yellow; those with $w_A(v_{k,a}) = 0$ are gray. Edges represent the connections defined in E_A.

This graph-based perspective on degenerate strings serves as a concrete starting point for the core topic of this chapter: the development of succinct data structures for general node-weighted DAGs to support path-based queries. We address the challenge of representing an arbitrary DAG $G = (V, E, w)$, where each vertex $v \in V$ carries a non-negative integer weight $w(v)$, in a compressed format that efficiently supports queries related to cumulative path weights. Such weighted DAGs model various phenomena beyond degenerate

strings. For example, in bioinformatics, pangenome graphs[1] can be interpreted through this lens: if each node corresponds to a DNA sequence (a string over $\{A, C, G, T\}$), the weight $w(v)$ could represent the count of a specific nucleotide (e.g., A) within that sequence; similarly for C, G, and T.

Our primary focus is on generalizing the rank query to this graph setting; the select query, while definable, will not be treated further in this work. For a given vertex N, the rank query aims to describe the set of possible cumulative weights achievable on paths originating from a designated source vertex s and terminating at N.

The combinatorial complexity of paths in a DAG - potentially exponential in the number of vertices - makes naive approaches based on explicit path enumeration or storage infeasible for large graphs. This motivated us to development of a *succinct* data structure. Our approach involves partitioning the vertices based on how their path weight information is represented: some vertices (*explicit*) will store this information directly, while others (*implicit*) will rely on indirect derivation through references facilitated by a carefully defined *successor* relationship, as detailed in Section 4.2.

4.1 MATHEMATICAL FRAMEWORK

To develop our data structure and associated algorithms, we first establish the necessary mathematical definitions and properties concerning weighted DAGs and path weights.

Weighted Directed Acyclic Graphs

We begin with the formal definition of the structure central to this chapter.

Definition 4.1 (Weighted DAG)**.** *A node-weighted Directed Acyclic Graph (weighted DAG) is a triple* $G = (V, E, w)$, *where:*

- V *is a finite set of vertices. We typically identify* V *with the set* $\{0, 1, \ldots, n-1\}$ *where* $n = |V|$, *thereby implicitly defining a total order on the vertices.*

- $E \subseteq V \times V$ *is a set of directed edges such that the graph* (V, E) *contains no directed cycles.*

---

1 Pangenome graphs may contain cycles. These cycles can be addressed by either removing them or by utilizing path information provided by modern pangenome graph formats.

- $w : V \to \mathbb{N}_0$ *is a weight function assigning a non-negative integer* $w(v)$ *to each vertex* $v \in V$, *where* $\mathbb{N}_0 = \{0, 1, 2, \dots\}$.

For a vertex $v \in V$, *we denote the set of its direct predecessors as*

$$\text{Pred}(v) = \{u \in V \mid (u, v) \in E\}$$

and the set of its direct successors as

$$\text{Succ}(v) = \{u \in V \mid (v, u) \in E\}.$$

A vertex v *with* $\text{Succ}(v) = \emptyset$ *is termed a sink vertex.*

This definition provides the fundamental object of study. We will often rely on the acyclic property, which guarantees the existence of topological orderings of the vertices.

Assumption 4.2 (Unique Source). *Without loss of generality, we assume that the DAG* G *possesses a unique source vertex* $s \in V$ *characterized by* $\text{Pred}(s) = \emptyset$. *If multiple sources exist in the original graph, a standard pre-processing step involves introducing a virtual source vertex* s' *with* $w(s') = 0$ *and adding edges* (s', v) *for all original source vertices* v. *Throughout this work, we assume such a transformation has been applied if necessary, and we identify the unique source with vertex* $s = 0$, *setting* $w(s) = 0$.

Having defined the graph structure, we now define paths and their associated weights, which are central to the queries we aim to support.

Definition 4.3 (Path in a DAG). *A path* P *from a vertex* u *to a vertex* v *in* G *is a sequence of vertices* $P = (v_0, v_1, \dots, v_k)$ *such that* $v_0 = u$, $v_k = v$, *and* $(v_{j-1}, v_j) \in E$ *for all* $1 \leqslant j \leqslant k$. *The length of the path* P *is* k, *the number of edges. Let* $\text{Path}(s, v)$ *denote the set of all paths originating from the unique source* s *and terminating at* v.

Definition 4.4 (Cumulative Path Weight). *The cumulative weight, denoted* $W(P)$, *for a path* $P = (v_0 = s, \dots, v_k = v)$ *as defined in* 4.3, *is the sum of the weights of the vertices along the path:*

$$W(P) = \sum_{j=1}^{k} w(v_j).$$

4.1.1 *Path Weight Aggregation*

A key challenge lies in efficiently representing the potentially vast collection of path weights terminating at each vertex. We introduce a set associated with each vertex to capture precisely this information.

Definition 4.5 ($\mathcal{O}$-Set)**.** *For each vertex $v \in V$ in a weighted DAG $G = (V, E, w)$ with source s, the $\mathcal{O}$-set, denoted $\mathcal{O}_v \subseteq \mathbb{N}_0$, is defined recursively. Let us assume a topological ordering of the vertices in V. The sets are constructed as follows: for the source vertex $v = s$:*

$$\mathcal{O}_s = \{0\}.$$

For any other vertex $v \neq s$:

$$\mathcal{O}_v = \bigcup_{u \in \mathtt{Pred}(v)} \{y + w(v) \mid y \in \mathcal{O}_u\}.$$

This definition implies that $\mathcal{O}_v$ contains only the distinct values generated by this union process. We consider $\mathcal{O}_v$ to be the set of these unique values, represented as a sorted sequence.
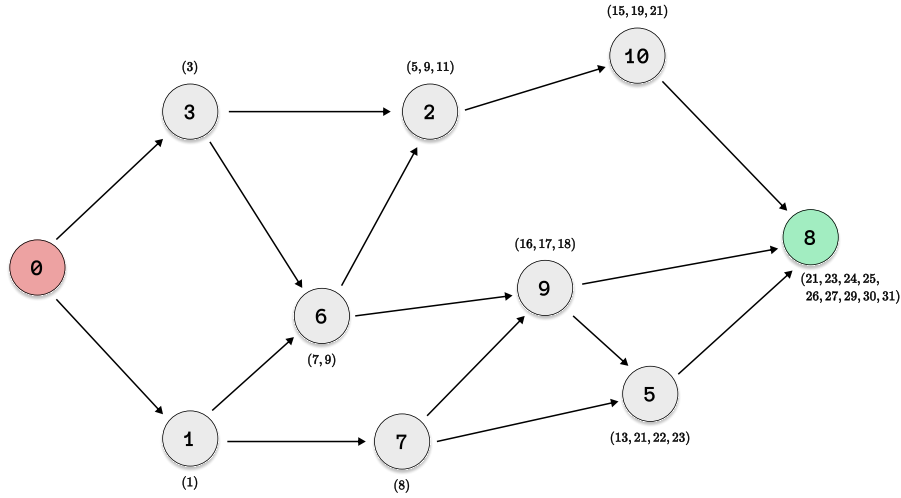

Figure 17: Example of a node-weighted DAG. Each node v contains its weight $w(v)$. The label associated with each node represents its calculated $\mathcal{O}$-set, $\mathcal{O}_v$, considered as a sorted sequence.

Example 4.6. [$\mathcal{O}$-Set Calculation] Consider the weighted DAG shown in Figure 17. Each node v is labelled with its weight $w(v)$ inside the circle. The label associated with each node displays its corresponding $\mathcal{O}$-set, calculated according to 4.5.

The following proposition establishes the semantic meaning of the $\mathcal{O}$-set, confirming that it correctly captures the set of all possible path weights (as defined in 4.4) ending at a vertex.

Proposition 4.7 (Characterization of the $\mathcal{O}$-Set). *For any vertex $v \in V$, the set $\mathcal{O}_v$ is equal to the set of cumulative path weights from the source s to v:*

$$\mathcal{O}_v = \{W(P) \mid P \in \mathrm{Path}(s, v)\}.$$

Proof. The proof proceeds by induction on the vertices $v \in V$, ordered according to a topological sort of G. *Base Case:* For the source vertex $v = s$, the only path in $\mathrm{Path}(s, s)$ is the trivial path $P = (s)$. According to Definition 4.4, $W(P) = 0$. By Definition 4.5, $\mathcal{O}_s = \{0\}$. Thus, the proposition holds for s. *Inductive Step:* Assume the proposition holds for all vertices u that strictly precede v in the topological order. In particular, this assumption holds for all $u \in \mathrm{Pred}(v)$, since the existence of an edge (u, v) implies u precedes v in any topological sort. We must show that $\mathcal{O}_v = \{W(P) \mid P \in \mathrm{Path}(s, v)\}$.

($\subseteq$) Let $x \in \mathcal{O}_v$. By Definition 4.5, since $v \neq s$, there must exist a predecessor $u \in \mathrm{Pred}(v)$ and a value $y \in \mathcal{O}_u$ such that $x = y + w(v)$. By the inductive hypothesis applied to u, $y = W(P')$ for some path $P' = (v_0 = s, \ldots, v_{k-1} = u) \in \mathrm{Path}(s, u)$. Consider the path $P = (v_0, \ldots, v_{k-1}, v_k = v)$ formed by appending the edge (u, v) to P'. This is a valid path in $\mathrm{Path}(s, v)$. Its weight according to Definition 4.4 is

$$W(P) = \sum_{j=1}^{k} w(v_j) = \left(\sum_{j=1}^{k-1} w(v_j) \right) + w(v_k)$$

$$= W(P') + w(v) = y + w(v) = x.$$

Therefore, any element $x \in \mathcal{O}_v$ corresponds to the weight of some path in $\mathrm{Path}(s, v)$.

($\supseteq$) Let $P = (v_0 = s, \ldots, v_k = v)$ be an arbitrary path in $\mathrm{Path}(s, v)$. Since $v \neq s$, the path must have length $k \geqslant 1$. Let $u = v_{k-1}$ be the vertex immediately preceding v on this path; thus, $u \in \mathrm{Pred}(v)$. Let $P' = (v_0, \ldots, v_{k-1})$ be the subpath of P ending at u. P' is a path in $\mathrm{Path}(s, u)$. By the inductive hypothesis, the weight $W(P') = \sum_{j=1}^{k-1} w(v_j)$ must be an element of $\mathcal{O}_u$. Let $y = W(P')$. By Definition 4.5, the value $y + w(v)$ is included in the construction of $\mathcal{O}_v$. We observe that

$$y + w(v) = W(P') + w(v_k) = \left(\sum_{j=1}^{k-1} w(v_j) \right) + w(v_k)$$

$$= \sum_{j=1}^{k} w(v_j) = W(P).$$

Thus, the weight $W(P)$ of any path in $\mathrm{Path}(s, v)$ is contained in $\mathcal{O}_v$.

Since both inclusions hold, we conclude that $\mathcal{O}_v = \{W(P) \mid P \in \mathrm{Path}(s, v)\}$. $\square$

An important property related to the sizes of these $\mathcal{O}$-sets is monotonicity along edges, which plays a fundamental role in the design of our succinct structure.

Lemma 4.8 ($\mathcal{O}$-Set Cardinality Monotonicity along Edges). *Let $v \in V$ and let $u \in \mathrm{Succ}(v)$ be any direct successor of v. Then, the cardinality of the $\mathcal{O}$-set of v is less than or equal to the cardinality of the $\mathcal{O}$-set of u, i.e., $|\mathcal{O}_v| \leqslant |\mathcal{O}_u|$.*

Proof. From Definition 4.5, the $\mathcal{O}$-set for u is given by

$$\mathcal{O}_u = \bigcup_{p \in \mathrm{Pred}(u)} \{y + w(u) \mid y \in \mathcal{O}_p\}.$$

Since u is a successor of v, it follows that v is a predecessor of u, i.e., $v \in \mathrm{Pred}(u)$. Therefore, the set $S_v = \{y + w(u) \mid y \in \mathcal{O}_v\}$ contributes to the union forming $\mathcal{O}_u$. Specifically

$$S_v \subseteq \bigcup_{p \in \mathrm{Pred}(u)} \{y + w(u) \mid y \in \mathcal{O}_p\}$$

Consider the mapping $f : \mathcal{O}_v \to S_v$ defined by $f(y) = y + w(u)$. Since $w(u) \geqslant 0$, this mapping is injective. If $y_1 \neq y_2$, then $y_1 + w(u) \neq y_2 + w(u)$. Consequently, the number of distinct elements in S_v is exactly equal to the number of distinct elements in $\mathcal{O}_v$, so $|S_v| = |\mathcal{O}_v|$. The set $\mathcal{O}_u$ is formed by taking the union of sets like S_v for all predecessors $p \in \mathrm{Pred}(u)$ and retaining only the unique values. Since the elements generated from v's contribution (namely, S_v) are a subset of the elements considered for $\mathcal{O}_u$, the total number of unique elements in $\mathcal{O}_u$ must be at least the number of unique elements contributed by v. Therefore, $|\mathcal{O}_u| \geqslant |S_v| = |\mathcal{O}_v|$. $\qquad\square$

4.1.2   *The Rank Query*

Having defined the $\mathcal{O}$-set, which precisely captures the set of all possible cumulative path weights terminating at a given vertex N, we now introduce the rank query. This query builds upon the $\mathcal{O}$-set to provide a richer description related to the path weights.

Intuitively, each value $x \in \mathcal{O}_N$ represents the total accumulated weight along some path from the source s ending exactly at N. We can think of the weight $w(N)$ of the node N itself as the contribution or cost associated with the final step or "activity" performed at N. The rank query, $\mathrm{rank}_G(N)$, aims to capture not just the final cumulative weights $x \in \mathcal{O}_N$, but rather the set of all possible cumulative values that could be considered "active" or relevant *during* the activity represented by node N.

Specifically, for a path P reaching N with total weight $W(P) = x$, the query considers the range of cumulative values from the point just before incorporating N's full weight up to the final value x. This corresponds mathematically to the integer interval

$$[\max(0, x - w(N) + 1), x]$$

This interval represents all possible integer cumulative weights observed during the *processing* of node N along that specific path. The rank query then aggregates these intervals over all possible paths ending at N.

This intuition leads to the following formal definition:

Definition 4.9 (Rank Query on Weighted DAG). *Given a vertex $N \in V$ in a weighted DAG $G = (V, E, w)$, the rank query, denoted $\mathrm{rank}_G(N)$, returns a representation of a specific set of integers derived from the $\mathcal{O}$-set $\mathcal{O}_N$. The target set, $S_N \subseteq \mathbb{N}_0$, is defined as the union of intervals generated from each element $x \in \mathcal{O}_N$:*

$$S_N = \bigcup_{x \in \mathcal{O}_N} \{z \in \mathbb{N}_0 \mid \max(0, x - w(N) + 1) \leqslant z \leqslant x\}.$$

These intervals are then maximally merged, meaning $r_k < l_{k+1} - 1$ for all $k = 1, \ldots, p - 1$. The query result is specified as a minimal collection of disjoint, closed integer intervals,

$$\mathcal{R}_N = \{[l_1, r_1], [l_2, r_2], \ldots, [l_p, r_p]\}$$

such that their union exactly covers S_N,

$$\bigcup_{k=1}^{p} [l_k, r_k] = S_N$$

Example 4.10. [Rank Query Calculation] Let us compute the rank query for vertex $N = 2$ in the DAG shown[2] in Figure 17. From Example 4.6, we know that the weight of node 2 is $w(2) = 2$, and its $\mathcal{O}$-set is $\mathcal{O}_2 = \{5, 9, 11\}$. These are the possible total weights of paths ending at node 2. Applying Definition 4.9, we associate an interval with each $x \in \mathcal{O}_2$, representing the values active during the processing of node 2:

- For path weight $x = 5$: Interval is $[\max(0, 5 - 2 + 1), 5] = [4, 5]$. These are the values active while accumulating the weight $w(2) = 2$ to reach 5.

- For path weight $x = 9$: Interval is $[\max(0, 9 - 2 + 1), 9] = [8, 9]$.

---

2 In this example, the weight function w assigns to each vertex v a weight equal to its identifier, i.e., $w(v) = v$. This is possible since it's just a small graph and we have taken unique weights

- For path weight $x = 11$: Interval is $[\max(0, 11 - 2 + 1), 11] = [10, 11]$.

The target set S_2 is the union of these intervals: $S_2 = [4, 5] \cup [8, 9] \cup [10, 11]$. We merge these intervals to obtain the minimal disjoint representation $\mathcal{R}_2$.

- Compare $[4, 5]$ and $[8, 9]$. Since $8 > 5 + 1$, they remain separate.

- Compare $[8, 9]$ and $[10, 11]$. Since $10 \leqslant 9 + 1$, they are merged into $[8, \max(9, 11)] = [8, 11]$.

The final minimal collection of disjoint intervals is:

$$\text{Rank}_G(2) = \{[4, 5], [8, 11]\}.$$

This collection represents the set $S_2 = \{4, 5\} \cup \{8, 9, 10, 11\}$, which encompasses all possible integer cumulative weights that could be considered active during the processing phase associated with node 2, across all possible paths leading to it.

4.2 THE SUCCINCT DAG REPRESENTATION

As established, the $\mathcal{O}$-sets can grow significantly in size, rendering their explicit storage for all vertices prohibitive for large graphs. This section details our proposed succinct representation strategy, designed to mitigate this space complexity while still enabling efficient query evaluation. The core idea is to partition the vertices and utilize indirect references guided by a successor relationship.

Successor Selection Heuristic

For an implicit representation of path information, we define a function σ that designates a specific successor for each non-sink vertex. This choice is guided by a simple heuristic aimed at minimizing the overall space required for storing the succinct representation.

Definition 4.11 (Successor Function σ). *For each vertex $v \in V$ that is not a sink (i.e., $\text{Succ}(v) \neq \emptyset$), we select a designated successor $\sigma(v) \in \text{Succ}(v)$ according to the following heuristic rule:*

$$\sigma(v) \in \underset{u \in \text{Succ}(v)}{\arg\min} \{|\mathcal{O}_u|\}.$$

In case of ties (multiple successors minimize the $\mathcal{O}$-set cardinality) we select the successor with the smallest vertex ID among the candidates.

The function σ is thus well-defined for all non-sink vertices.

Node Partitioning

The successor function σ determines a partition of the vertex set V, influencing how path information is represented for each vertex.

Definition 4.12 (Explicit and Implicit Vertices). *The set of vertices V is partitioned into the set of explicit vertices V_E and the set of implicit vertices V_I. The set V_E contains all sink vertices of the graph G, formally defined as*

$$V_E = \{v \in V \mid \text{Succ}(v) = \emptyset\}.$$

The set V_I contains all remaining vertices:

$$V_I = V \setminus V_E = \{v \in V \mid \text{Succ}(v) \neq \emptyset\}.$$

The path weight information ($\mathcal{O}$-sets) for vertices in V_E is stored explicitly within the representation, while for vertices in V_I, this information is derived implicitly through references involving the designated successor $\sigma(v)$.

4.2.1 *Structure Components*

We now outline the main components of our data structure designed to represent the weighted DAG $G = (V, E, w)$ succinctly. These components can be seen as arrays indexed by vertex ID (from 0 to $n - 1$), enabling a Struct of Arrays (SoA) memory layout [3].

1. *Weights $\mathcal{W}$:* An array storing the weight $w(v)$ for each vertex $v \in V$, $\mathcal{W}[v] = w(v)$.

2. *Successor Information Σ:* An array encoding the successor function σ and identifying explicit nodes. For an implicit vertex $v \in V_I$, $\Sigma[v]$ stores the identifier (ID) of its designated successor $\sigma(v)$. For an explicit vertex $v \in V_E$, $\Sigma[v]$ contains a special marker indicating its status.

3. *Associated Data $\mathcal{D}$:* An array or structure holding the core path weight information, structured differently depending on whether a vertex is explicit or implicit. For a vertex v, $\mathcal{D}[v]$ stores either its full $\mathcal{O}$-set (if $v \in V_E$) or an offset sequence $\mathcal{I}_v$ (if $v \in V_I$) that enables reconstruction of $\mathcal{O}_v$ via reference to the data associated with $\sigma(v)$ (and eventually all its successors up to a node in V_E).

---

3 The SoA organization can be advantageous for cache performance and allows for independent compression strategies for different data types (weights, pointers, path data) that we will discuss in Section 4.4.

The content stored within the Associated Data component $\mathcal{D}$ is determined by the classification of the vertex according to the partitioning defined in 4.12. Specifically:

For $v \in V_E$ (*Explicit Vertex*), $\mathcal{D}[v]$ stores the sorted sequence $\mathcal{O}_v$. We denote this stored data representation as $\mathcal{D}_E(v)$. In practice, $\mathcal{D}_E(v)$ would be implemented using a suitable (potentially compressed) representation of the sequence $\mathcal{O}_v$.

For $v \in V_I$ (*Implicit Vertex*), let $u = \sigma(v)$ be the designated successor. $\mathcal{D}[v]$ stores the *offset sequence* $\mathcal{I}_v$. This sequence $\mathcal{I}_v = (j_0, j_1, \ldots, j_{m-1})$ is a strictly monotonically increasing sequence of $m = |\mathcal{O}_v|$ indices. The index j_k (stored at position k in $\mathcal{I}_v$) indicates that the k-th element of $\mathcal{O}_v$ (let it be x_k) can be computed from the j_k-th element of $\mathcal{O}_u$ (let it be y_{j_k}) using the reconstruction rule: $x_k = y_{j_k} - w(u)$. We denote this stored sequence representation as $\mathcal{D}_I(v)$.

Proposition 4.13. *For any implicit node $v \in V_I$, let $u = \sigma(v)$ be its designated successor chosen according to Definition 4.11. Then $|\mathcal{O}_v| \leqslant |\mathcal{O}_u|$.*

Proof. This is a direct consequence of Lemma 4.8. Since $\sigma(v)$ is chosen from the set $\mathrm{Succ}(v)$ of direct successors of v, the lemma applies, yielding $|\mathcal{O}_v| \leqslant |\mathcal{O}_{\sigma(v)}|$. □

This inequality guarantees that the length of the offset sequence $\mathcal{I}_v$ (which is $m = |\mathcal{O}_v|$) is no greater than the length of the sequence $\mathcal{O}_u$ (which is $|\mathcal{O}_u|$) from which values are derived. Furthermore, the reconstruction rule $x_k = y_{j_k} - w(u)$ implies that each $x_k \in \mathcal{O}_v$ originates from some element in $\mathcal{O}_u$ (shifted by $-w(u)$). The offset sequence $\mathcal{I}_v$ stores the index j_k in $\mathcal{O}_u$ corresponding to the k-th element x_k in $\mathcal{O}_v$.

The heuristic choice of $\sigma(v)$ (4.11) aims to minimize $|\mathcal{O}_{\sigma(v)}|$. While this is a greedy, local optimization, the intuition is that choosing a successor with a smaller $\mathcal{O}$-set might lead to offset sequences $\mathcal{I}_v$ that are structurally simpler or involve smaller index values, potentially improving the compressibility of the $\mathcal{D}_I(v)$ component. In Chapter 5, we will discuss alternative strategies for selecting successors that considers the overall structure of the DAG.

Remark 4.14. [Unique Sink Transformation] A DAG with multiple sinks can be transformed into one with a unique sink by adding a virtual sink t' ($w(t') = 0$) and connecting all original sinks to it. This transformation preserves the $\mathcal{O}$-sets for all original vertices. The main advantage for our succinct structure is space efficiency: instead of storing potentially numerous and large $\mathcal{O}$-sets for all original sinks (explicit nodes), we only need to store the $\mathcal{O}$-set for the single virtual sink t'. This significantly reduces the cost associated with explicit

nodes, which are generally more space-intensive than implicit nodes, especially for sinks deep within the DAG. We can thus assume, without loss of generality, that our DAG has a unique sink.

Example of the Structure

To illustrate the succinct representation, we apply the principles from Section 4.2.1 to the example DAG introduced in Figure 17. The resulting structure is visualized in Figure 18.
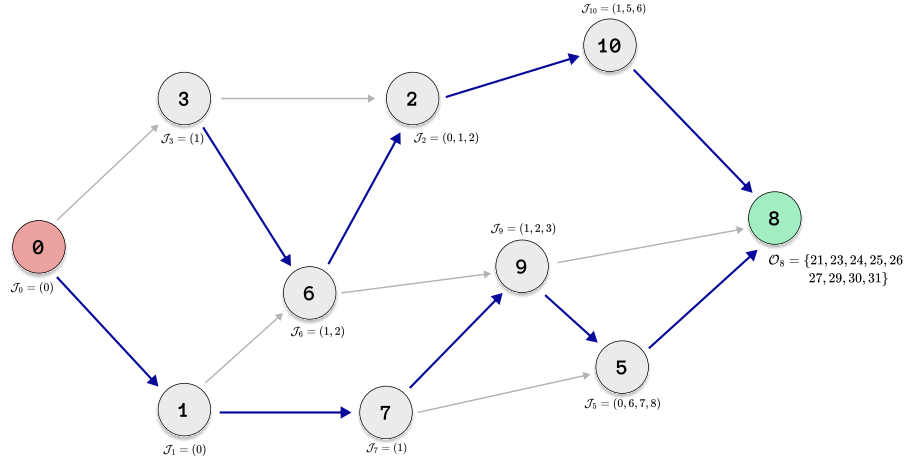

Figure 18: Illustration of the succinct DAG representation for the graph in Figure 17. Implicit nodes are shown with standard borders, while the explicit sink node (8) is shaded green. The source node (0) is red. Highlighted blue edges indicate the chosen successor $\sigma(v)$ for each implicit node v, selected according to 4.11. Labels show the stored associated data $\mathcal{D}[v]$: the full $\mathcal{O}$-set for the explicit node, and the offset sequence $\mathcal{I}_v$ for all implicit nodes.

The construction proceeds in three main steps:

1. *Partitioning:* Vertices are partitioned into explicit sinks $V_E = \{v \mid \mathrm{Succ}(v) = \emptyset\}$ and implicit non-sinks $V_I = V \setminus V_E$. In the example (Figure 18), $V_E = \{8\}$.

2. *Successor Selection:* For each $v \in V_I$, a successor $\sigma(v)$ is chosen from $\mathrm{Succ}(v)$ to minimize $|\mathcal{O}_{\sigma(v)}|$. The selected successors are shown as blue edges in Figure 18. For example, $\sigma(0) = 1$, $\sigma(1) = 7$, $\sigma(3) = 6$, etc.

3. *Associated Data Determination:* The data $\mathcal{D}[v]$ depends on the vertex type: For $v \in V_E$, the full $\mathcal{O}$-set is stored: $\mathcal{D}[v] = \mathcal{D}_E(v) = \mathcal{O}_v$. E.g., $\mathcal{D}[8] = \mathcal{O}_8$ in the figure.

   For $v \in V_I$, the offset sequence $\mathcal{I}_v$ is stored: $\mathcal{D}[v] = \mathcal{D}_I(v) = \mathcal{I}_v$. Let $u = \sigma(v)$. The sequence $\mathcal{I}_v = (j_0, \ldots, j_{m-1})$ where $m = |\mathcal{O}_v|$, provides the indices j_k such that the k-th element x_k of $\mathcal{O}_v$

is reconstructed from the j_k-th element y_{j_k} of $\mathcal{O}_u$ via the rule $x_k = y_{j_k} - w(u)$.

For example, consider $v = 3$. We have $\sigma(3) = 6$, $w(6) = 6$, $\mathcal{O}_3 = \{3\}$ (so $x_0 = 3$), and $\mathcal{O}_6 = \{7, 9\}$ (so $y_0 = 7, y_1 = 9$). We need j_0 such that $x_0 = y_{j_0} - w(6)$, i.e., $3 = y_{j_0} - 6$. This gives $y_{j_0} = 9$, which corresponds to index $j_0 = 1$ in $\mathcal{O}_6$. Thus, $\mathcal{I}_3 = (1)$.

The offset sequences for all implicit nodes are computed similarly and displayed as labels in Figure 18.

This representation stores $\mathcal{O}$-sets only for explicit (sink) nodes. For implicit nodes, it stores references (via σ) and transformations (via $\mathcal{I}_v$ and weights $\mathcal{W}$), enabling reconstruction of path information, as detailed in the next section.

4.3 QUERY ALGORITHMS

This section details the algorithms operating on the succinct DAG representation introduced in Section 4.2. The core idea is to reconstruct the necessary path weight information for a queried node v by traversing the successor path starting from v until an explicit node is reached, using the stored offset sequences and weights to transform the query along the way.

4.3.1 *Reconstructing $\mathcal{O}$-Sets*

To compute queries like rank, we first need a mechanism to retrieve elements of the $\mathcal{O}$-set for any given vertex v. If v is explicit ($v \in V_E$), this is straightforward as $\mathcal{O}_v$ is stored directly (or in a recoverable compressed format) in $\mathcal{D}[v]$. If v is implicit ($v \in V_I$), the value must be reconstructed recursively by following the successor path defined by σ.

Consider the task of retrieving the k-th element of $\mathcal{O}_v$, denoted $\mathcal{O}_v[k]$. The stored offset sequence $\mathcal{I}_v = \mathcal{D}[v]$ provides the corresponding index $j_k = \mathcal{I}_v[k]$ in the $\mathcal{O}$-set of the successor $u = \sigma(v)$, such that $\mathcal{O}_v[k] = \mathcal{O}_u[j_k] - w(u)$. This relation forms the basis of a traversal process. We start at node v with the target index k. We find the successor $u = \sigma(v)$ and update the target index to $j_k = \mathcal{I}_v[k]$. We also accumulate the weight $w(u)$. We repeat this process from u with the new index j_k, following the successor path $v \rightarrow u \rightarrow \cdots \rightarrow e$, where e is the first explicit node encountered. Let the final index reached at node e be K, and let the sum of weights accumulated along the path (excluding $w(v)$ but including $w(e)$ if $e \neq v$) be W_{sum}. The desired value $\mathcal{O}_v[k]$ is then calculated as $\mathcal{O}_e[K] - W_{sum}$.

Figure 19 provides a concrete illustration of this query process, showing the computation of $\mathcal{O}_7[0]$ using the succinct structure from Figure 18.
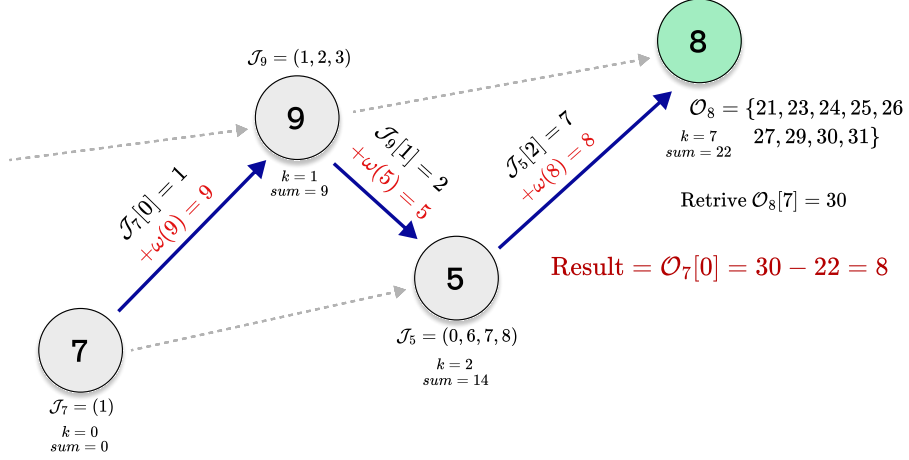

Figure 19: Visualization of the query process for retrieving the element at index $k = 0$ of $\mathcal{O}_7$ using the succinct representation (Figure 18). The query follows the successor path $7 \rightarrow 9 \rightarrow 5 \rightarrow 8$. At each step from an implicit node v to its successor $u = \sigma(v)$, the current index $k_{current}$ is updated using the stored offset $k_{next} = \mathcal{I}_v[k_{current}]$, and the weight $w(u)$ is added to an accumulator (sum). The path starts with $k = 0$ at node 7. It proceeds to node 9 using index $\mathcal{I}_7[0] = 1$, accumulating $w(9) = 9$. Then to node 5 using index $\mathcal{I}_9[1] = 2$, accumulating $w(5) = 5$ (total sum 14). Then to node 8 using index $\mathcal{I}_5[2] = 7$, accumulating $w(8) = 8$ (total sum 22). Node 8 is explicit, so the value at the final index 7, $\mathcal{O}_8[7] = 30$, is retrieved. The result is obtained by subtracting the total accumulated weight: $30 - 22 = 8$. This correctly reconstructs $\mathcal{O}_7[0]$.

The general procedure to compute the k-th element (0-indexed) of $\mathcal{O}_v$ is formalized in Algorithm 10. It implements the traversal and accumulation process described above, relying on accessing the structure components: weights $\mathcal{W}$, successor information Σ (to get $\sigma(v)$ and check for explicit nodes), and associated data $\mathcal{D}$ (to retrieve $\mathcal{I}$ sequences or $\mathcal{O}$-sets)

The correctness of Algorithm 10 follows inductively from the definition of the offset sequence $\mathcal{I}_v$. Let $x_k^{(v)}$ denote the k-th element of $\mathcal{O}_v$. If v is implicit with successor $u = \sigma(v)$, then by construction $x_k^{(v)} = x_{j_k}^{(u)} - w(u)$, where $j_k = \mathcal{I}_v[k]$. The algorithm iteratively applies this relation: if $v \rightarrow u \rightarrow \cdots \rightarrow e$ is the successor path ending at an explicit node e, and the indices transform as

$$k \rightarrow j_k^{(v)} \rightarrow j_{j_k^{(v)}}^{(u)} \rightarrow \cdots \rightarrow K$$

Algorithm 10 GETVALUE(v, k): Compute the k-th element of $\mathcal{O}_v$

Require: Vertex ID v, index $k \in \{0, \dots, |\mathcal{O}_v| - 1\}$.
Ensure: The value of the k-th smallest element in $\mathcal{O}_v$.
1: current_node $\leftarrow v$
2: current_index $\leftarrow k$
3: weight_sum $\leftarrow 0$
4: **while** current_node $\notin V_E$ **do**
5:     successor $\leftarrow \Sigma[\text{current\_node}]$
6:     weight_sum $\leftarrow$ weight_sum $+ \mathcal{W}[\text{successor}]$
7:     $\mathcal{I}_{\text{current\_node}} \leftarrow \mathcal{D}[\text{current\_node}]$
8:     next_index $\leftarrow \mathcal{I}_{\text{current\_node}}[\text{current\_index}]$
9:     current_node $\leftarrow$ successor
10:    current_index $\leftarrow$ next_index
11: **end while**
12: $\mathcal{O}_{\text{explicit}} \leftarrow \mathcal{D}[\text{current\_node}]$
13: base_value $\leftarrow \mathcal{O}_{\text{explicit}}[\text{current\_index}]$
14: **return** base_value $-$ weight_sum

---

then the algorithm computes

$$x_K^{(e)} - \sum_{z \in \text{path } v \to e, z \neq v} w(z)$$

which correctly yields $x_k^{(v)}$.

To reconstruct the entire $\mathcal{O}$-set for a vertex v, we can repeatedly call GETVALUE(v, k) for $k = 0, 1, \dots, |\mathcal{O}_v| - 1$. This requires knowing the size $|\mathcal{O}_v|$. We assume this size information is either stored explicitly for each node or can be efficiently derived (e.g., potentially stored alongside $\mathcal{I}_v$ or $\mathcal{O}_v$ in the $\mathcal{D}$ component). Let LENGTH(v) be an operation that returns $|\mathcal{O}_v|$. This procedure is implemented in Algorithm 11.

Algorithm 11 GETOSET(v): Reconstruct the $\mathcal{O}$-set for vertex v

---

Require: Vertex ID v.
Ensure: The sorted sequence $\mathcal{O}_v$.
1: size $\leftarrow$ LENGTH(v)
2: Initialize an empty list O_list of size size.
3: **for** k from 0 to size $- 1$ **do**
4:     value $\leftarrow$ GETVALUE(v, k)
5:     O_list[k] $\leftarrow$ value
6: **end for**
7: **return** O_list

4.3.2 *Computing the Rank Query*

Equipped with the ability to reconstruct $\mathcal{O}_N$ for any query vertex N via Algorithm 11, we can now implement the rank query as specified

in 4.9. The procedure involves two main steps: first, generate the initial set of intervals based on the elements of $\mathcal{O}_N$ and the weight $w(N)$; second, merge these potentially overlapping or adjacent intervals into a minimal set of disjoint intervals.

The interval merging step is a standard procedure. Given a list of intervals sorted by their starting points, we can merge them efficiently. The core idea is to iterate through the sorted intervals, merging the current interval with the next one if they overlap or are directly adjacent (i.e., the start of the next interval is less than or equal to the end of the current interval plus one). Algorithm 12 formalizes this merging process, which requires linear time with respect to the number of initial intervals

---

Algorithm 12 MERGEINTERVALS(Intervals): Merge sorted intervals

---

Require: A list $\text{Intervals} = \{[l_1, r_1], [l_2, r_2], \dots\}$ sorted by start points l_i.
Ensure: A minimal list MergedIntervals of disjoint intervals
  1: Initialize an empty list MergedIntervals.
  2: **if** Intervals is not empty **then**
  3:     $\text{current\_interval} \leftarrow \text{Intervals}[0]$.
  4:     **for** i from 1 to $\text{length}(\text{Intervals}) - 1$ **do**
  5:         $\text{next\_interval} \leftarrow \text{Intervals}[i]$.
  6:         **if** $\text{next\_interval.l} \leqslant \text{current\_interval.r} + 1$ **then**
  7:             $\text{current\_interval.r} \leftarrow \max(\text{current\_interval.r}, \text{next\_interval.r})$
  8:         **else**
  9:             Append current_interval to MergedIntervals.
 10:             $\text{current\_interval} \leftarrow \text{next\_interval}$.
 11:         **end if**
 12:     **end for**
 13:     Append current_interval to MergedIntervals.
 14: **end if**
 15: **return** MergedIntervals.

Algorithm 13 implements the Rank query defined in 4.9. It begins by reconstructing the set $\mathcal{O}_N$ using GETOSET (Algorithm 11). Then, for each path weight $x \in \mathcal{O}_N$, it generates the interval $[\max(0, x - w_N + 1), x]$ according to the transformation rule specified in Definition 4.9, where $w_N = \mathcal{W}[N]$. The union of these generated intervals constitutes the set S_N:

$$S_N = \bigcup_{x \in \mathcal{O}_N} [\max(0, x - w_N + 1), x].$$

Since these intervals may overlap or be adjacent, they are first sorted by their starting points. The sorted intervals are then merged via Algorithm 12 (line 10) to compute the final result $\mathcal{R}_N$, which is the minimal representation of S_N as disjoint intervals.

Algorithm 13 $\text{Rank}_G(N)$: Compute the Rank query for vertex N

Require: Vertex ID N.
Ensure: A minimal set of disjoint intervals $\mathcal{R}_N$ representing S_N
1: $\mathcal{O}_N \leftarrow \text{GETOSET}(N)$
2: $w_N \leftarrow \mathcal{W}[N]$
3: Initialize an empty list InitialIntervals.
4: **for** each $x \in \mathcal{O}_N$ **do**
5:      $l \leftarrow \max(0, x - w_N + 1)$
6:      $r \leftarrow x$
7:      Append the interval $[l, r]$ to InitialIntervals.
8: **end for**
9: Sort InitialIntervals based on the starting point l.
10: MergedIntervals $\leftarrow \text{MERGEINTERVALS}(\text{InitialIntervals})$
11: **return** MergedIntervals.

Example: Rank Query Computation

We illustrate the execution of Algorithm 13 to compute $\text{Rank}_G(N)$ for vertex $N = 2$. Referring to the example structure presented in Figure 17 and Figure 18, this vertex has weight $w(2) = 2$.

First, the computation requires the $\mathcal{O}$-set for node 2. The algorithm calls $\text{GETOSET}(2)$ (Algorithm 11), which utilizes $\text{GETVALUE}(2, k)$ (Algorithm 10) for $k = 0, 1, \ldots, |\mathcal{O}_2| - 1$. As described previously (Section 4.3.1 and Figure 19 show a similar process), GETVALUE traverses the successor path determined by σ. For node 2, this path is $2 \to 10 \to 8$. By following this path, applying the offset indices $\mathcal{I}_2 = \mathcal{D}[2]$ and $\mathcal{I}_{10} = \mathcal{D}[10]$, accumulating the weights $w(10) = \mathcal{W}[10]$ and $w(8) = \mathcal{W}[8]$, and retrieving the base value from the explicit node's data $\mathcal{D}[8] = \mathcal{O}_8$, the set $\mathcal{O}_2 = \{5, 9, 11\}$ is reconstructed.

Next, the weight of the query node, $w_N = w(2) = 2$, is retrieved (from $\mathcal{W}[2]$).

The algorithm then proceeds to generate the initial set of intervals. Each element $x \in \mathcal{O}_2$ is transformed into an interval $[\max(0, x - w_2 + 1), x]$ using the rule from Definition 4.9:

$$\begin{aligned}
x = 5 &\longrightarrow [\max(0, 5 - 2 + 1), 5] = [4, 5] \\
x = 9 &\longrightarrow [\max(0, 9 - 2 + 1), 9] = [8, 9] \\
x = 11 &\longrightarrow [\max(0, 11 - 2 + 1), 11] = [10, 11]
\end{aligned}$$

This yields the initial list of intervals

$$\text{InitialIntervals} = \{[4, 5], [8, 9], [10, 11]\}.$$

Finally, MERGEINTERVALS (Algorithm 12) is applied to this list[4]. The intervals $[8, 9]$ and $[10, 11]$ merge because $10 \leqslant 9 + 1$, resulting in

---

4 after sorting, which does not change the order in this specific case.

[8, 11]. The interval [4, 5] remains distinct as $8 > 5 + 1$. The final result returned by $\text{Rank}_G(2)$ is the minimal set of disjoint intervals $\mathcal{R}_2 = \{[4, 5], [8, 11]\}$.

4.4 COMPRESSION STRATEGIES

The succinct representation presented in Section 4.2 consists of arrays for weights ($\mathcal{W}$), successor information (Σ), and associated data ($\mathcal{D}$). To further reduce the memory footprint beyond the gains achieved by the explicit/implicit node partitioning, this section discusses compression techniques for each component.

We primarily consider variable-length integer coding (Section 2.6), Elias-Fano encoding (Section 2.6.4), and Run-Length Encoding (RLE), aiming to preserve efficient access needed for query evaluation (Algorithms 10 and 13), potentially using structures like the compressed integer vectors from Appendix A.

4.4.1 *Weights and Successors*

The components $\mathcal{W}$ and Σ are arrays of integers, both without any guarantee of monotonicity or specific distribution patterns a priori.

- $\mathcal{W}$: An array of length $n = |V|$, where $\mathcal{W}[v] = w(v) \in \mathbb{N}_0$. The values are non-negative integers representing vertex weights.

- Σ: An array of length n, where $\Sigma[v]$ stores either the integer ID $\sigma(v) \in \{0, \ldots, n - 1\}$ if $v \in V_I$, or a special marker (which can also be represented as an integer) if $v \in V_E$.

Since both $\mathcal{W}$ and Σ are integer sequences, variable-length coding schemes from Section 2.6 (e.g., Unary, Elias Gamma/Delta, Rice codes) are applicable. The choice of the best code depends on the observed distribution of weights and successor IDs.

To combine compression with efficient random access (retrieving $\mathcal{W}[v]$ or $\Sigma[v]$), the compressed-intvec structure (Appendix A) is a suitable implementation choice. It allows selecting an appropriate integer codec and uses sampling to achieve constant expected time access, with sub-linear space overhead for samples.

Alternatively, if the range of values (maximum weight or n) is small, treating them as symbols from a small alphabet α allows using Wavelet Trees (Section 3.2) or related structures (Section 3.2.3). These offer $O(\log |\alpha|)$ access time. However, for general graphs with potentially large weights or vertex counts, direct integer coding via compressed-intvec is often more practical.

4.4.2 *Associated Data Sequences*

The associated data component $\mathcal{D}$ stores sequences that encode path weight information. Specifically, for an explicit vertex $v \in V_E$, $\mathcal{D}[v]$ holds the $\mathcal{O}$-set $\mathcal{O}_v = (x_0, \ldots, x_{m-1})$, and for an implicit vertex $v \in V_I$, it holds the offset sequence $\mathcal{I}_v = (j_0, \ldots, j_{m-1})$. Both $\mathcal{O}_v$ and $\mathcal{I}_v$ are sequences of non-negative integers which are strictly increasing ($x_k < x_{k+1}$ and $j_k < j_{k+1}$ respectively), as established by their definitions and construction rules.

This strictly monotonic property makes these sequences suitable for specialized compression techniques. Elias-Fano encoding (Section 2.6.4), discussed previously, is a strong candidate offering both good compression ratios and efficient support for operations like random access. An alternative approach, particularly effective when sequences contain long stretches of consecutive integers, is Run-Length Encoding (RLE). We detail the RLE representation below.

Run-Length Encoding (RLE) Representation

Run-Length Encoding compresses a monotonic sequence by identifying and representing consecutive values efficiently. Consider a generic strictly increasing sequence $Y = (y_0, y_1, \ldots, y_{m-1})$. A *run* is a maximal contiguous subsequence $(y_i, y_{i+1}, \ldots, y_{i+l-1})$ where each element is exactly one greater than its predecessor ($y_{j+1} = y_j + 1$ for $i \leqslant j < i + l - 1$). A run can have length $l = 1$. RLE represents the sequence Y by encoding each run using its starting value and its length.

The RLE process generates two auxiliary sequences:

- The *run starts sequence*, $S = (s_1, s_2, \ldots, s_p)$, contains the first value s_i of the i-th run in Y. Since runs are maximal and Y is strictly increasing, S is also strictly increasing.

- The *run lengths sequence*, $L = (l_1, l_2, \ldots, l_p)$, contains the length $l_i \geqslant 1$ of the i-th run. L is a sequence of positive integers with no other guaranteed properties.

The pair (S, L) allows for the exact reconstruction of Y. Algorithm 14 outlines the procedure to compute S and L from Y.

The space efficiency of RLE relies on effectively compressing the resulting sequences S and L. The run starts sequence $S = (s_1, \ldots, s_p)$ is strictly monotonic. Consequently, it is an ideal candidate for Elias-Fano encoding (Section 2.6.4).

Algorithm 14 ENCODERLE(Y): RLE encoding of a monotonic sequence

---

Require: Monotonic sequence $Y = (y_0, y_1, \ldots, y_{m-1})$, where $m = |Y|$.
Ensure: Run starts sequence S, Run lengths sequence L.
  1: Initialize $S \leftarrow \emptyset$, $L \leftarrow \emptyset$.
  2: **if** $m = 0$ **then**
  3:     **return** (S, L)
  4: **end if**
  5: $i \leftarrow 0$
  6: **while** $i < m$ **do**
  7:     current_start $\leftarrow y_i$
  8:     current_length $\leftarrow 1$
  9:     **while** $i + 1 < m$ and $y_{i+1} = y_i + 1$ **do**
 10:         current_length $\leftarrow$ current_length $+ 1$
 11:         $i \leftarrow i + 1$
 12:     **end while**
 13:     Append current_start to S.
 14:     Append current_length to L.
 15:     $i \leftarrow i + 1$
 16: **end while**
 17: **return** (S, L)

The run lengths sequence $L = (l_1, \ldots, l_p)$ is a sequence of positive integers without guaranteed structure. Standard variable-length integer codes (Section 2.6), such as Elias Gamma or Delta codes, can be applied. In practice, employing a structure like the compressed-intvec (Appendix A) allows choosing an appropriate codec and provides efficient random access.

Random Access with RLE Sequences

Retrieving the element y_k (the element at index k in the original sequence Y, $0 \leqslant k < m$) from the RLE representation (S, L) requires identifying the run to which y_k belongs. This necessitates finding the unique run index i^* (where $1 \leqslant i^* \leqslant p$) such that:

$$\sum_{j=1}^{i^*-1} l_j \leqslant k < \sum_{j=1}^{i^*} l_j$$

where the sum is defined as 0 if $i^* = 1$. Once i^* is found, the value y_k is given by:

$$y_k = s_{i^*} + \left(k - \sum_{j=1}^{i^*-1} l_j \right)$$

Computing the prefix sums $\sum l_j$ on the fly requires iterating through L, potentially leading to $O(p)$ time complexity for access, which is inefficient if the number of runs p is large.

To accelerate random access, one can precompute and store the sequence of prefix sums of the run lengths:

$$P = (p_1, p_2, \ldots, p_p) \qquad p_i = \sum_{j=1}^{i} l_j.$$

Since $l_j \geqslant 1$ for all j, the sequence P is strictly increasing. As a strictly monotonic sequence, P itself can be compressed effectively, for instance, using Elias-Fano encoding.

With the prefix sum sequence P available, finding the index i^* corresponding to the query index k reduces to searching for the smallest i^* such that $p_{i^*} > k$. This is a successor search problem on the monotonic sequence P. Using binary search on P (if stored as an array) takes $O(\log p)$ time. If P is stored in a structure supporting faster searches (like rank/select structures built upon certain Elias-Fano constructions), this lookup time might be further improved. Algorithm 15 formalizes access using prefix sums.

Algorithm 15 GETVALUERLE(S, L, P, k): Retrieve element from RLE

Require: $S = (s_1, \ldots, s_p)$, $L = (l_1, \ldots, l_p)$, $P = (p_1, \ldots, p_p)$, $k \in [0, m-1]$.
Ensure: The value y_k of the element at index k.
1: Find smallest $i^* \in \{1, \ldots, p\}$ such that $P[i^*] > k$.
2: **if** $i^* = 1$ **then**
3: $\quad$ previous_cumulative_length $\leftarrow 0$
4: **else**
5: $\quad$ previous_cumulative_length $\leftarrow P[i^* - 1]$
6: **end if**
7: offset $\leftarrow k -$ previous_cumulative_length
8: start_value $\leftarrow S[i^*]$
9: **return** start_value $+$ offset

Choosing Between Elias-Fano and RLE

The choice between direct Elias-Fano encoding and Run-Length Encoding (RLE) for representing the strictly increasing sequences $\mathcal{O}_v$ and $\mathcal{I}_v$ depends on their structure. RLE is advantageous when the sequence exhibits significant clustering, meaning the number of runs p is substantially smaller than the total number of elements m ($p \ll m$). In such cases, the combined compressed size of the run starts S and run lengths L (and potentially the prefix sums P) might be less than direct Elias-Fano encoding of the original sequence.

On the other hand, if sequences are sparse or lack significant runs (p is close to m), direct Elias-Fano is likely more straightforward and potentially more space-efficient.

Regardless of the chosen compression method, representing the entire associated data component $\mathcal{D}$ practically involves concatenating

the compressed representations of all sequences ($\{\mathcal{D}_E(v)\}_{v \in V_E}$ and $\{\mathcal{D}_I(v)\}_{v \in V_I}$) into a single buffer. An auxiliary index structure is then needed to map each vertex ID v to the starting position and metadata of its compressed sequence. The space overhead for this index is typically negligible compared to the compressed data itself

4.5 ACHIEVING SUB-ENTROPY SPACE FOR PATH QUERIES

To evaluate the space efficiency of our proposed structure, we establish a baseline based on the information content in the weighted DAG itself. Drawing upon the principles of information theory outlined in Chapter 2, we can define a measure of entropy for the graph $G = (V, E, w)$.

Any *lossless* representation of the graph G must, at a minimum, encode the information required to uniquely define its structure (the edges E) and the associated weights (the function w). We formulate a 0th-order entropy measure, denoted $\mathcal{H}_0(G)$, as a lower bound on the number of bits required to represent these components, assuming no prior knowledge about correlations or higher-order statistical properties.

The information content required to represent the sequence of vertex weights $(w(v))_{v \in V}$ constitutes the first component. A fundamental lower bound, denoted $\mathcal{H}_W(G)$, can be established by considering the minimal binary representation length for each individual weight:

$$\mathcal{H}_W(G) = \sum_{v \in V} \lceil \log_2(w(v) + 1) \rceil \quad \text{bits.}$$

This measure reflects the space needed assuming each weight is encoded independently, using the minimal bits for its value, without leveraging potential statistical correlations or distribution patterns suitable for techniques like variable-length integer coding (Section 2.6).

The second component relates to the graph's topology, specifically the set of edges E. With $n = |V|$ vertices, there exist $n(n-1)$ possible directed edges (excluding self-loops). Encoding the topology requires identifying which $m = |E|$ of these potential edges are present. Assuming all directed graphs with n vertices and m edges are equally probable a priori, the information content is determined by the number of ways to choose these m edges. This leads to the topological information component, $\mathcal{H}_E(G)$:

$$\mathcal{H}_E(G) = \log_2 \binom{n(n-1)}{m} \quad \text{bits.}$$

This quantity can be approximated using Stirling's formula,

$$\log_2 \binom{N}{k} \approx k \log_2(N/k) + O(k)$$

yielding

$$\mathcal{H}_E(G) \approx m \log_2 \left(\frac{n(n-1)}{m} \right) + O(m) \quad \text{bits}$$

Combining these components gives us a formal definition for the 0th-order entropy of the weighted DAG.

Definition 4.15 (0th-Order Weighted DAG Entropy). *For a weighted DAG $G = (V, E, w)$ with $n = |V|$ vertices and $m = |E|$ edges, its 0th-order entropy $\mathcal{H}_0(G)$ is defined as the sum of the information content required for the weights and the topology:*

$$\mathcal{H}_0(G) = \underbrace{\sum_{v \in V} \lceil \log_2(w(v) + 1) \rceil}_{\mathcal{H}_W(G)} + \underbrace{\log_2 \binom{n(n-1)}{m}}_{\mathcal{H}_E(G)} \quad \textit{bits.}$$

The value $\mathcal{H}_0(G)$ represents a theoretical lower bound on the space required by any lossless encoding of the graph (V, E, w) based solely on its zero-order statistics.

Our proposed succinct data structure (Section 4.2), however, is designed differently. While lossless for rank query computation (4.9), it is inherently *lossy* concerning the reconstruction of the original graph G, as it does not store the complete edge set E. It retains only vertex weights W, successor information Σ, and associated data $\mathcal{D}$. This distinction allows the structure's space usage, $S(G)$, to potentially fall below the $\mathcal{H}_0(G)$ bound.

To illustrate this, we analyze space performance on a weighted DAG derived from unrolling a Bitcoin temporal network graph [33] (details of the unrolling process are beyond the scope of this thesis), having $n = 22,210$ vertices and $m = 50,514$ edges. For this specific DAG, the calculated 0th-order entropy $\mathcal{H}_0(G)$ amounts to 1,525,730 bits, comprising $\mathcal{H}_W(G) = 60,824$ bits for weights and $\mathcal{H}_E(G) = 1,464,906$ bits for topology according to 4.15.

We compare this theoretical lower bound $\mathcal{H}_0(G)$ against theoretical estimates of the space required by our succinct structure and alternative approaches based on precomputation.

For sequences composed of general non-negative integers x, such as the vertex weights W, the successor identifiers Σ, or the interval endpoints in baseline precomputation results, the space estimation is based on summing the minimal binary representation cost for each

integer independently. This cost is calculated as $\lceil \log_2(x+1) \rceil$ bits per integer x.

When representing strictly monotonic sequences, like the run start values in RLE or interval endpoints compressed using Elias-Fano (Section 2.6.4), our space estimation relies on its established theoretical complexity. Theorem 2.36 guarantees an upper bound of

$$n \log_2(u/n) + 2n$$

bits for encoding n integers within the range $[0, u)$ using Elias-Fano.

Finally, the space for the offset sequences $\mathcal{I}_v$ when stored using the Run-Length Encoding (RLE) scheme described in Section 4.4 is estimated by combining the previous principles. It requires the sum of the space estimate for the strictly monotonic sequence of run start values (using the Elias-Fano estimation) and the space estimate for the sequence of corresponding run lengths (using the minimal binary representation cost for each length).

Component / Method	Estimated Bits
Theoretical Lower Bound ($\mathcal{H}_0(G)$)	
0th-Order Entropy Total	1,525,730
Weights Component ($\mathcal{H}_W(G)$)	60,824
Topology Component ($\mathcal{H}_E(G)$)	1,464,906
Precomputed Rank Queries	
Explicit Storage (Minimal Binary)	4,854,533
Elias-Fano Compressed Storage	2,211,849
Succinct DAG Representation (RLE)	
Total Space ($S(G)$)	602,808
Weights $\mathcal{W}$ (Minimal Binary)	60,824
Successors Σ (Minimal Binary)	297,700
Associated Data $\mathcal{D}$ (RLE Offsets)	244,284

Table 2: Theoretical space estimates (in bits) for the example Bitcoin DAG ($n = 22,210$, $m = 50,514$).

Table 2 presents the results of this theoretical space estimation for the example DAG. The total estimated space for our succinct DAG representation using RLE for the offsets, $S(G)$, is 602,808 bits. This value is notably less than half of the 0th-order graph entropy $\mathcal{H}_0(G)$ (1,525,730 bits), demonstrating the benefit of storing only query-relevant information rather than the full graph topology.

Furthermore, the comparison against precomputation strategies underscores the practical advantages of our approach. Precomputing and storing all rank query results explicitly represents a baseline for

achieving minimal query time (potentially $O(1)$ access), but at a significant space cost, estimated at 4,854,533 bits even with minimal binary encoding. Attempting to mitigate this by compressing the precomputed results using Elias-Fano still requires 2,211,849 bits. While this compression offers substantial savings over the explicit form, the resulting space remains considerably larger than both the graph entropy bound $\mathcal{H}_0(G)$ and, more importantly, the space achieved by our succinct structure $(S(G))$.

Therefore, our analysis indicates that the proposed succinct DAG representation provides not only a mechanism to answer complex path queries but does so with remarkable space efficiency. It avoids the prohibitive space overhead associated with direct precomputation strategies, offering a compact alternative that surpasses even optimized precomputation methods in terms of storage footprint, and falls below conventional entropy bounds for lossless graph representation due to its targeted, query-specific information retention.

5

CONCLUSION AND FUTURE DIRECTIONS

This thesis began by covering data compression, succinct data structures and sequence queries. Building on that foundation, Chapter 4 introduced our primary contribution: a space-efficient method for representing node-weighted Directed Acyclic Graphs (DAGs). This representation is specifically designed to support rank (4.9) queries, which aggregate cumulative path weights ending at a particular vertex.

The core contribution presented in Chapter 4 is a succinct representation strategy for weighted DAGs. Motivated initially by the reinterpretation of the degenerate string problem as a graph problem, we generalized the approach to arbitrary weighted DAGs. The key idea involves partitioning the vertices into two sets: explicit vertices (V_E), typically comprising the sink nodes, for which path weight information ($\mathcal{O}$-sets) is stored directly; and implicit vertices (V_I), for which this information is derived indirectly. This derivation relies on a carefully defined successor function, σ, which designates a specific successor for each implicit node, guiding a traversal path. Associated with each implicit node v, an offset sequence $\mathcal{I}_v$ stores the necessary indices to reconstruct its $\mathcal{O}$-set elements from the $\mathcal{O}$-set of its designated successor $\sigma(v)$. Query algorithms, notably GETVALUE (10) and GETOSET (11), were presented, demonstrating how to reconstruct the path weight information by traversing these successor paths until an explicit node is reached.

Furthermore, we investigated compression strategies for the components of our structure, vertex weights W, successor information Σ, and the associated data $\mathcal{D}$ (containing $\mathcal{O}$-sets or $\mathcal{I}$ sequences). Techniques such as variable-length integer coding and Run-Length Encoding, coupled with methods like Elias-Fano encoding for monotonic sequences, were discussed to minimize space occupancy. A significant finding highlighted in Section 4.5 is that the space usage of our proposed structure can fall below the established 0th-order entropy lower bound for lossless graph representation. This is possible because our structure is tailored specifically for the rank query and does not retain the full topological information (the complete edge set E) of the original DAG, thereby achieving high space efficiency for its designated task compared to both lossless graph encodings and methods based on precomputing query results.

FUTURE DIRECTIONS

While the developed succinct DAG representation offers substantial space savings, a potential performance consideration arises from the query evaluation process itself. The time required to compute a query for an implicit node v depends directly on the length of the successor path that must be traversed from v until an explicit node is encountered (as seen in Algorithm 10). In large or deep DAGs, these paths could potentially become long, leading to variability and potentially slow query times in the worst case for certain nodes. This observation motivates a primary direction for future research: enhancing the query time predictability and efficiency by ensuring that all implicit nodes are reasonably close to an explicit node within the successor path structure.

To address this, instead of relying solely on the sink nodes as the base cases for path traversal, we propose a strategy based on ensuring a maximum traversal distance, denoted by a predefined integer k. The core idea is to augment the original set of explicit nodes V_E (initially, the sinks) with a carefully selected subset of currently implicit nodes, resulting in a new, larger set of explicit nodes $V_E' \supseteq V_E$. This target set V_E' must satisfy a specific property related to the successor function σ: every vertex v that remains implicit (i.e., $v \in V \setminus V_E'$) must be able to reach some node $u \in V_E'$ by following the successor path defined by σ, using at most k steps. More formally, let the successor path starting from v be the sequence $v_0 = v, v_1 = \sigma(v_0), v_2 = \sigma(v_1), \ldots$. Then, for every $v \in V \setminus V_E'$, there must exist an index j, where $0 \leqslant j \leqslant k$, such that $v_j \in V_E'$.

The challenge then becomes selecting such a set V_E' that is as small as possible, in order to minimize the additional space overhead associated with storing the 0-sets explicitly for these newly designated explicit nodes. This optimization problem is conceptually analogous to finding a minimum distance-k dominating set in a graph [25]. In the standard definition, a distance-k dominating set D is a subset of vertices such that every vertex not in D is within a distance of k (measured by the number of edges in a shortest path) from at least one vertex in D. Our formulation adapts this concept: the distance is measured specifically along the directed paths induced by the successor function σ, and the goal is to find a set V_E' of minimum cardinality that *dominates* all other vertices within k steps along these σ-paths. Finding a minimum distance-k dominating set is known to be an NP-hard problem for general graphs [25]. Furthermore, the problem of finding a minimum cardinality set V_E' satisfying our k-step σ-path constraint on a DAG is also NP-hard; this can be demonstrated through a reduction from the Set Cover problem, indicating

that finding an optimal solution is likely computationally intractable for large DAGs.

Consequently, a practical direction for future investigation involves the design and analysis of efficient heuristics. Such heuristics would aim to construct a set V'_E satisfying the k-distance requirement along σ-paths, while keeping its size reasonably small, even if not guaranteeing absolute minimality. The choice of heuristic would need to balance the quality of the solution (size of V'_E) with the computational cost of finding it.

Once a suitable set V'_E has been determined (whether optimally or via a heuristic), the successor selection function σ needs to be redefined to leverage this structure. For an implicit node $v \in V \setminus V'_E$, the choice of its designated successor $σ(v)$ from the set $Succ(v)$ should prioritize reaching *any* node within the target set V'_E as quickly as possible along the subsequent σ-path. That is, $σ(v)$ should ideally be selected as the node $u \in Succ(v)$ which minimizes the length of the σ-path starting from u to the nearest node in V'_E. Ties in path length could be resolved using secondary criteria, such as minimizing the $\mathcal{O}$-set cardinality $|\mathcal{O}_u|$ (as in the original heuristic) or simply selecting the successor with the minimum vertex identifier.

Implementing this refined strategy directly imposes an upper bound of k on the number of iterations performed by the main loop in Algorithm 10. This provides a worst-case guarantee on the time complexity of the path traversal component for any rank query, making the overall query performance significantly more predictable and uniform across all nodes, regardless of their position within the DAG. The main trade-off shifts to the selection of the parameter k: smaller values of k yield faster worst-case query times but likely necessitate larger (and thus more space-consuming) sets V'_E, whereas larger values of k may permit smaller sets V'_E at the expense of a higher query time bound.

A

ENGINEERING A COMPRESSED INTEGER VECTOR

This appendix outlines the design principles and engineering considerations behind *compressed-intvec*, a software library that we developed for the efficient storage and retrieval of integer sequences [34]. The library leverages the variable-length integer coding techniques discussed in Section 2.6 to achieve significant space savings compared to standard fixed-width representations, while providing mechanisms for fast random access.

BITSTREAM ABSTRACTION   Storing sequences of integers, particularly when many values are small or follow predictable patterns, using standard fixed-width types (such as 64-bit integers) is inherently wasteful. Variable-length integer codes, such as Unary, Gamma, Delta, and Rice codes (Section 2.6), offer a solution by representing integers using a number of bits closer to their information content, assigning shorter codes to smaller or more frequent values.

However, codes produce binary representations of varying lengths, not necessarily aligned to byte or machine word boundaries. Therefore, storing a sequence of integers compressed with these methods requires packing their binary codes contiguously into a single, undifferentiated sequence of bits, commonly referred to as a bitstream. This necessitates the use of specialized bitstream reading and writing capabilities, abstracting away the complexities of bit-level manipulation. The implementation described here relies on the `dsi-bitstream` library for this purpose [56], ensuring that the variable-length codes can be written to and read from memory efficiently. The fundamental requirement for correctly decoding the concatenated sequence is the prefix-free (self-delimiting) property of the chosen integer code, which guarantees that the end of one codeword can be determined without ambiguity before reading the next.

RANDOM ACCESS VIA SAMPLING   While bitstream concatenation enables compression, it introduces a significant challenge for random access. Retrieving the i-th integer from the original sequence cannot be done by calculating a simple memory offset, as the bit lengths of preceding elements are variable. A naive approach would require sequentially decoding the first i integers from the beginning of the bitstream, resulting in an unacceptable $O(i)$ access time.

To provide efficient random access, the *compressed-intvec* library employs a *sampling* technique. During the encoding phase, the absolute starting bit position of every k-th integer in the sequence is recorded. These positions, or samples, are stored in an auxiliary data structure, typically a simple array. The value k is a user-configurable sampling parameter that dictates a trade-off between random access speed and the memory overhead incurred by storing the samples.

To retrieve the i-th integer, the library first determines the index of the sample corresponding to the block containing the i-th element: `sample_idx` $= \lfloor i/k \rfloor$. It retrieves the bit offset `start_bit` associated with this sample. The bitstream reader can then jump directly to this position. From `start_bit`, the decoder only needs to perform $i \pmod k$ sequential decoding operations to reach and return the desired i-th integer. If k is considered a constant, this reduces the expected time complexity for random access to $O(1)$[1]. The space overhead for the samples is approximately $O((n/k)\log(\text{total\_bits}))$, which is generally sub-linear in the size of the compressed data for practical values of k. The choice of k allows tuning the balance between faster access (smaller k) and lower memory usage (larger k).

CODEC FLEXIBILITY   The compression effectiveness of various integer coding techniques, as detailed in Section 2.6, is highly contingent upon the statistical properties of the integer sequence being encoded. For instance, Gamma coding is generally well-suited for distributions exhibiting decay proportional to $1/x^2$, Rice codes demonstrate efficiency for geometrically distributed data, and Minimal Binary coding provides optimal compression for integers uniformly distributed within a known range $[0, u)$.

This data-dependent performance necessitates adaptability in the choice of coding scheme (*codec*). The *compressed-intvec* library achieves this through an abstraction mechanism based on Rust traits. These traits define a formal interface that different codec implementations must satisfy, allowing the library's core logic to remain agnostic to the specific encoding details. Consequently, the user can parameterize the compressed vector type with the most suitable codec implementation for their particular data distribution at compile time. The selection of an inappropriate codec relative to the data's characteristics can substantially degrade compression performance, potentially yielding a representation larger than the uncompressed equivalent.

---

1 The underlying bitstream operations and single-integer decoding are sufficiently fast to assume that

BIBLIOGRAPHY

[1] Jarno N Alanko, Simon J Puglisi, and Jaakko Vuohtoniemi. "Small searchable κ-spectra via subset rank queries on the spectral burrows-wheeler transform." In: *SIAM Conference on Applied and Computational Discrete Algorithms (ACDA23)*. SIAM. 2023, pp. 225–236.

[2] Jarno N. Alanko et al. "Subset Wavelet Trees." In: *21st International Symposium on Experimental Algorithms (SEA 2023)*. Ed. by Loukas Georgiadis. Vol. 265. Leibniz International Proceedings in Informatics (LIPIcs). Schloss Dagstuhl – Leibniz-Zentrum für Informatik, 2023, 4:1–4:14.

[3] Mai Alzamel et al. "Degenerate string comparison and applications." In: *WABI 2018-18th Workshop on Algorithms in Bioinformatics*. Vol. 113. 2018, pp. 1–14.

[4] David Benoit et al. "Representing trees of higher degree." In: *Algorithmica* 43 (2005), pp. 275–292.

[5] Philip Bille, Inge Li Gørtz, and Tord Stordalen. *Rank and Select on Degenerate Strings*. 2023.

[6] Michael Burrows. "A block-sorting lossless data compression algorithm." In: *SRS Research Report* 124 (1994).

[7] Bernard Chazelle. "A Functional Approach to Data Structures and Its Use in Multidimensional Searching." In: *SIAM Journal on Computing* 17.3 (1988), pp. 427–462.

[8] David Clark. "Compact pat trees." In: (1997).

[9] Francisco Claude, Gonzalo Navarro, and Alberto Ordónez. "The wavelet matrix: An efficient wavelet tree for large alphabets." In: *Information Systems* 47 (2015), pp. 15–32.

[10] T.M. Cover and J.A. Thomas. *Elements of Information Theory*. Wiley, 2012.

[11] P. Elias. "Universal codeword sets and representations of the integers." In: *IEEE Transactions on Information Theory* 21.2 (1975), pp. 194–203.

[12] Robert Mario Fano. *On the number of bits required to implement an associative memory*. Massachusetts Institute of Technology, Project MAC, 1971.

[13] P. Ferragina. *Pearls of Algorithm Engineering*. Cambridge University Press, 2023.

[14] Paolo Ferragina, Raffaele Giancarlo, and Giovanni Manzini. "The myriad virtues of Wavelet Trees." In: *Information and Computation* 207.8 (2009), pp. 849–866.

[15] Paolo Ferragina and Giovanni Manzini. "Opportunistic data structures with applications." In: *Proceedings 41st annual symposium on foundations of computer science*. IEEE. 2000, pp. 390–398.

[16] Paolo Ferragina et al. "Compressed representations of sequences and full-text indexes." In: *ACM Transactions on Algorithms (TALG)* 3.2 (2007), 20–es.

[17] Michael J Fischer and Michael S Paterson. "String-matching and other products." In: (1974).

[18] Simon Gog et al. "From theory to practice: Plug and play with succinct data structures." In: *Experimental Algorithms: 13th International Symposium, SEA 2014, Copenhagen, Denmark, June 29–July 1, 2014. Proceedings 13*. Springer. 2014, pp. 326–337.

[19] Solomon Golomb. "Run-length encodings (corresp.)" In: *IEEE transactions on information theory* 12.3 (1966), pp. 399–401.

[20] Alexander Golynski. "Rank/Select Operations on Large Alphabets: a Tool for Text." In: *Proceedings of the Seventeenth Annual ACM-SIAM Symposium on Discrete Algorithms*. Vol. 122. SIAM. 2006, p. 368.

[21] Roberto Grossi, Ankur Gupta, and Jeffrey Vitter. "High-Order Entropy-Compressed Text Indexes." In: *Proceedings of the Annual ACM-SIAM Symposium on Discrete Algorithms* (Nov. 2002).

[22] Roberto Grossi, Ankur Gupta, Jeffrey Scott Vitter, et al. "When indexing equals compression: experiments with compressing suffix arrays and applications." In: *SODA*. Vol. 4. 2004, pp. 636–645.

[23] Roberto Grossi, Jeffrey Scott Vitter, and Bojian Xu. "Wavelet Trees: From Theory to Practice." In: *2011 First International Conference on Data Compression, Communications and Processing*. 2011, pp. 210–221.

[24] T.S. Han and K. Kobayashi. *Mathematics of Information and Coding*. Fields Institute Monographs. American Mathematical Society, 2002.

[25] Teresa W Haynes, Stephen Hedetniemi, and Peter Slater. *Fundamentals of domination in graphs*. CRC press, 2013.

[26] David A Huffman. "A method for the construction of minimum-redundancy codes." In: *Proceedings of the IRE* 40.9 (1952), pp. 1098–1101.

[27] David A. Huffman. "A Method for the Construction of Minimum-Redundancy Codes." In: *Proceedings of the IRE* 40.9 (1952), pp. 1098–1101.

[28] G. Jacobson. "Space-efficient static trees and graphs." In: *30th Annual Symposium on Foundations of Computer Science*. 1989, pp. 549–554.

[29] Guy Joseph Jacobson. *Succinct static data structures*. 1988.

[30] J Kärkkäinen. "Repetition-based text indexing." PhD thesis. Ph. D. thesis, Department of Computer Science, University of Helsinki, Finland, 1999.

[31] Juha Kärkkäinen and Simon J Puglisi. "Fixed block compression boosting in FM-indexes." In: *International Symposium on String Processing and Information Retrieval*. Springer. 2011, pp. 174–184.

[32] S Rao Kosaraju and Giovanni Manzini. "Compression of low entropy strings with Lempel–Ziv algorithms." In: *SIAM Journal on Computing* 29.3 (2000), pp. 893–911.

[33] Srijan Kumar et al. "Rev2: Fraudulent user prediction in rating platforms." In: *Proceedings of the Eleventh ACM International Conference on Web Search and Data Mining*. ACM. 2018, pp. 333–341.

[34] Luca Lombardo. *compressed-intvec: Compressed Integer Vector Library*. Rust Crate. Accessed: May 2025. URL: https://crates.io/crates/compressed-intvec.

[35] Veli Mäkinen and Gonzalo Navarro. "New search algorithms and time/space tradeoffs for succinct suffix arrays." In: *Technical rep. C-2004-20 (April). University of Helsinki, Helsinki, Finland* (2004).

[36] Veli Mäkinen and Gonzalo Navarro. "Position-Restricted Substring Searching." In: *LATIN 2006: Theoretical Informatics*. Ed. by José R. Correa, Alejandro Hevia, and Marcos Kiwi. Springer Berlin Heidelberg, 2006, pp. 703–714.

[37] Veli Mäkinen and Gonzalo Navarro. "Rank and select revisited and extended." In: *Theoretical Computer Science* 387.3 (2007), pp. 332–347.

[38] Giovanni Manzini. "An analysis of the Burrows—Wheeler transform." In: *Journal of the ACM (JACM)* 48.3 (2001), pp. 407–430.

[39] Rossano Venturini Matteo Ceregini Florian Kurpicz. *Faster Wavelet Trees with Quad Vectors*. 2024.

[40] Alistair Moffat, Radford M Neal, and Ian H Witten. "Arithmetic coding revisited." In: *ACM Transactions on Information Systems (TOIS)* 16.3 (1998), pp. 256–294.

[41] G. Navarro. *Compact Data Structures: A Practical Approach*. Cambridge University Press, 2016.

[42]   Gonzalo Navarro. "Wavelet trees for all." In: *Journal of Discrete Algorithms* 25 (2014). 23rd Annual Symposium on Combinatorial Pattern Matching, pp. 2–20. ISSN: 1570-8667.

[43]   Gonzalo Navarro and Veli Mäkinen. "Compressed full-text indexes." In: *ACM Computing Surveys (CSUR)* 39.1 (2007), 2–es.

[44]   Giuseppe Ottaviano and Rossano Venturini. "Partitioned Elias-Fano indexes." In: *Proceedings of the 37th International ACM SIGIR Conference on Research & Development in Information Retrieval*. SIGIR '14. Association for Computing Machinery, 2014, pp. 273–282. ISBN: 9781450322577.

[45]   Richard Clark Pasco. "Source coding algorithms for fast data compression." PhD thesis. Stanford University CA, 1976.

[46]   Mihai Patrascu. "Succincter." In: *2008 49th Annual IEEE Symposium on Foundations of Computer Science*. 2008, pp. 305–313.

[47]   Eli Plotnik, Marcelo J Weinberger, and Jacob Ziv. "Upper bounds on the probability of sequences emitted by finite-state sources and on the redundancy of the Lempel-Ziv algorithm." In: *IEEE transactions on information theory* 38.1 (1992), pp. 66–72.

[48]   Rajeev Raman, Venkatesh Raman, and S. Srinivasa Rao. "Succinct indexable dictionaries with applications to encoding k-ary trees and multisets." In: *Proceedings of the Thirteenth Annual ACM-SIAM Symposium on Discrete Algorithms*. SODA '02. Society for Industrial and Applied Mathematics, 2002, pp. 233–242. ISBN: 089871513X.

[49]   Robert F Rice. *Some practical universal noiseless coding techniques*. Tech. rep. 1979.

[50]   Jorma J Rissanen. "Generalized Kraft inequality and arithmetic coding." In: *IBM Journal of research and development* 20.3 (1976), pp. 198–203.

[51]   Kunihiko Sadakane and Roberto Grossi. "Squeezing succinct data structures into entropy bounds." In: *Proceedings of the seventeenth annual ACM-SIAM symposium on Discrete algorithm*. 2006, pp. 1230–1239.

[52]   K. Sayood. *Lossless Compression Handbook*. Communications, Networking and Multimedia. Elsevier Science, 2002, pp. 55–64.

[53]   Hinrich Schütze, Christopher D Manning, and Prabhakar Raghavan. *Introduction to information retrieval*. Vol. 39. Cambridge University Press Cambridge, 2008.

[54]   C. E. Shannon. "A mathematical theory of communication." In: *The Bell System Technical Journal* 27.3 (1948), pp. 379–423.

[55]   Sebastiano Vigna. "Broadword implementation of rank/select queries." In: *International Workshop on Experimental and Efficient Algorithms*. Springer. 2008, pp. 154–168.

[56] Sebastiano Vigna et al. *Dsi-bitstream: Bitstream readers/writers for the DSI utilities*. Rust Crate. Accessed: May 2025. URL: https://crates.io/crates/dsi-bitstream.

[57] Sebastiano Vigna. "Quasi-succinct indices." In: *Proceedings of the Sixth ACM International Conference on Web Search and Data Mining*. WSDM '13. Association for Computing Machinery, 2013, pp. 83–92.

[58] Ian H Witten, Alistair Moffat, and Timothy C Bell. *Managing gigabytes: compressing and indexing documents and images*. Morgan Kaufmann, 1999.